Philipps Universität Marburg

On the Mechanism of Electron-Bifurcation by Electron Transferring Flavoprotein and Butryl-CoA Dehydrogenase

Dissertation
zur Erlangung des Doktorgrades
der Naturwissenschaften
(Dr. rer. nat.)

dem Fachbereich Biologie
der Philipps-Universität Marburg
vorgelegt von

Nilanjan Pal Chowdhury
aus Kalkutta, Indien

Marburg/Lahn 2014

Die Untersuchungen zur vorliegenden Arbeit wurden von Oktober 2011 bis September 2014 am Max Planck Institute für Terretrische Mikrobiologie und Fachbereich Biologie der Philipps-Universität Marburg unter der Leitung von Herrn Prof. Dr. W. Buckel durchgeführt.

Vom

Fachbereich Biologie der Philipps-Universität Marburg als Dissertation am _____ angenommen.

Erstgutachter: Prof. Dr. Wolfgang Buckel

Zweitgutachter: Prof. Dr. Johann Heider

Tag der mündlichen Prüfung: _____

Dedicated to those people…..

Who lost hope to come back to science.

Die im zeitlichen Rahmen dieser Dissertation erzielten Ergebnisse sind in folgenden Publikationen veröffentlicht:

Anutthaman Parthasarathy, Jörg Kahnt, Nilanjan Pal Chowdhury & Wolfgang Buckel (2013) Phenylalanine catabolism in Archaeoglobus fulgidus VC-16
Arch Microbiol, 195:781–797, doi: 10.1007/s00203-013-0925-3

Nilanjan Pal Chowdhury, Amr M. Mowafy, Julius K. Demmer, Vikrant Upadhyay, Sebastian Koelzer, Elamparithi Jayamani, Joerg Kahnt, Marco Hornung, Ulrike Demmer, Ulrich Ermler & Wolfgang Buckel(2014) Studies on the Mechanism of Electron Bifurcation Catalyzed by Electron Transferring Flavoprotein (Etf) and Butyryl-CoA Dehydrogenase (Bcd) of *Acidaminococcus fermentans*. J. Biol. Chem., 289:5145-5157. doi: 10.1074/jbc.M113.521013

Nilanjan Pal Chowdhury, Katharina Klomann & Wolfgang Buckel (2014) Flavodoxin and flavin-based electron bifurcation**.** (To be submitted)

Nilanjan Pal Chowdhury, Jorg Kahnt & Wolfgang Buckel (2014) Generation of reactive oxygen species by flavin-based electron bifurcation**.** (To be submitted)

Work under progress

Nilanjan Pal Chowdhury, Arno Fricke & Wolfgang Buckel. Lactate dehydrogenase and electron transferring flavoprotein from *Megasphaera elsdenii*.

Contents

Abbreviations

AHT	Anhydrotetracyline
DMSO	Dimethyl sulfoxide
DTNB	5,5'-Dithiobis(2-nitrobenzoic acid)
DTT	Dithiothreitol
EPR	Electron Paramagnetic Resonance
FAD	Flavin Adenine Dinucleotide
FMN	Riboflavin-5'-phosphate
HPLC	High Performance Liquid Chromatography
β-IPTG	beta-Isopropyl thiogalactoside
MALDI-TOF	Matrix-assisted laser desorption ionisation – time of flight (mass spectrometry)
MOPS	4-Morpholinepropanesulfonic acid
O.D	Optical Density
SDS	Sodium dodecylsulfate
TEMED	N, N, N', N'- Tetraethylethylenediamine
TFA	Trifluoroacetic acid
THF	Tetrahydrofuran
Tris	2-Amino-2-(hydroxymethyl)-1, 3-propanediol
UV-vis	Ultraviolet visible
KPP	Potassium phosphate buffer

Zusammenfassung

Die auf Flavinen basierende Elektronen-Bifurkation (FBEB), die 2008 erstmalig beschrieben wurde, ist eine neue Art der der energetischen Kopplung in anaeroben Bakterien und Archaeen. Der Komplex aus dem Elektronen-transferierenden Flavoprotein und Butyryl-CoA-Dehydrogenase (Etf/Bcd) katalysiert die die Reduktion von Crotonyl-CoA zu Butyryl-CoA (E_0'=−10 mV) mit NADH (E_0'= −320 mV) nur in Gegenwart von Ferredoxin (E_0'= −420 mV). Während der Elektronenbifurkation finden die beiden Elektronen des NADH ihre Ziele in verschiedenen Richtungen, eines geht exergon zum Crotonyl-CoA während das andere endergon zum Ferredoxin übertragen wird. Wiederholung dieses Prozesses liefert Butyryl-CoA und ein zweites reduziertes Ferredoxin. Letzteres reduziert entweder Protonen mit einer löslichen Hydrogenase unter Bildung von Wasserstoff oder NAD^+ mit einer membranständigen Ferredoxin-NAD-Reduktase (Rnf) unter Bildung eines elektrochemischen Na^+-Gradienten, der zur ATP-Synthese dient.

In der vorliegenden Arbeit habe ich den dissoziierbarenEtf/Bcd Komplex aus *Acidaminococcus fermentans* untersucht. Die Kristallstruktur des heterodimeren Etfs zeigte das Vorhandensein von zwei FAD-Molekülen, jedes in einer Untereinheit, wobei NAD^+ neben dem FAD der β-Untereinheit (β-FAD) bindet. Bei stufenweiser Zugabe von NADH zum Etf wird zuerst das FAD der α-Untereinheit (α-FAD) über das stabile anionische Semichinon (α-$FAD^{\bullet-}$) zum $FADH^-$ reduziert, während das zweite NADH das β-FAD zum β-$FADH^-$ reduziert. In Gegenwart von Bcd benötigte die Reduktion zum α-$FAD^{\bullet-}$ ein ganzes Äquivalent NADH. Bei der Bifurkation erhöhte die stufenweise Zugabe von Etf zur Bcd die Oxidation sgeschwindigkeit von NADH bis eine molares Verhältnis von Etf:Bcd (tetramer) = 2 erreicht war. Die nicht dissoziierbaren Etf/Bcd Komplexe der Clostridien sind ebenso zusammengesetzt. Das optimale Verhältnis Ferredoxin:Etf:Bcd = 4:2:1 in Gegenwart von Hydrogenaselässt vermuten, dass Ferredoxin (Fd) unter Fließ gleichgewichtsbedingungen (steady state) zwischen einfach (Fd^-) und doppelt reduziertem Zustand (Fd^{2-}) hin und her pendelt. Unser postulierter Mechanismus der Elektronen-bifurkation beginnt mit der Reduktion des β-FAD durch NADH zum $FADH^-$. Dann nähert sich das α-FAD, das auf einer flexiblen Domäne sitzt, und schnappt sich ein Elektron, das es zum stablisierten α-$FAD^{\bullet-}$ reduziert. Das zurückbleibende hochreaktive β-$FADH^{\bullet}$ reduziert unverzüglich Ferredoxin.Das α-$FAD^{\bullet-}$ überträgt sein Elektron weiter auf Bcd. Bei Wiederholung der Bifurkation wird ein zweites Ferredoxin reduziert und Bcd bekommt das zweite Elektron zur Reduktion von Crotonyl-CoA.

Weiterhin zeige ich, dass das gelbe Flavodoxindas braune Ferredoxin ersetzen kann. NAD^+ oxidiert die farblose Hydrochinon-Form des Flavodoxins (E_0'= −420 mV) mit Rnf zur blauen Semichinon-Form (E_0'= −60 mV) und pendelt so zwischen den Hydrochion- und Semchinon-Formen hin und her.

Ich untersuchte auch den sehr ähnlichen bifurkierenden Etf/Bcd Komplex aus *Megasphaera elsdenii*. Nach früheren Arbeiten benötigt die scheinbare Reduktion von Crotonyl-CoA zu Butyryl-CoA mit NADH kein Ferredoxin. Ich fand, dass unter aeroben Bedingungen der Sauerstoffanstelle von Ferredoxin als Elektronenakzeptor dient und zu H_2O_2 reduziert wurde. Die bis zu 50% ige Hemmung der NADH-Oxidation durch Superoxid-Dismutase lässt vermuten, dass die langsame Reduktion von O_2 zu $O_2^{\bullet-}$ von einer sehr schnellen Reduktion von $O_2^{\bullet-}$ zu H_2O_2 gefolgt wird. Interessanterweise wurden die gleichen NADH Oxidationsraten auch in Gegenwart von Butyryl-CoA beobachtet. Wir postulieren, dass die Oxidation von Butyryl-CoA zu Crotonyl-CoA durch Sauerstoff von einer bifurkierenden Reduktion von Crotonyl-CoA durch NADH gefolgt wird. Demnach fungiert der Etf/Bcd Komplex an Luft in Gegenwart von katalytischen Mengen an Crotonyl-CoA oder Butyryl-CoA als NADH-Oxidase.

Summary

Flavin-based electron bifurcation (FBEB), discovered in 2008, is a novel mode of energy coupling in anaerobic bacteria and archaea. The complex of electron-transferring flavoprotein and butyryl-CoA dehydrogenase (Etf/Bcd) mediates the reduction of crotonyl-CoA (E_0'=−10 mV) by NADH (E_0'= −320 mV) only in presence of ferredoxin (E_0'= −420 mV). During electron bifurcation, the two electrons from NADH find their destination in two different directions; one goes exergonicllay to crotonyl-CoA and the other moves endergonically to ferredoxin. Repetition of this process yields butyryl-CoA and a second reduced ferredoxin. The latter reduces either protons to give hydrogen via a soluble hydrogenase or NAD^+ via the membrane-bound ferredoxin-NAD^+ reductase (Rnf). The thereby formed electrochemical Na^+-gradient is used for ATP synthesis.

In this thesis, I have studied the dissociable Etf/Bcd complex from *Acidaminococcus fermentans*. The crystal structure of the heterodimeric Etf revealed the presence two FAD molecules, each bound to one subunit. NAD^+ binds near the FAD of the smaller β-subunit (β-FAD). Upon stepwise addition of NADH to Etf, first the FAD of the α-subunit (α-FAD) was reduced to $FADH^-$ via the stable anionic semiquinone (α-$FAD^{\bullet-}$). The second equivalent NADH reduced β-FAD.In the presence of Bcd, reduction to α-$FAD^{\bullet-}$ required a whole equivalent of NADH. During the bifurcation process, stepwise addition of Etf to Bcd increased the rate of NADH oxidation until a molar ratio of Etf:Bcd (tetramer) = 2 was reached. The non-dissociable clostridial Bcd/Etf complexes have the same composition. The optimal ratio of ferredoxin: Etf: tetrameric Bcd in the presence of hydrogenase was 4:2:1, suggesting that under steady state conditions ferredoxin shuttles between the semireduced (Fd^-) and completely reduced states (Fd^{2-}). Our postulated mechanism of electron bifurcation starts with the reduction of β-FAD by NADH to $FADH^-$. Then α-FAD, which is located on a flexible domain, approaches and takes one electron to yield the stabilized semiquinone α-$FAD^{\bullet-}$. The remaining highly reactive electron on β-$FADH^{\bullet}$ is not stabilized and immediately reduces ferredoxin. The α-$FAD^{\bullet-}$ transfers its electron further to Bcd. After repetition of the bifurcation, a second reduced ferredoxin is formed and Bcd gets a second electron to reduce crotonyl-CoA.

FurtherI illustrate that the brownish ferredoxin can be replaced by the bright yellow flavodoxin in the bifurcation process. The colorless hydroquinone of flavodoxin (E_0'= −420 mV) can be reoxidized by NAD^+ via Rnf to its blue semiquinone form (E_0'= −60 mV) and thus shuttles between the semiquinone and hydroquinone forms.

I also investigated the very similar bifurcating Etf/Bcd complex from *Megasphaera elsdenii*. In older studies, an apparent reduction of crotonyl-CoA by NADH was achieved without the need of ferredoxin. I found that under aerobic conditions oxygen fulfilled the need of ferredoxin and was reduced to hydrogen peroxide (H_2O_2). The up to 50% inhibition of the rate of NADH oxidation by superoxide dismutase suggested that the slow reduction of oxygen to superoxide ($O_2^{\bullet-}$) was followed by a fast reduction of $O_2^{\bullet-}$ to H_2O_2. Interestingly, the same rates of NADH oxidation were observed by replacing crotonyl-CoA with butyryl-CoA. We propose an oxidation of butyryl-CoA by oxygen followed by the bifurcating reduction of crotonyl-CoA by NADH. Hence, under air and in the presence of catalytic amounts of crotonyl-CoA or butyryl-CoA, Etf/Bcd acts as NADH oxidase.

1. Introduction

1.1 Anaerobic Energy Metabolism

Most energy conserving reactions in living organisms consists of two basic mechanisms, substrate level phosphorylation (SLP) and electron transport coupled to phosphorylation (ETP), which more generally is called ion gradient phosphorylation (IGP). Ion gradient phosphorylation works with an ATP synthase driven by an electrochemical gradient of ions (H^+ or Na^+) across a membrane. Most ion gradients are formed by redox reactions in which one substrate is oxidized and another substrate is reduced. In aerobic organisms, the electron donor is usually an organic compound such as glucose and the acceptor is molecular oxygen. In the oxidative branch of metabolism, energy is conserved via SLP and in the reductive branch, ATP synthesis is coupled to the electron transport (ETP) with H^+ (in few cases, with Na^+) as coupling ion.
However many bacteria are able to live under anoxic conditions where molecular oxygen is absent and use organic or inorganic compounds as electron acceptors instead of oxygen. All these anaerobic energy conserving processes in which electron transport is coupled to phosphorylation are called anaerobic respiration. In contrast all anaerobic energy-conserving metabolic processes with SLP and no ETP are called fermentations. In bacterial fermentations the substrate serves not only as an electron donor but also as a terminal electron acceptor, since oxygen, nitrate, fumarate, etc. are absent [1]. It was apparently accepted that fermentations usually occur in the cytoplasm and anaerobic respirations involve an ion pump driven by an electron transport in combination with an ATP synthase. Though the definition of fermentation excludes the participation of an electron transport chain, some strict anaerobic bacteria like *Clostridium perfringens* [2, 3], *Clostridium tertium* [4] and species of *Propionibacterium* [5]have been reported to contain components of dissimilatory nitrate reduction which provides the electron sink for oxidative substrate-level phosphorylation. In general, fermentation cannot be completely separated from a membrane electron transport because many redox processes cause ion (H^+/Na^+) extrusion from the cytoplasm which contributes to an electrochemical gradient resulting in energy conservation via ion import via ATP synthase (e.g. decarboxylation of glutaconyl-CoA to crotonyl-CoA by biotin dependent glutaconyl-CoA decarboxylase discussed later). In recent years the discovery of a membrane bound NADH: ferredoxin oxidoreductase responsible for generation of a Na^+ gradient and its link to the F-type ATPase in anaerobic bacteria has completely changed our outlook on energy conservation in anaerobic living systems [6-8].

1.2 Anaerobic food chain

Aerobic organisms are able to degrade organic compounds like carbohydrates and proteins completely to CO_2 and H_2O. In contrast, anaerobes perform this process in several steps, called the anaerobic food chain, in which at least five different groups of bacteria and archaea participate. These include primary fermenting bacteria, acetogens, secondary fermenting bacteria (syntrophs) and methanogens [9]. Extracellular hydrolytic enzymes released by primary fermenting bacteria like clostridia break down polymers to oligomers and monomers (sugars and amino acids). These are then fermented to short chain fatty acids, ammonia, CO_2, acetate and molecular hydrogen. H_2 and $CO_2$are used by acetogenic bacteria as the energy source. The short chain fatty acids and aromatic compounds are oxidized by syntrophic bacteria to acetate, CO_2 and H_2 or formate. Syntrophic bacteria can only live if the methanogenic bacteria

keep the partial pressure of H_2 and the concentration of formate at very low values by reducing CO_2 to CH_4, hence the name syntrophism = living together. A simple illustration is shown as below:

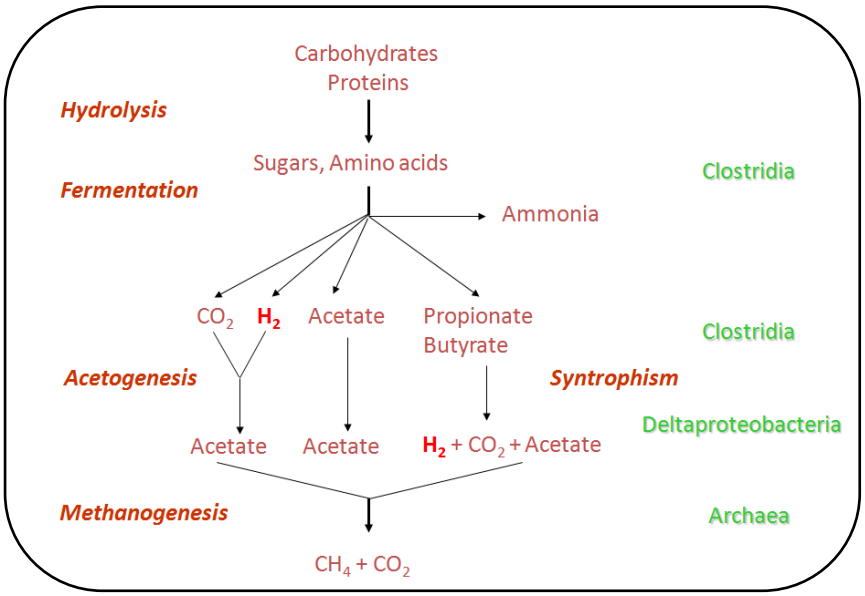

Fig. 1.1 Anaerobic food chain

Anaerobic bacteria of orders Clostridiales (phylum Firmicutes) and Fusobacteriales (phylum Fusobacteria) [10] and few other anaerobes are able to use amino acids as sole energy substrates [11, 12]. The 20 proteinogenic amino acids have an average redox state similar to the sugars and are therefore suitable for fermentative redox reactions. The oxidative deamination of amino acids and decarboxylation of keto acids involves many interesting reactions in anaerobic energy metabolism. It mostly involves special and unique radical enzymes which have been discovered and well studied in recent past. During 1930s, L.H.Stickland showed that pairs of amino acids were fermented by *Clostridium sporogenes* [13] where one amino acid (e.g.alanine) served as electron donor, whereas a different amino acid (e.g. glycine) was used an electron acceptor, famously known as Stickland reaction (shown in schematic below).

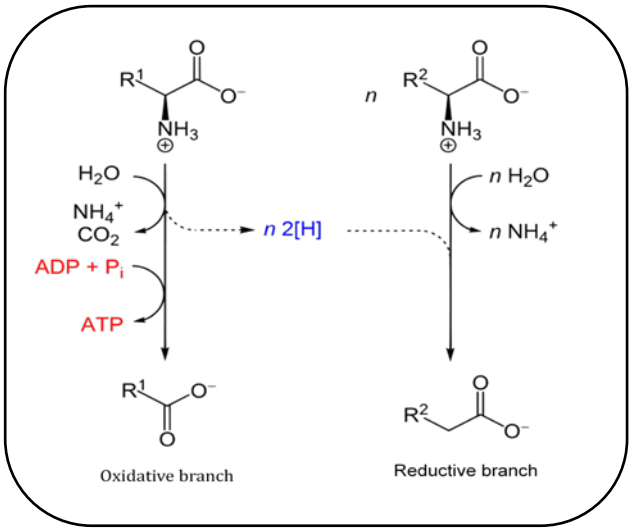

Fig. 1.2 General scheme of amino acid fermentation

Later in 1940s, H.A.Barker and coworkers isolated clostridia and related non sporulating anaerobic bacteria (e.g.*Clostridium propionicum*) which fermented single amino acids. *C. propionicum* uses alanine both as an electron donor and acceptor.

In amino acid fermentation pathways it was thought energy could only be conserved in the oxidative branch of fermentation which is coupled to SLP. A common acyl-CoA is formed which is converted to acetyl-CoA by a CoA-transferase, which is followed by a phosphate acetyltransferase and acetate kinase to release ATP and acetate.

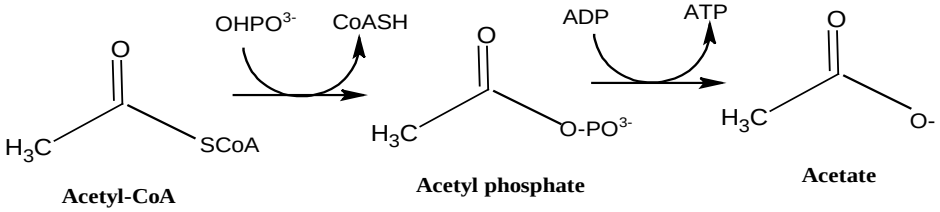

Fig. 1.3 Energy conservation by substrate level phosphorylation

However the discovery of flavin based electron bifurcation in 2008[14, 15] has completely changed our perspective regarding the energy conservation in anaerobic bacteria and archaea. An example of glutamate fermentation by *Acidaminococcus fermentans*, which ferments glutamate to ammonia, CO_2, acetate ,butyrate and hydrogen throws more light on how energy is not only conserved by SLP but also by flavin based bifurcation.

1.3 Glutamate Fermentation

Glutamate is fermented mainly by anaerobic bacteria from the order Clostridiales and Fusobacteriales by atleast 5 different pathways [16]. Three of these pathways lead to the formation of butyrate.The major two pathaways that occur in glutamate fermentation are the methylaspartate and the hydroxyglutarate pathway named after their intermediates. Both of the pathways lead to the formation of ammonia, CO_2, acetate, butyrate and hydrogen [17, 18] as shown in the equation below:

$$5\ \text{Glutamate}^- + 6\ H_2O + 2\ H^+ \longrightarrow 5\ NH_4 + 5\ CO_2 + 6\ \text{Acetate}^- + 2\ \text{Butyrate}^- + H_2$$

$\Delta G^{\circ\prime} = -63.5$ kJ/mol glutamate

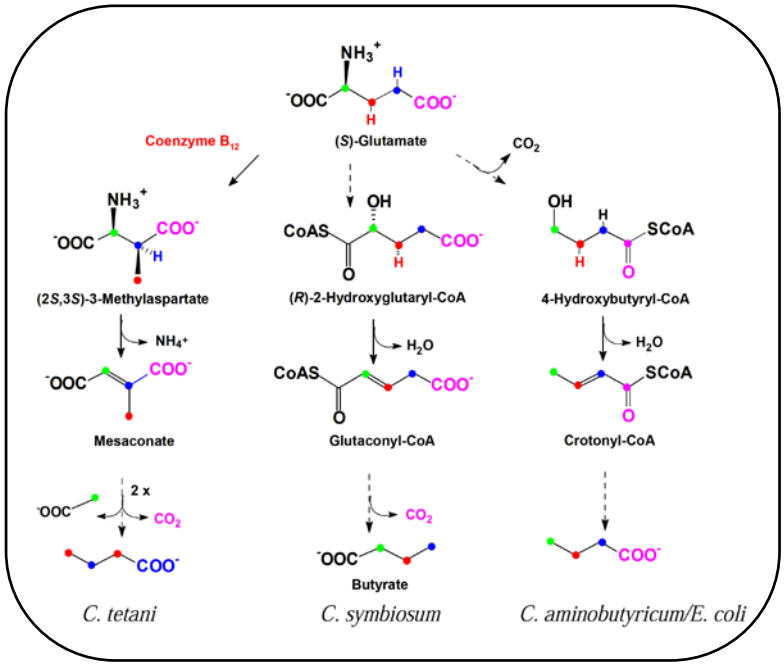

Fig. 1.4 Glutamate fermentation pathways

C. tetanomorphum and *C. tetani* ferment glutamate (first 2 pathways) via 3-methylaspartate to ammonia, acetate and pyruvate mediated by coenzyme B_{12}-dependent glutamate mutase [19] and three further enzymes [20]. The third pathway via 2-hydroxyglutarate is described and discussed in this thesis. The remaining two pathways demand more than one organism for the complete catabolism of glutamate to short chain fatty acids. For example, glutamate is decarboxylated to 4-aminobutyrate which is fermented by a second organism to acetate and butyrate by unusual dehydratase that catalyzes the reversible dehydration of 4-hydroxybutyryl-CoA to crotonyl-CoA. The last pathway does not involve any decarboxylation, proceeds via proline and 5-aminovalerate to acetate, propionate and n-valerate.

1.3.1 Hydroxyglutarate pathway

The pathway, which does not use the coenzyme B_{12}, has been found in *Acidaminococcus fermentans*, *C. sporosphaeroides*, *C. symbosium*, *Fusobacterium nucleatum* and *Peptostreptococcus asaccharolyticus* [17, 21]. The organisms ferment glutamate via (*R*)-2-hyrdoxyglutaryl-CoA, glutaconyl-CoA and crotonyl-CoA. Crotonyl-CoA disproportionates to acetate, butyrate and H_2. The products of the hydroxyglutarate pathway are identical to those of the methylaspartate pathway. The first step of the hydroxyglutarate pathway is the oxidative NAD^+-dependent deamination of glutamate to 2-oxogluarate, which is carried out by the glutamate dehydrogenase and followed by hydroxyglutarate dehydrogenase to form (*R*)-2-hydroxyglutarate. Glutaconate-CoA transferase then transfers the CoA moiety from an incoming acetyl-CoA to 2-hydroxyglutarate to release 2-hydroxyglutaryl-CoA which is dehydrated by 2-hydroxygluratryl-CoA dehydratase to (*E*)-glutaconyl-CoA. This transformation of hydroxyglutaryl-CoA to glutaconyl-CoA differed from conventional biochemical transformation [22-24]. A mechanistically difficult reaction of reversible *syn*-elimination of water is achieved where the 3-*Si* proton is removed from the non-activated β-position, whereas a hydroxyl anion is expelled from the α-position adjacent to the electron withdrawing

CoA ester. The dehydratase has been purified from *A. fermentans* and *C. symbosium*, which consists of two protein components A and D. The extremely oxygen sensitive homodimeric component A (hgdC, 2x27 kDa) contains one $[4Fe\text{-}4S]^{2+}$ cluster between two subunits and acts as an activator of the dehydratase. Dehydratase activity requires both components A and D, $MgCl_2$, catalytic amounts of ATP and a reducing agent. In vivo reduced ferredoxin or flavodoxin act an electron donor [24].

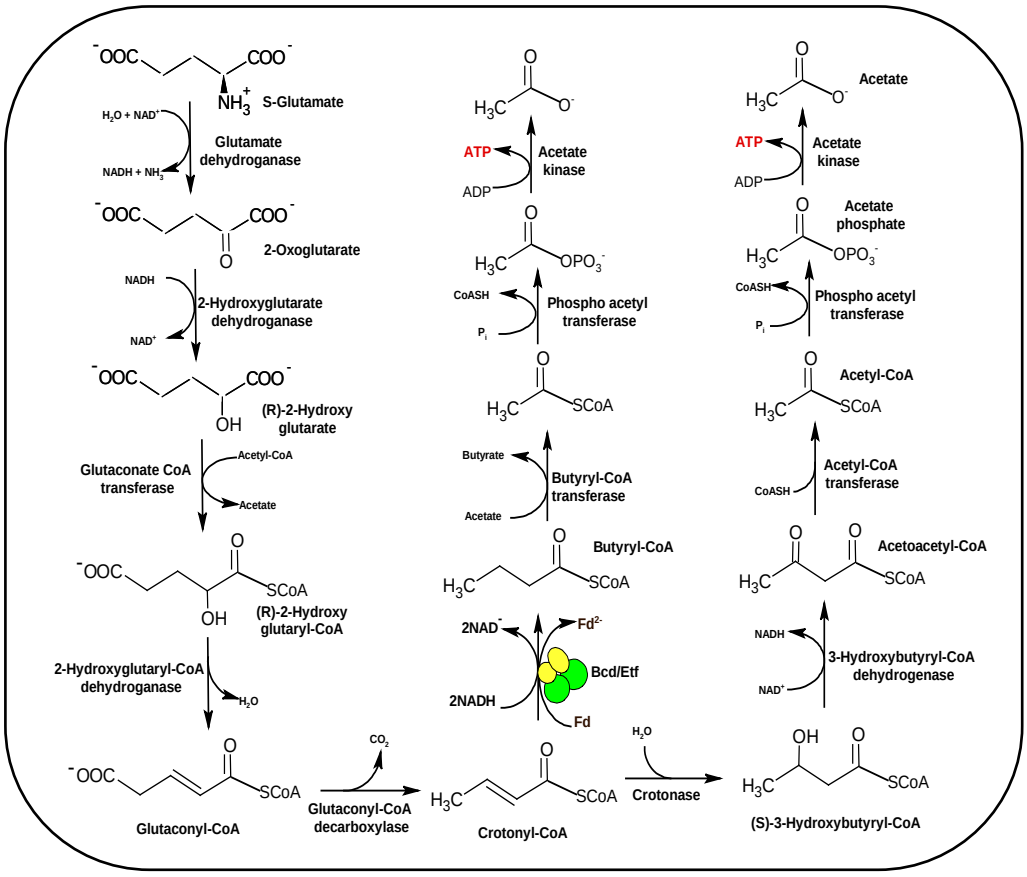

Fig. 1.5 Hydroxyglutarate pathway of glutamate fermentation

The glutaconyl-CoA so formed is then decarboxylated to crotonyl-CoA by glutaconyl-CoA decarboxylase (Gcd). This is decarboxylation step is found to be very interesting in the metabolism of *A. fermentans*, which was later realized to be one the main contributors to the formation of ATP by ion gradient phosphorylation. The salient feature of this enzyme GcdABCD is its integration into the cytoplasmic membrane, its biotin content and Na^+ dependency of the enzymatic reaction [25-27]. Gcd shares similar features with oxaloacetate decarboxylase from Gammproteobacteria [28] and *P. modestum* [29]. Glutaconyl-CoA decarboxylases are complexes of four to five functional domains or subunits, a carboxytransferase (α), a 9-11 transmembrane helix containing Na^+-dependent carboxybiotin decarboxylase (β), 1-2 mobile biotin carrier (γ) and a membrane anchor (δ) [30, 31]. A simple illustration is as shown below:

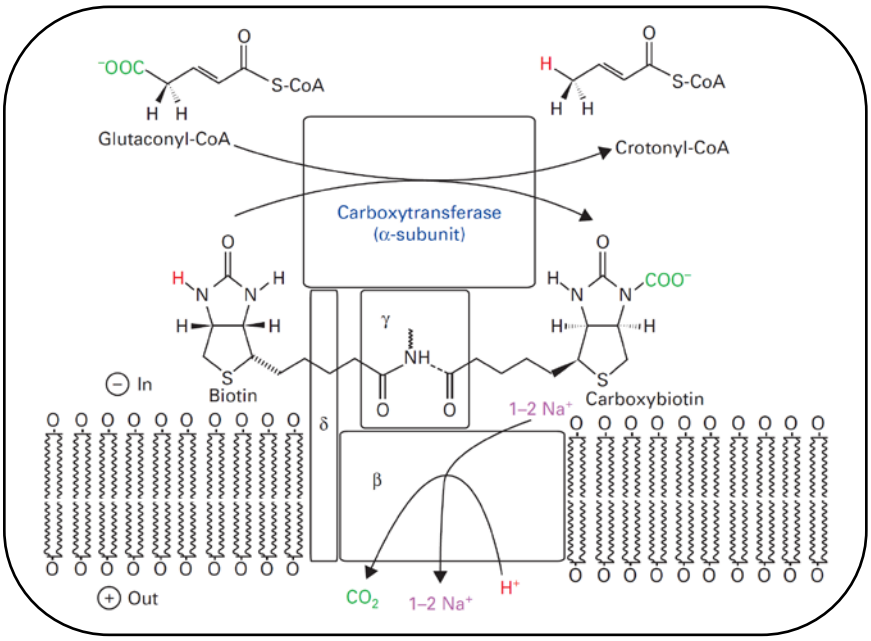

Fig. 1.6. A simplistic model of glutaconyl-CoA decarboxylase. The array in the lower part resembles the cytoplasmic membrane in which the β and δ is embedded. (Model adapted from Boiangiu et al, 2005)

The beauty of the decarboxylation lies in the fact that the free energy of decarboxylation is converted to an electrochemical Na^+ gradient resulting in $\Delta\mu Na^+$ [32]. According to stoichiometric calculations, 5 glutamate leads to the formation of 5 glutaconyl-CoA which are then decarboxylated to 5 crotonyl-CoA and 10 Na^+ ions are pumped out of the cell.

After the decarboxylation of glutaconyl-CoA to crotonyl-CoA, the 2-hydroxyglutarate pathway forks into oxidative and reductive branch. The NAD^+-dependent oxidation of crotonyl-CoA proceeds after a 'normal' hydration to (*S*)-3-hydroxybutyryl-CoA. After oxidation by NAD^+ the product acetoacetyl-CoA is subsequently cleaved by CoASH into two acetyl-CoA, which finally give rise to 2 ATP by SLP via acetyl phosphate (as shown above). In reductive branch, crotonyl-CoA is reduced to butyryl-CoA. CoA transfer to acetate releases the final product butyrate and additional acetyl-CoA. This acetyl-CoA pool is used to convert 2-hydroxyglutarate to the thiol ester and to synthesize ATP via acetyl-phosphate.

The apparently simple reduction of crotonyl-CoA to butyryl-CoA requires NADH as an electron donor and a protein complex of electron transferring flavoprotein (Etf)-butyryl-CoA dehydrogenase (Bcd). The activities of the individual proteins, Etf and Bcd could be identified separately by a diaphorase assay and a butyryl-CoA dehydrogenase assay, respectively. But when combined together the physiological oxidation of NADH by crotonyl-CoA under strict anoxic conditions was not detected. In 2008 it was hypothesized that the exergonic electron transfer from NADH to crotonyl-CoA was coupled to the concomitant enedergonic reduction of ferredoxin by a process called **electron bifurcation** (Herrmann et al.) [14].This hypothesis was verified with the Etf-Bcd complex from *C. kluyveri* [14, 15].

$$\mathbf{2\ Fd_{ox}^{-} + 2\ NADH + crotonyl\text{-}CoA \rightarrow 2\ Fd^{2-}_{red} + 2\ NAD^{+} + butyryl\text{-}CoA;\ \Delta G^{\circ\prime} = -44 kJ/mol}$$

The Etf is a heterodimer consisting of two subunits of α (36 kDa) and β (28 kDa) and the Bcd a tetramer of 41 kDa subunits. The enzymes in *C. tetanomorphum* [33], *C. kluyveri* [15] and *C. difficile* [34] form tight complexes and do not dissociate during purification. In *A. fermentans* [35] the yellow Etf and the

green butyryl-CoA dehydrogenase were isolated as separate molecules. The only cofactor present in Etf and Bcd is flavin adenine dinucleotide (FAD) and hence the name **flavin based electron bifurcation** was coined. First the electrons from NADH are passed on to the β-FAD of the Etf, one electron then moves to the α-FAD of the Etf, the second electron which is quite unstable at β-FAD$^{\bullet}$ quickly reduces a ferredoxin. In the second round another NADH binds and the same thing is repeated once again, resulting in two reduced ferredoxins and butyryl-CoA. The reduced ferredoxins can either give rise to H_2 via the hydrogenase present which increases the energy conservation by SLP or get reoxidized via the Rnf (discussed later) giving rise to NADH. While the ferredoxin is reoxidized, the redox potential difference between ferredoxin and NAD^+($\Delta E'$ =220 mV) is sufficient to allow the build-up of an electrochemical ion potential ($\Delta\mu H^+/\Delta\mu Na^+$) that in turn could be used to drive the phosphorylation of ADP via membrane associated F_0F_1 or A_0A_1 ATP synthase complexes. Thus flavin-based electron bifurcation indirectly either conserves energy by increasing SLP by H_2 formation or by giving rise to ion gradient phosphorylation (according to following equations).

$Fd^{2-}_{red} + 2\ H^+ = Fd_{ox} + H_2$

$Fd^{2-}_{red} + NAD^+ + H^+ = Fd_{ox} + NADH + (\Delta\mu H^+/\Delta\mu Na^+)$

So the overall reaction combining earlier equations:

Crotonyl-CoA + NADH + H^+= butyryl-CoA + NAD^+ + ($\Delta\mu H^+/\Delta\mu Na^+$)

1.4 Rnf complex

The phototrophic bacterium *Rhodobacter capsulatus* is able to fix nitrogen. Its genome contains a cluster of six genes designated as ***rnfABCDEG*** that is thought to be involved in electron transfer to nitrogenase (*Rhodobacter nitrogen fixation* = Rnf) [36, 37]. The reducing power for nitrogen fixation in these bacteria, which is a limiting factor, is solved by the Rnf. Mutant strains failed to grow diazotrophically and exhibited no acetylene reduction activity. Insertion or deletion of Rnf genes showed that it plays an important role in electron transfer reaction to the nitrogenase. Using cell free extracts, nitrogenase activities could be determined using diothionite as an artificial electron donor in Rnf mutant strains. These studies showed that the Rnf system is involved in nitrogen fixation by acting as electron donor for the nitrogenase.

Homologus clusters like Rnf, which code for such a membrane bound NAD^+-ferredoxin oxidoreductase, are found in over a hundred aerobic and anaerobic bacteria but only in two archaea [38]. Genome sequence of *C. tetani* [39] showed the abundance of FeS clusters within the proteins encoded by a putative operon of six genes, homologous to Rnf. Membrane vesicles of *C. tetanomorphum* catalyze the oxidation of NADH by hexacyanoferrate (III) (ferricyanide) at a rate of 20 Umg^{-1}protein and the reduction of NAD^+ by ferredoxin [reduced with Ti (III) citrate] with 1.5 Umg^{-1} protein. This provides the missing link of how the reduced ferredoxin, generated by flavin-based electron bifurcation is reoxidized and NADH is regenerated. This process also gives rise to$\Delta\mu Na^+$ that can be used for ATP synthesis. Recent studies in *A. woodii* showed that Rnf containing membrane vesicles can indeed couple the reduction of NAD^+ by reduced ferredoxin with formation of $\Delta\mu Na^+$ that can be used for ATP-synthesis or transport process [8]. The entire co-ordination between flavin-based electron bifurcation and redoxidation of ferredoxin is shown in the simple illustration below:

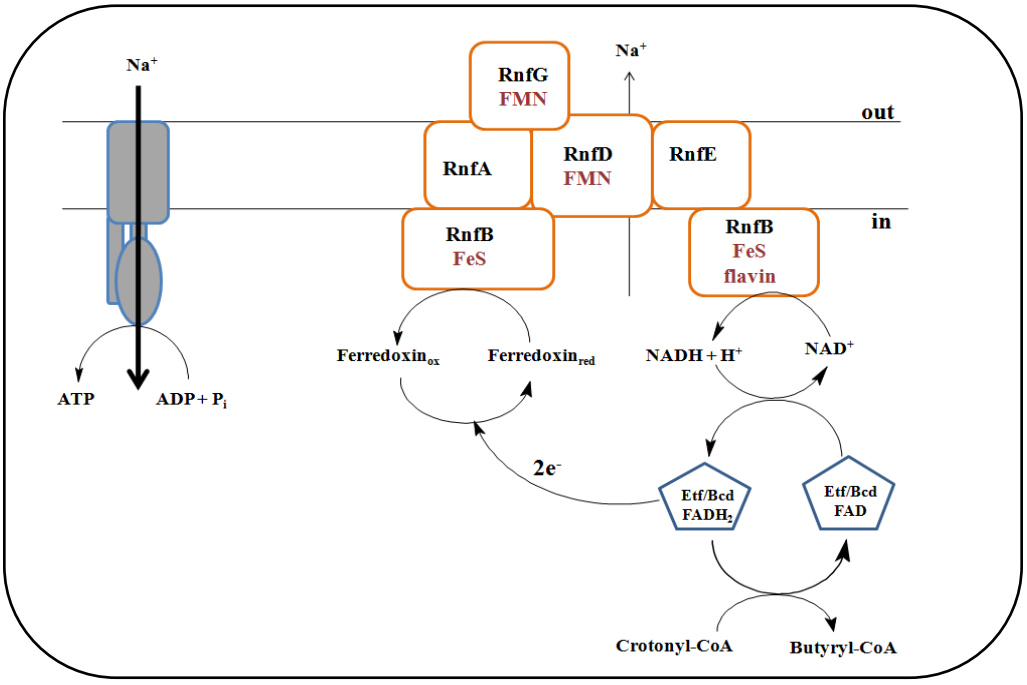

Fig. 1.7 Scheme showing reduction of crotonyl-CoA to butyryl-CoA by NADH with subsequent generation of reduced ferredoxin and its mode of reoxidation by the membrane-bound Rnf complex.

1.5 Flavin-based electron bifurcation

Flavin containing cytoplasmic multienzyme complexes from anaerobic bacteria and archaea that catalyze the reduction of the low potential ferredoxin by electron donors with higher potentials, such as NAD(P)H or H_2 at ≤100 kPa follow the process called flavin-based electron bifurcation (FBEB). In this process, the endergonic reactions are driven by concomitant oxidation of the electron donor with higher potential acceptors like crotonyl-CoA, pyruvate, NAD^+ or heterodisulfide (CoM-S-S-CoB). This can be regarded as the **Third Mode of Energy Conservation** in addition to substrate level phosphorylation (**SLP**) and electron transport phosphorylation (**ETP**). As mentioned earlier FBEB was first discovered in Etf/Bcd complex from *C. kluyveri* in 2008, since then reports of bifurcating complexes are increasing with time. The multisubunit [Fe-Fe] hydrogenase from *Thermatoga maritima* (HydABC) [40] and from acetogenic bacteria [41], the [Ni-Fe] hydrogenase/heterodisulfide reductase (MvhADG-HdrABC) from methanogenic archaea [42], the transhydrogenase (NfnAB) from *C. kluyveri* [43], the formate dehydrogenase from *Clostridium acidiurici* [44], the lactate dehydrogenase from *A. woodii* [45], all were shown to be either electron bifurcating or confurcating complexes. All the complexes reported so have FAD/FMN as co-factor and one or more (Fe-S) clusters as cofactors apart the Etf/Bcd complex from clostridia, which have FAD as the only cofactor. This makes the Etf/Bcd an attractive candidate to study, as the sole role play in electron transmission is played by either the FAD or the protein itself unlike in other cases presence of multiple (Fe-S) clusters makes the situation more complex. A simple illustration shown below explains the mechanism in detail.

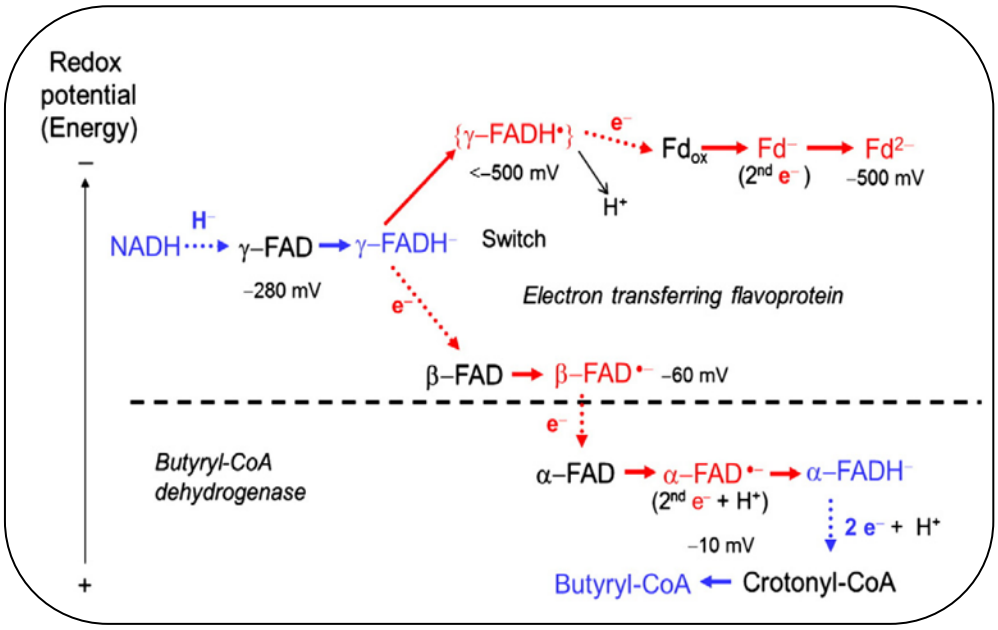

Fig. 1.8 Illustration of flavin-based electron bifurcation (adapted from Buckel and Thauer 2013)

Later in this thesis a detailed working mechanism of the Etf-Bcd complex has been well described and discussed. Studies both at the biochemical and structural level from gives a mechanistic picture of how the Etf-Bcd might work in-vivo. As a model system the dissociating complex of Etf-Bcd from *A. fermentans* and *M. elsdenii* was chosen.

1.6 Organisms

1.6.1 *Acidaminococcus fermentans*

A. fermentans is a non-motile, non-sporulating and strict anaerobic bacterium. It was first isolated from the pig alimentary tract along with 48 other Gram-negative strains by Fuller in 1966 [46]. Later it was characterized by Rogosa in 1969 [47]. It is a member of the phylum *Firmicutes* and is Gram-negative diplococci. Amino acids, mainly glutamic acid serves as the sole energy source for growth in the gastrointestinal tract of homothermic animals. It ferments glutamate via the hydroxyglutarate pathway to ammonia, carbon dioxide, acetate, butyrate and molecular hydrogen (ArchMicrobiol (1985) 142:128-135)

1.6.2 *Megasphaera elsdenii*

M. elsdenii was first isolated and characterized by Elsden in 1956 from rumen contents of sheep [48]. Like *A. fermentans* it belongs to the phyla *Firmicutes* and a strict Gram-negative anaerobic bacterium. It metabolizes DL-lactate principally to carbon dioxide, hydrogen, propionate, acetate, butyrate and traces of valerate [49, 50]. The metabolic pathway of *M. elsdenii* is still not well understood, we here study the working mechanism of the Etf-Bcd complex (discussed in Chapter 2.3.1) in reduction of crotonyl-CoA. Later in Chapter 2.3.2, lactate oxiding protein lactate-dehydrogenase has been reported but the work is still under progress and initial results have been presented.

2. Results

This section has been divided in to three chapters and a subchapter.

Chapter 2.1 describes the biochemical and structural study of the electron transferring flavoprotein and butyryl-CoA dehydrogenase of *Acidaminococcus fermentans*. This chapter is presented as a publication reprint.

Chapter 2.2 describes the role of flavodoxin in anaerobic energy metabolism; biochemical studies present forward the model of flavodoxin involvement in energy conservation in *A. fermentans*. This chapter is presented as a publication draft (to be submitted)

Chapter 2.3 has been divided in to 2.3.1and 2.3.2

Chapter 2.3.1 deals with the Etf-Bcd complex of *Megasphaera elsdenii*. (To be submitted)
Chapter 2.3.2 presents a short study on the role of Etf and lactate dehydrogenase in lactate metabolism by *M. elsdenii*. (Work under progress)

Chapter 2.2 and 2.3.1 are presented as draft manuscripts which will be submitted soon. Each chapter has been summarized in short at the beginning of the chapter.

2.1 Flavin Based Electron-Bifurcation: A Biochemical and structural study

Summary

Hydrogen production in several glutamate fermenting bacteria has remained obscure over many years. Until recently the hypothesis of electron bifurcation in non-dissociable electron transferring flavoprotein/butyryl-CoA dehydrogenase complex (Herrmann et. al.) explains how it enables anaerobic bacteria and archaea to reduce the low-potential [4Fe-4S] clusters of ferredoxin, which was later proved by Li. et.al (2008). Reduced ferredoxin can be reoxidized by hydrogenase by reducing protons to molecular hydrogen or generates an electrochemical gradient across the membrane. Reoxidation of ferredoxin results in increase in efficiency of substrate level phosphorylation or better energy conservation by electron transport phosphorylation.

In this study we have studied the dissociable Etf/Bcd complex of the glutamate fermenting bacterium, *Acidaminococcus fermentans*. With the help of biochemical and spectroscopic experiments we have characterized the protein complex. Crystallization study revealed the enzyme active site and the co-factor binding sites, single FADs are bound at the α- and β-subunit. NAD^+ is found to be bound next to the β-FAD. The structure can be modeled which fits to the working mechanism of electron-bifurcation. We propose a stepwise electron transfer within the Etf and to the ferredoxin which affords reduction of crotonyl-CoA by NADH. Reduced ferredoxin when coupled with hydrogenase releases hydrogen which explains the hydrogen production during glutamate fermentation.

This study finds its importance as this elucidated mechanism can be extended to understand other bifurcating systems reported which has FAD as the bifurcating cofactor.

THE JOURNAL OF BIOLOGICAL CHEMISTRY VOL. 289, NO. 8, pp. 5145–5157, February 21, 2014

Studies on the Mechanism of Electron Bifurcation Catalyzed by Electron Transferring Flavoprotein (Etf) and Butyryl-CoA Dehydrogenase (Bcd) of *Acidaminococcus fermentans**

Received for publication, September 24, 2013, and in revised form, December 20, 2013 Published, JBC Papers in Press, December 30, 2013, DOI 10.1074/jbc.M113.521013

Nilanjan Pal Chowdhury[‡§1], Amr M. Mowafy[‡§¶1], Julius K. Demmer[§‖], Vikrant Upadhyay[‖2], Sebastian Koelzer[‡], Elamparithi Jayamani[‡§3], Joerg Kahnt[§], Marco Hornung[‡§], Ulrike Demmer[‖], Ulrich Ermler[‖], and Wolfgang Buckel[‡§4]

From the [‡]Laboratorium für Mikrobiologie, Fachbereich Biologie and SYNMIKRO, Philipps-Universität, 35032 Marburg, Germany, the [§]Max-Planck-Institut für terrestrische Mikrobiologie, Karl-von-Frisch-Str. 10, 35043 Marburg, Germany, the [¶]Faculty of Science, Mansoura University, Mansoura 35516, Egypt, and the [‖]Max-Planck-Institut für Biophysik, Max-von-Laue-Str. 3, 60438 Frankfurt am Main, Germany

Background: Flavin-based electron bifurcation explains the energy metabolism of anaerobic microorganisms.
Results: Kinetic, structural, and spectral data revealed a detailed picture of the bifurcation process.
Conclusion: NADH reduces β-FAD of Etf, which bifurcates one electron to Bcd via α-FAD and the other to ferredoxin. Repetition leads to reduction of crotonyl-CoA.
Significance: The mechanism can be extended to other bifurcating systems.

Electron bifurcation is a fundamental strategy of energy coupling originally discovered in the Q-cycle of many organisms. Recently a flavin-based electron bifurcation has been detected in anaerobes, first in clostridia and later in acetogens and methanogens. It enables anaerobic bacteria and archaea to reduce the low-potential [4Fe-4S] clusters of ferredoxin, which increases the efficiency of the substrate level and electron transport phosphorylations. Here we characterize the bifurcating electron transferring flavoprotein (Etf_{Af}) and butyryl-CoA dehydrogenase (Bcd_{Af}) of *Acidaminococcus fermentans*, which couple the exergonic reduction of crotonyl-CoA to butyryl-CoA to the endergonic reduction of ferredoxin both with NADH. Etf_{Af} contains one FAD (α-FAD) in subunit α and a second FAD (β-FAD) in subunit β. The distance between the two isoalloxazine rings is 18 Å. The Etf_{Af}-NAD^+ complex structure revealed β-FAD as acceptor of the hydride of NADH. The formed β-$FADH^-$ is considered as the bifurcating electron donor. As a result of a domain movement, α-FAD is able to approach β-$FADH^-$ by about 4 Å and to take up one electron yielding a stable anionic semiquinone, α-$FAD^{\bullet-}$, which donates this electron further to Dh-FAD of Bcd_{Af} after a second domain movement. The remaining non-stabilized neutral semiquinone, β-$FADH^{\bullet}$, immediately reduces ferredoxin. Repetition of this process affords a second reduced ferredoxin and Dh-$FADH^-$ that converts crotonyl-CoA to butyryl-CoA.

Electron bifurcation proposed by Peter Mitchell in 1976 (1) is the key event of the Q (ubiquinone)-cycle used by the bc_1 complex to double the efficiency of the proton-motive process. In 2008, a second type of electron bifurcation was discovered that is based on flavin cofactors bound to a soluble cytoplasmic protein complex and not on ubiquinone used by the transmembrane bc_1 complex (2, 3). This so-called flavin-based electron bifurcation, considered as a new mode of energy coupling, plays a crucial role in diverse energy-limited anaerobic organisms and is proposed to operate since the early evolution of life (4). So far, five such systems are experimentally established; for a recent review, see Ref. 5. The latest additions are caffeyl-CoA reductase of *Acetobacterium woodii* (6) and formate dehydrogenase of *Clostridium acidiurici* (7). All enzyme complexes possess at least one flavin, either FAD or riboflavin 5′-phosphate, and catalyze the reduction of a low-potential ferredoxin. The functional understanding of these enzyme complexes allows an explanation of the bioenergetics of many fermenting bacteria, methanogens, and acetogens.

The best studied flavin-based electron bifurcating system is the electron transferring flavoprotein-butyryl-CoA dehydrogenase (Etf-Bcd)[5] complex, which is a key enzyme in butyrate producing clostridia. This Etf-Bcd complex couples the exergonic reduction of crotonyl-CoA to butyryl-CoA ($E_0' = -10$ mV) by NADH with the endergonic reduction of ferredoxin (Fd) also by oxidation of NADH to NAD^+ ($E_0' = -320$ mV). According to current knowledge, the electron pair of NADH is

* This work was supported by grants from the Max-Planck Society, the German Research Foundation (DFG), and SYNMIKRO of the Philipps-Universität Marburg.

The atomic coordinates and structure factors (codes 4KPU, 4L21, and 4L1F) have been deposited in the Protein Data Bank (http://wwpdb.org/).

[1] Both authors contributed equally to this work and are considered as first authors.

[2] Present address: Dept. of Anesthesiology, Weill Cornell Medical College, 52 East St., NY, New York 10065.

[3] Present address: Division of Infectious Diseases, MA General Hospital, Harvard Medical School, Boston, MA 02114.

[4] To whom correspondence should be addressed: Laboratorium für Mikrobiologie, Fachbereich Biologie, Philipps-Universität, 35032 Marburg, Germany. Tel.: 49-6421-2822088; Fax: 49-6421-2828979; E-mail: buckel@staff.uni-marburg.de.

[5] The abbreviations used are: Etf, electron transferring flavoprotein; Etf_{Af}, Etf of *A. fermentans*; Etf_{Me}, Etf of *M. elsdenii*; Bcd, butyryl-CoA dehydrogenase; Bcd_{Af}, Bcd of *A. fermentans*; Fd/$Fd^{\bullet-}$/Fd^{2-}, oxidized/semi-reduced/reduced ferredoxin; BisTris propane, 1,3-bis[tris(hydroxymethyl)methylamino]propane; Dh-FAD, dehydrogenase FAD.

split at the two-electron acceptor and one-electron donor FAD; one electron reduces the Dh-FAD (dehydrogenase FAD) of Bcd and the other goes to ferredoxin (Fd^-) characterized by a low redox potential ($E_0' = -405$ mV) (8). Repetition of this process leads to a second reduced ferredoxin and butyryl-CoA upon hydride transfer from $FADH^-$ of Bcd to crotonyl-CoA. The "energy-rich" reduced ferredoxin contributes to the energy conservation of the organism either by regeneration of NADH via the H^+/Na^+-pumping ferredoxin-NAD^+ reductase also called Rnf (9–11) or by reduction of protons to H_2, which increases the substrate-level phosphorylation via the oxidative branch of the fermentation.

To gain detailed mechanistic insights into electron bifurcation, we chose as a model Etf_{Af} and Bcd_{Af} of the Gram-negative glutamate fermenting *Acidaminococcus fermentans*, in which Etf and Bcd are separate proteins (12), in contrast to the non-dissociable Etf-Bcd complexes of several clostridia. We solved the crystal structures of Etf_{Af} and Bcd_{Af}, and characterized the proteins further by biochemical, kinetic, and spectroscopic methods.

EXPERIMENTAL PROCEDURES

Crotonyl-CoA and Butyryl-CoA—Both were synthesized by acylation of CoASH in aqueous 1 M $KHCO_3$ using 1 M crotonic anhydride or butyric anhydride in acetonitrile with a slight molar excess. After acidification the CoA-thioesters were purified on C18 columns and stored as lyophilized powders at −80 °C (13). The concentration of crotonyl-CoA was determined by the NAD^+-dependent β-oxidation to acetyl-CoA and acetyl phosphate as described for the assay of glutaconyl-CoA decarboxylase (14). HPLC of crotonyl-CoA and butyryl-CoA was performed on a C18 Kinetex column (5-μm particle size, 100 Å pore size, 250 × 4.6 mm, Phenomenex, Aschaffenburg, Germany) at a flow rate of 1 ml/min in 50 mM KH_2PO_4, pH 5.3, and 5% acetonitrile. During 20 min a linear gradient up to 60% acetonitrile was applied. The ferricenium (Fc^+) solution for the Bcd assay was prepared in 10 mM HCl to a final concentration of 2 mM set at 617 nm with $\epsilon_{617} = 0.41\ mM^{-1}\ cm^{-1}$ (15).

Protein concentrations were estimated with the Bradford assay (16) (Bio-Rad-Microassay reagent, Bio-Rad-Laboratories). Bovine serum albumin (Sigma) served as standard. SDS-PAGE was performed as described by the method of Laemmli (17).

Purification of Etf_{Af}—A. fermentans VR4 (DSM 20731) was grown in a 100-liter glutamate-yeast extract medium under anaerobic conditions at 37 °C (14). Wet packed cells (10 g) were suspended in 20 ml of 50 mM potassium phosphate, pH 7.0 (buffer A), and opened by three passages through a French press. The supernatant, obtained by centrifugation at 150,000 × *g* for 1 h at 4 °C was loaded on a DEAE column and fractionated with 10 column volumes of 0–100% 1 M NaCl in buffer A. Etf eluted from the column at around 19% NaCl. The fractions with the highest activity (iodonitrosotetrazolium chloride assay) were combined and dialyzed overnight against buffer A. The dialysate was concentrated by ultrafiltration and mixed with an equal volume of 3 M $(NH_4)_2SO_4$ to make a final concentration of 1.5 M. This mixture was loaded on a phenyl-Sepharose column and fractionated with 10 column volumes of 0–100% 1.5 M $(NH_4)_2SO_4$ in buffer A. The fractions eluting around 58% were run on SDS-PAGE, which showed both the subunits of Etf_{Af}.

Heterologous Production of Etf_{Af}—The genes *Acfer_0555* (β-subunit) and *Acfer_0556* (α-subunit) were cloned in this order as one fragment by applying the Stargate™ system according to the instructions of IBA, Göttingen, Germany. Genomic DNA of *A. fermentans* was used for PCR as template with the forward primer 5′-AGCTCTTCAATGAACATCGTTGTATGTGT-3′ and the reverse primer 5′-AAGCTCTTCACCCGGATTCTTTGAAGCCTTGA-3′. The PCR product was cloned into the *p*-ENTRY vector and introduced into *Escherichia coli* DH5α by chemical transformation. After confirmation of the desired sequence, the genes were transferred from the donor vector to expression vector pASG IBA33 and further into *E. coli* BL21(GroEL). The recombinant cells were cultivated in 4 liters of Standard I nutrient broth (Merck, Darmstadt, Germany) containing ampicillin (100 μg/ml) and chloramphenicol (34 μg/ml). When the $A_{600\ nm}$ was 0.5, both anhydrotetracycline (0.2 μg/ml) and 0.1 mM isopropylthiogalactoside were added to the culture medium to induce the overproduction of Etf and GroEL. The cultures were incubated at room temperature overnight. After harvesting, the cells (17 g wet mass) were suspended in 34 ml of 10 mM imidazole in 10 mM sodium phosphate, pH 7.4, and disrupted by passing the suspension three times through a French press cell at 140 megapascals. Cell debris was removed by centrifugation at 30,000 × *g* for 1 h and 4 °C to obtain 34 ml of cell extract containing 34 mg of protein/ml. The purification process was performed under oxic conditions at 4 °C. The supernatant was applied on a 20 ml of nickel-nitrilotriacetic acid column, which was equilibrated with buffer A. The recombinant protein was eluted with 500 mM NaCl and 150 mM imidazole in 10 mM sodium phosphate, pH 7.4. The purified protein was concentrated by ultrafiltration, washed with 50 mM potassium phosphate, pH 7.0, and stored at −80 °C. The prosthetic group was quantitatively extracted with both trichloroacetic acid and heat denaturation of the protein and identified by thin layer chromatography on TLC plates (Silica Gel 60 F_{254}) from Merck KGaA, Germany. The solvent system was *n*-butyl alcohol:acetic acid:water (4:3:3) (18). The titration of Etf_{Af} with NADH was performed under anoxic conditions in 50 mM potassium phosphate, pH 7.0.

Purification of Butyryl-CoA Dehydrogenase (Bcd_{Af})—The supernatant obtained by centrifugation at 150,000 × *g* (see purification of Etf) was saturated with ammonium sulfate to 60%. After centrifugation at 50,000 × *g* for 1 h at 4 °C, the clear supernatant was dialyzed against buffer A. The supernatant was then loaded on a DEAE-Sepharose column equilibrated with buffer A. After washing with this buffer, proteins were eluted by linear gradient from 0 to 1 M NaCl in buffer A. The fractions containing green Bcd_{Af} were analyzed by SDS-PAGE. The purest fractions were collected, washed with buffer A by ultrafiltration, and stored at −80 °C.

The yellow form of Bcd_{Af} was prepared by adding a molar excess of solid dithionite to the solution in buffer A under anaerobic conditions. After standing on ice for 1 h the enzyme was desalted by passing through a PD10 column in anaerobic 0.1 M potassium phosphate, pH 6.8. Then the enzyme was washed three times under air with the same but aerobic buffer by ultrafiltration using Centricon 30 (19).

Partial Purification of Hydrogenase—*Clostridium pasteurianum* (DSM 525) was grown on a medium containing 100 mM glucose, 70 mM $NaHCO_3$, and yeast extract (2 g/liter). Wet packed cells (10 g) were suspended in 50 mM potassium phosphate, pH 7.4 (buffer B), and broken by three passages through a French press at 140 megapascal (20,000 p.s.i.). The broken cells were centrifuged at 7,000 × *g* for 20 min. The supernatant was heated at 55–60 °C for 10 min under a hydrogen atmosphere. After keeping on ice for 10 min, precipitated protein was removed by centrifugation at 20,000 × *g* for 20 min. The supernatant containing the hydrogenase (6 mg of protein/ml) was stored at −20 °C until use (20).

Purification of Ferredoxin—*Clostridium tetanomorphum* (DSM 526) was grown on the same medium as used for *A. fermentans* from which biotin was omitted. The purification was carried out under strictly anoxic conditions in an atmosphere of 95% N_2 and 5% H_2 (Coy Anaerobic Chamber). Wet packed cells (10 g) were suspended in buffer B. After sonication, the supernatant, obtained by centrifugation at 150,000 × *g* for 1 h at 4 °C, was loaded on a DEAE column that was equilibrated by buffer B. After washing the unbound proteins, ferredoxin was eluted with a linear gradient from 0 to 100% 2 M NaCl in buffer B. The active fractions found by the bifurcation assay were collected and concentrated with a 3-kDa ultrafiltration membrane. The concentrated sample was loaded to a Superdex 75 column that was equilibrated with 150 mM NaCl in buffer B. The fractions containing ferredoxin were concentrated and stored under anoxic conditions at −80 °C. To calculate the concentration of ferredoxin, a molecular mass of 6 kDa was used (8).

Enzyme Assays—Etf_{Af} activity was measured in a 1-ml cuvette (d = 1 cm) containing 50 mM potassium phosphate, pH 7.0, 250 μM NADH, and 100 μM iodonitrosotetrazolium chloride. The formation of the red formazane was followed at 492 nm, ϵ = 19.2 mM^{-1} cm^{-1} (12). Bcd_{Af} activity was measured in 50 mM potassium phosphate, pH 7.0, with 0.2 mM ferricenium hexafluorophosphate (Fc^+) and 0.1 mM butyryl-CoA. The decrease of absorbance was followed at 310 nm, ϵ = 2 × 4.3 mM^{-1} cm^{-1}, because 2 mol of Fc^+ are required to oxidize 1 mol of butyryl-CoA (21). Unless otherwise indicated the assay for Etf_{Af}/Bcd_{Af} activity (bifurcation assay) was done under anoxic conditions containing 250 μM NADH, 100 μM crotonyl-CoA, 0.5 μM Etf_{Af}, 1 μM Bcd_{Af}, 1 μM ferredoxin, crude hydrogenase (30 μg/ml), and 50 mM potassium phosphate, pH 7.0 (3). The decrease in NADH concentration was monitored at 340 nm, ϵ = 6.3 mM^{-1} cm^{-1} (22). When appropriate the data were fitted to the Michealis-Menten equation using GraphPad Prism 5 software.

X-ray Structure Analysis of Etf_{Af} and Bcd_{Af}—Etf_{Af} was concentrated to 20 mg/ml in 10 mM MOPS and 1 mM FAD, pH 7.0, Bcd_{Af} to 15 mg/ml in 10 mM MOPS, pH 6.8, and 1 mM FAD. Crystallization experiments were performed with the sitting drop method at 4 and 18 °C using a CrystalMation™ system from Rigaku and commercially available screens. Initial conditions for both enzymes were found in the PACT++ screen, which were further optimized (see Table 1). Data were collected at the PXII beamline at the Swiss-Light-Source in Villigen and processed with XDS (23). Phase determination is described in Table 1. Crystallization of the Etf_{Af}-NAD^+ complex was performed under related conditions (Table 1). The structure of Bcd_{Af} was solved by molecular replacement using the coordinates of Bcd of *Megasphaera elsdenii* (1buc) as model (24). Model errors were corrected within COOT (25). The refinement was performed with REFMAC5 (26). Data quality and refinement statistics were listed in Table 1. Figs. 3–7 were generated with PyMOL (Schrödinger, LLC).

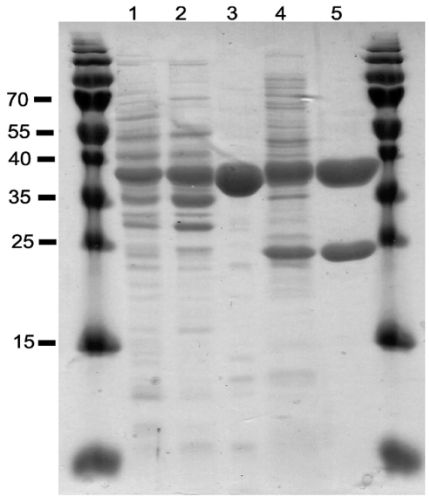

FIGURE 1. **SDS-PAGE of native Bcd_{Af} (*lanes 1–3*) and recombinant His-tagged Etf_{Af} (*lanes 4* and *5*) at different purification stages.** Each lane contained 10 μg of protein. *Lane 1*, cell-free extract of *A. fermentans*. *Lane 2*, supernatant after ammonium sulfate precipitation at 60% saturation. *Lane 3*, DEAE-Sepharose eluate. *Lane 4*, cell-free extract of *E. coli* producing Etf_{Af}. *Lane 5*, eluate from the nickel-nitrilotriacetic acid column. Etf_{Af} has an apparent molecular mass of 34 kDa for subunit α and 27 kDa for subunit β.

RESULTS AND DISCUSSION

Biochemical Characterization—To find out which of the two gene clusters encoding Etf_{Af} are expressed under the conditions of glutamate fermentation by *A. fermentans* VR4 (DSM 20731) (27), the protein was purified from a cell-free extract, kinetically characterized by a formazane producing NADH-dependent assay (specific activity 2.5 units/mg of protein) (12) and analyzed by N-terminal sequencing and peptide mapping with MALDI-TOF mass spectrometry for gene identification. Accordingly, Etf_{Af} is encoded by the genes *Acfer_0556* and *Acfer_0555*, composed of 340 and 263 amino acids for subunits α and β, respectively.

To obtain Etf_{Af} in higher amounts, we overproduced the enzyme with a C-terminal His tag at subunit α in *E. coli*. According to gel filtration, the pure protein (Fig. 1) is a heterodimer with a molecular mass of around 66 kDa (theoretically 37.6 + 28.4 kDa). Non-covalently bound FAD (and not AMP and other flavins such as riboflavin, riboflavin-5′-phosphate or hydroxylated flavins (28)) was identified by HPLC and MALDI-TOF analysis. Quantitative analyses using UV-visible spectroscopy (ϵ_{450} = 11.3 mM^{-1} cm^{-1}) (29) revealed about 0.7 FAD/heterodimer, which could be raised to 2 upon incubation with 1 mM FAD, which agrees well with the structural data (see below). Thereby the specific activity of the Etf_{Af} in the formazane assay increased 4-fold. Bcd of *A. fermentans* (Bcd_{Af}) was purified (Fig. 1) as homotetrameric flavoprotein (4 × 42 kDa) with a specific

Mechanism of Electron Bifurcation

activity of 20 units/mg of protein (21). Bcd_{Af} is encoded by the *Acfer_1477* gene (acyl-CoA dehydrogenase, 383 amino acids).

Kinetic Characterization—Although Etf_{Af} and Bcd_{Af} are stable under air, all the following experiments were performed in an anaerobic chamber under an atmosphere of 95% N_2 and 5% H_2, since ferredoxin and the reduced forms of flavin are oxygen sensitive. Incubation of catalytic amounts of Etf_{Af} and Bcd_{Af} with NADH and crotonyl-CoA caused oxidation of NADH at the low rate of 0.01 units mg^{-1} of Etf (units = μmol min^{-1}). However, upon addition of catalytic amounts of ferredoxin (1 μM) and hydrogenase the rate increased to 1.5 units mg^{-1}. The products of the reaction were besides NAD^+, butyryl-CoA (determined by MALDI-TOF mass spectrometry and HPLC) and molecular hydrogen (determined by gas chromatography (3)). Hence, Etf_{Af} + Bcd_{Af} catalyzed the reduction of crotonyl-CoA to butyryl-CoA coupled to the reduction of ferredoxin (Fd; Equation 1), whereby hydrogenase recycled the oxidized ferredoxin (Equation 2) resulting in Equation 3 (3).

$$\text{Crotonyl-CoA} + 2\,\text{NADH} + 2\,\text{Fd}^- \rightarrow \text{butyryl-CoA} + 2\,\text{NAD}^+ + 2\,\text{Fd}^{2-} \quad \text{(Eq. 1)}$$

$$2\,\text{Fd}^{2-} + 2\,\text{H}^+ \rightleftharpoons 2\,\text{Fd}^- + \text{H}_2 \quad \text{(Eq. 2)}$$

$$\text{Crotonyl-CoA} + 2\,\text{NADH} + 2\,\text{H}^+ \rightarrow \text{butyryl-CoA} + 2\,\text{NAD}^+ + \text{H}_2 \quad \text{(Eq. 3)}$$

Omission of Etf_{Af}, Bcd_{Af}, ferredoxin, or crotonyl-CoA gave no activity. No reaction was observed when NADH was replaced by NADPH or crotonyl-CoA by butyryl-CoA. The required stoichiometry of NADH:crotonyl-CoA = 2.1 ± 0.1 was measured (Fig. 2*A*) with a solution of the CoA thioester, whose concentration was calibrated by a coupled NAD-dependent assay using β-oxidation enzymes from *A. fermentans* (14). Because Etf_{Af} and Bcd_{Af} are found as separated proteins in solution, a transient Bcd-Etf complex is sufficient to perform a bifurcation process.

Titration of Etf_{Af} with Bcd_{Af} increased the rate of NADH oxidation until a molar ratio of 2 Etf:1 Bcd (tetramer) was reached (Fig. 2*B*). This optimal ratio agrees well with the molecular masses of the stable clostridial Bcd-Etf complexes of *Clostridium kluyveri* (3), *Clostridium difficile* (30), and *C. tetanomorphum* (31, 32) with compositions of Etf_1-Bcd(dimer) or Etf_2-Bcd(tetramer) (see also Fig. 5) (5).

The optimal ratio of ferredoxin:Etf: tetrameric Bcd was determined to be 2:1:0.5 based on the titration of the Etf_{Af}-Bcd_{Af} system with ferredoxin in the presence of hydrogenase (Fig. 2*C*). These data suggest that during steady state ferredoxin takes up only one electron and hands it over to the hydrogenase. Most likely the electron acceptor is the semi-reduced form (Fd^-), which is completely reduced to Fd^{2-} (see Equations 1 and 2). This behavior agrees well with the different redox potentials of the *A. fermentans* ferredoxin ($E_0' = -340$ for Fd/Fd^- and -405 mV for Fd^-/Fd^{2-}) (8).

The dependence of the NADH oxidation rate on the concentration of crotonyl-CoA followed Michaelis-Menten kinetics, K_m = 12 μM. By increasing the NADH concentrations the rate passed through a maximum already at about 70 μM NADH (Fig. 2*D*). This inhibition suggests equilibrium between the free proteins and their complex (Etf_{Af} + Bcd_{Af} ⇌ Etf_{Af}-Bcd_{Af}) whereby some of the free Etf_{Af} gets fully reduced by NADH (see spectroscopic characterization) and cannot participate in electron bifurcation. In contrast, the tight non-dissociating bifurcating Etf-Bcd complex of *C. difficile* exhibits normal Michaelis-Menten kinetics for NADH, K_m = 145 μM (30).

Using stoichiometric amounts of ferredoxin (15 μM) in the absence of hydrogenase, identical spectra in the range of 400–500 nm were observed, regardless of whether the reduction was performed by dithionite or by NADH and crotonyl-CoA mediated by Etf_{Af}-Bcd_{Af} (Fig. 2*E*). As demonstrated for other flavin-based electron bifurcating systems (5, 6, 30), ferredoxin reduction is almost 100% indicating a tight energetic coupling between ferredoxin and crotonyl-CoA reduction. Limiting amounts of crotonyl-CoA under these conditions resulted in the reduction of 1 mol of ferredoxin/mol of crotonyl-CoA; hence at equilibrium the completely oxidized Fd accepts two electrons, one by each [4Fe-4S] cluster. In contrast to flavodoxin (33) the fully oxidized and half-reduced ferredoxins absorb at the same wavelength and therefore cannot be distinguished spectroscopically.

Structural Characterization—The structural basis of FAD-based electron bifurcation requires information about (i) the proteins Etf containing α-FAD and β-FAD, and Bcd containing Dh-FAD, (ii) the complexes of Etf-NAD^+, Etf-ferredoxin, and Etf-Bcd, as well as (iii) the electron transfer routes between the redox centers.

Overall Structure of Etf_{Af}—Structural analysis of recombinantly produced Etf_{Af} resulted in an R/R_{free} factor of 16.1/19.1% at 1.6-Å resolution (see Table 1). As crystallization was performed under aerobic conditions without reducing agents, both FADs are oxidized. Architecturally, heterodimeric Etf is composed of three domains: domains I (5–199) and II (215–340) from subunit α and domain III (1–219) from subunit β (Fig. 3*A*). A comparison with the structurally related electron-accepting Etfs (34–36) is presented in Fig. 3*B*. Domains I and III, essentially sharing the same fold (root mean square deviation of 4.6 Å; 208 C_α atoms used), consist of an α/β structure and a tightly associated β-meander. The polypeptides of subunits α and β proceed by strands 200:213 and 220:228 that enlarges the β-meander of the respective other subunit to a four-stranded antiparallel β-sheet. The major difference between domains I and III is an exposed β-hairpin-like segment following strand 2:7 of domain III (Fig. 3*A*). Domain II of subunit α is composed of a flavodoxin-like fold enlarged by a sixth strand and one helix from subunit β termed as the C-terminal arm (229–262) (Fig. 3*A*). Domains I and III are tightly associated (contact area of 4200 $Å^2$). Domain II sits above this base in a shallow bowl and is hung up on opposite sides by the flexible linker connecting domains I and II (B-factor 210:213: >50 $Å^2$) and the mentioned C-terminal arm of subunit β (Fig. 3*A*). Domains I + III and domain II are only loosely attached via a layer of solvent molecules mostly visible in the electron density at 1.6 Å but only by a few direct non-covalent polypeptide interactions.

α-FAD Binding—The completely occupied, non-covalently bound α-FAD is present in a stretched conformation (Fig. 4*A*) similar to that found in other Etf family members (34). The planar isoalloxazine ring embedded into a pocket at the domain

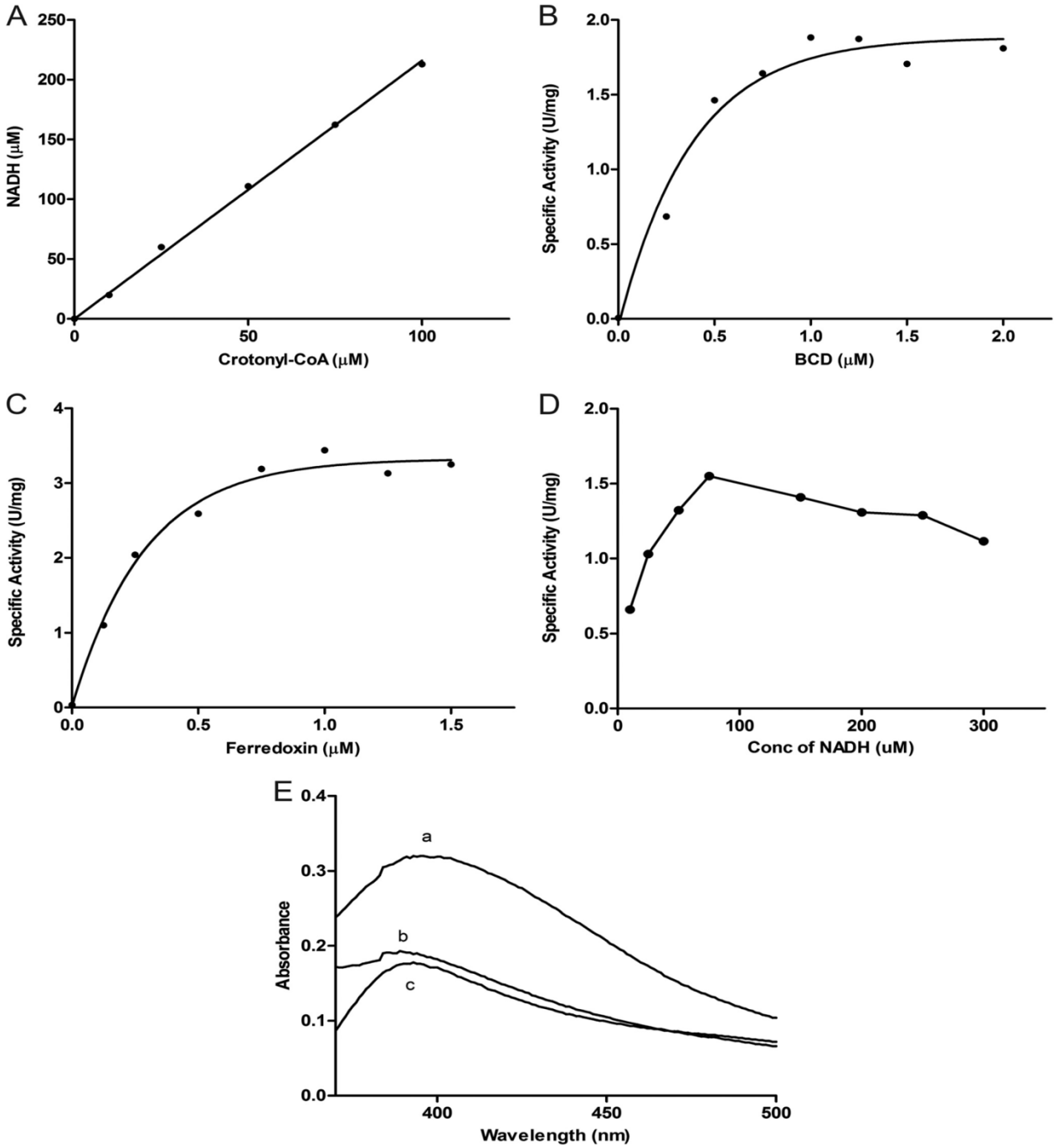

FIGURE 2. **Bifurcation assays.** See "Experimental Procedures" for details. *A,* stoichiometry between NADH and crotonyl-CoA of 2.1:1. The assays were performed with limiting amounts of crotonyl-CoA. *B,* dependence of the specific activity of NADH oxidation (μmol of NADH/mg of Etf_{Af}) on the concentration of the Bcd_{Af} monomer. Each assay contained 0.5 μM Etf_{Af}, 1 μM ferredoxin and hydrogenase (30 μg/ml). *C,* dependence of the specific activity of NADH oxidation (μmol of NADH/mg of Etf_{Af}) on the concentration of ferredoxin used in the assay. Each assay contained 0.5 μM Etf_{Af}, 1 μM Bcd_{Af} monomer and hydrogenase; K_m (ferredoxin) = 0.2 μM. *D,* dependence of the specific activity of NADH oxidation (μmol of NADH/mg of Etf_{Af}) on the concentration of NADH used in the assay. Each bifurcation assay contained 0.5 μM Etf_{Af}, 1 μM Bcd_{Af} monomer, 1 μM ferredoxin and hydrogenase. *E,* complete reduction of 15 μM ferredoxin in the bifurcation assay without hydrogenase. (*a*) Spectrum of oxidized ferredoxin before starting the bifurcation; (*b*) excess dithionite was added; (*c*) after bifurcation has terminated due to limiting amounts of ferredoxin.

II-III interface is flanked from the *re*-face by Arg-α253 and Tyr-β40 and from the *si*-face by Gln-α269, Gln-α289, and His-α290 (Fig. 4*A*). In contrast to the other structurally characterized Etfs, the guanidinium group of Arg-α253 is oriented coplanar to the isoalloxazine ring and interacts with subunit β via Tyr-β40, Asp-β182 (solvent-mediated) and via Arg-β173. Both gua-

Mechanism of Electron Bifurcation

TABLE 1
Crystallization conditions and x-ray analysis statistics

Data set	Etf_{Af}	Etf_{Af} (Hg edge)[a]	Etf_{Af} + NAD^+	Bcd_{Af}
Crystallization Conditions[b]	18% PEG 3350, 0.1 M Bistris propane, pH 7.5 0.1 M Na formate 1 mM FAD	18% PEG 3350, 0.1 M Bistris propane, pH 7.5 0.1 M Na formate 1 mM FAD	17% PEG 3350, 0.1 M Bistris propane, pH 7.5 0.1 M Na formate 1 mM FAD	225% PEG1500, 10% SPG buffer, pH 9.0
Protein concentration	20 mg/ml	20 mg/ml	20 mg/ml	15 mg/ml
Temperature	4 °C	4 °C	4 °C	4 °C
Soaking conditions		0.1 mM CH_3HgAc, 5 h		
Freezing conditions	+25% (w/v) glycerol	+25% (w/v) glycerol	+25% (w/v) glycerol	25% (v/v) 1,2-propandiol
Data collection				
Wavelength (Å)	1.0	1.006	1.0	0.9999
Space group	$P2_12_12_1$	$P2_12_12_1$	$P2_12_12_1$	$P2_12_12$
Unit cell parameter				
a, *b*, *c* (Å)	80.2, 84.9, 106.7	78.2, 85.7, 106.6	79.5, 84.8, 106.4	109.1, 141.4, 64.1
Number of molecules per asymmetric unit	1	1	1	1
Resolution range (Å)	30.0-1.6	30.0-3.0	30.0-1.45	30.0-1.8
(highest shell)	(1.7-1.6)	(3.1-3.0)	(1.55-1.45)	(1.9-1.8)
Redundancy	2.4 (2.4)	4.6 (4.8)	3.9 (4.0)	7.9 (8.1)
Completeness (%)	93.2 (91.8)	99.6 (99.8)	97.6 (96.4)	99.9 (100)
R_{merge} (%)	6.9 (48.8)	9.6 (150.9)	4.5 (63.5)	14.4 (78.8)
$I/\sigma(I)$	11.8 (2.5)	11.8 (1.5)	15.6 (3.0)	13.2 (3.9)
Refinement				
Resolution limit (Å)	1.6-50.0		1.45-50.0	1.8-50.0
(highest shell)	1.6-1.64		1.45-1.49	1.8-1.84
R_{work}/R_{free} (%)	16.1/19.1		15.1/20.8	15.3/18.3
(highest shell)	26.4/28.1		24.5/37.5	22.0/25.2
Root mean square deviation bond lengths (Å)	0.024		0.023	0.022
Root mean square deviation bond angles (°)	2.3		2.36	2.13
Average *B* ($Å^2$)	18.2		23.3	18.7

[a] Phase determination. Initial SIRAS phases were obtained from native Etf data and from measurements of a crystal soaked with CH_3HgAc using SHELXD (50), SHARP (51), and SOLOMON (52). After phase determination the model was built automatically at 2.5-Å resolution with PHENIX (53) supported by a model of human Etf that could be correctly placed into the unit cell and further improved at 1.6-Å resolution with ARP/WARP (54).
[b] Applied crystallization screens: JBScreen HTS I+II, pentaerythritol, PACT++ (JBS), JCSG Core Suite I–IV (Qiagen), and PGA (MDL).

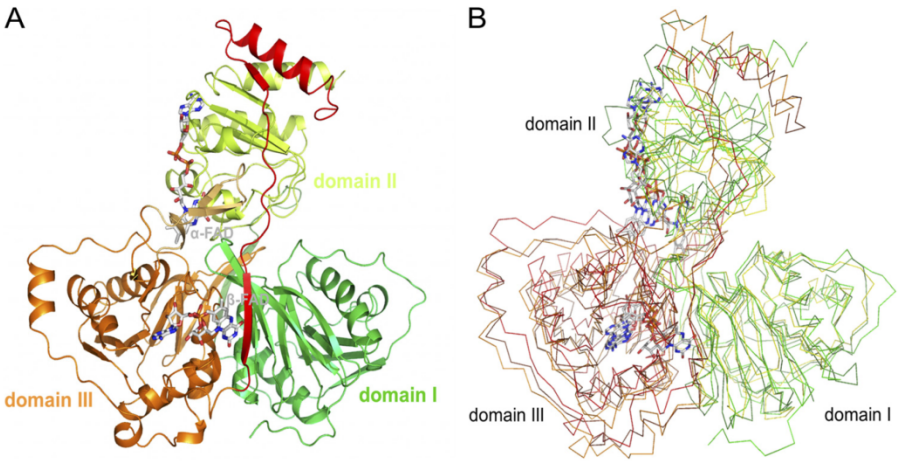

FIGURE 3. **Structures of Etf.** *A*, Etf of *A. fermentans*. Subunit α is composed of domains I (*green*) and II (*yellow green*) and subunit β of domain III (*orange*), the β-hairpin (*light orange*), and the C-terminal arm (*red*). α-FAD and β-FAD are drawn as stick models with the carbons in *gray*. *B*, structures of Etf_{Af}, human Etf, and *Methylophilus methylotrophus* Etf superimposed. Domains I (*green*, *yellow*, *forest*; 5–199. Etf_{Af} numbering) and II (*green*, *yellow*, *forest*; 215–340) form subunit α and domain III (*orange*, *brown*, *red*; 1–219) forms subunit β.

nidinium groups are stacked to each other (Fig. 4*A*). The N5 atom of the dihydropyrazine ring is completely shielded from bulk solvent and hydrogen bonded to Ser-α270-OG. The N1-C2 = O group of the pyrimidine ring is hydrogen bonded to the 4′-OH of ribityl, Val-α267-O, His-α290-ND1, and Arg-α253-NH, respectively, the latter being positioned at the N-terminal end of helix 253:258. These interactions, well conserved in Etfs (34–36) are considered a major structural feature to neutralize the negatively charged $FAD^{\cdot-}$ and $FADH^-$ states (Fig. 4*A*) reflected in high redox potentials of the α-FAD/α-$FAD^{\cdot-}$ couple ($E_0' = +81$ mV for Etf_{Me}) and in a weakened form also of the α-$FAD^{\cdot-}$/α-$FADH^-$ couple ($E_0' = -136$ mV for Etf_{Me}) (37, 38). The higher value of the latter couple is attributable to the unfavorable Ser-α270-OG-N5(protonated) interactions. Etf_{Me} is the Etf of *M. elsdenii*, a relative of *A. fermentans*, which also contains two FAD per heterodimer and shares 49%

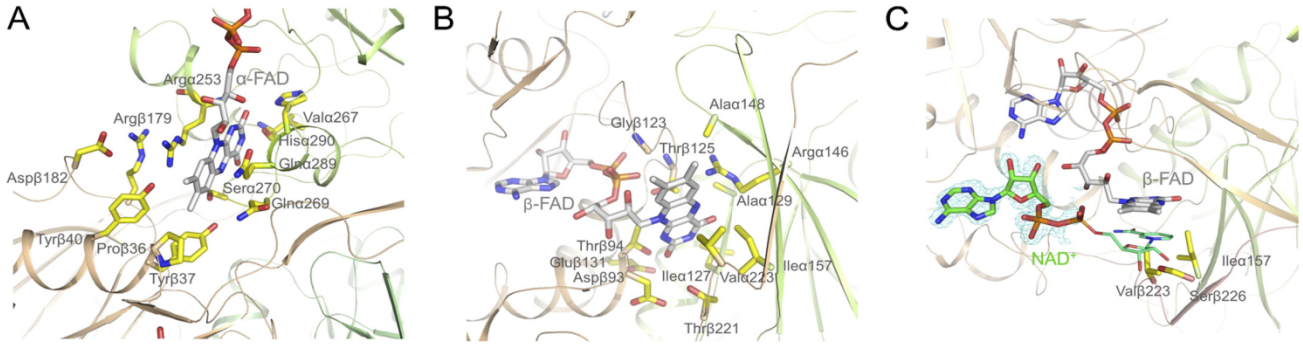

FIGURE 4. *A*, binding mode of α-FAD. The isoalloxazine ring is located between domains II and III. One side of α-FAD is attached along the C-terminal side of the parallel β-sheet of domain II and the opposite side is largely exposed to bulk solvent. N5 is hydrogen-bonded to Ser-270-OG. *B*, binding mode of β-FAD. The isoalloxazine ring of compressed β-FAD primarily binds to domains III and I. Arg-α146-NH_2 is projected toward the bottom of the isoalloxazine ring and interacts with N5 of the isoalloxazine ring. *C*, binding of NAD^+. The ADP part (in stick mode) of NAD^+ (carbons in *green*) is predominantly fixed by its contacts to β-FAD. The nicotinamide-ribose part (in line mode) is disordered but can be modeled to the *re*-face of the isoalloxazine. Ile-α157, Val-β223, and Ser-β226 interfere with the nicotinamide-ribose in the conformation capable for hydride transfer and have to be displaced upon NADH binding. The electron density (in *blue*) is contoured at 1.5.

sequence identity. Altogether, α-FAD is not attractive as bifurcating flavin due to the high redox potential and the accompanied weak reduction power.

β-FAD Binding—The 1.6-Å electron density of Etf_{Af} revealed that the non-covalently bound β-FAD is also completely occupied but arranged in a compressed S-shaped conformation at the C-terminal side of the central β-sheet of domain III (Figs. 3*A* and 4*B*). The AMP binding mode of Etf_{Af} corresponds to that of the other structurally characterized Etfs (34) (Fig. 4*B*). The isoalloxazine ring protrudes beyond domain III toward domain I (Fig. 3*A*) with its nonpolar xylene ring being largely exposed to bulk solvent. The planar tricyclic ring is flanked from the *si*-face by Thr-β25, Gly-β123, Arg-α146, and Ala-α148 and from the *re*-face by Ile-α157, Thr-β221, and Val-β223 (Fig. 4*B*). The pyrimidine ring of β-FAD and the polypeptide are hydrogen-bonded via N3 and Leu-α127-O, O4 and Ala-α129-NH as well as O2 and Thr-β94-NH and -OG1, the latter being located at the positively charged N-terminal side of helix 94:108. Interestingly, O2 is further contacted by the carboxylate groups of Asp-β93 and Glu-β131 (exchanged in human Etf by Gly and Lys), which destabilizes a negatively charged state of the isoalloxazine ring (Fig. 4*B*). This finding is in agreement with the rather low redox potential ($E_0' = -280$ mV) of the β-FAD/β-$FADH^-$ couple and the observation that in Etf_{Me} β-FAD binds stronger than α-FAD, and α-$FADH^-$ stronger than β-$FADH^-$ (38). An important function is also attributed to Arg-α146-NH_2 in adjusting an even lower β-FAD/β-$FADH^•$ potential as it forms a stronger hydrogen bond with N5 in β-FAD than in β-$FADH^•$ and β-$FADH^-$. As a result, β-FAD appears to be suitable as bifurcating flavin.

Structure of the Etf_{Af}-NAD^+ Complex—Binding of NAD^+ was characterized on the basis of an Etf_{Af}-NAD^+ structure at 1.5-Å resolution after co-crystallizing Etf_{Af} and NAD^+ (Table 1). Its electron density only exhibits the ADP part, whereas the ribose-nicotinamide part is completely disordered (Fig. 4*C*). NAD^+ appears to be primarily fixed to its binding site by interactions with β-FAD. A hydrogen bond is formed between the 2′-OH of the AMP-ribose of NAD^+ and the ribitol hydroxyl groups of β-FAD. The diphosphate and ribose fraction of ADP is largely exposed to bulk solvent, whereas the adenine ring is sandwiched between the loops following strands 56:61 and 80:84. In agreement with the kinetic data, NADPH cannot replace NADH due to a collision between the 2′-phospho group and the protein scaffold.

Considering the ADP moiety as anchor point, the ribose-nicotinamide moiety can be reasonably modeled to the *re*-side of β-FAD in a stacking arrangement thereby underlining the biological relevance of the detected ADP as part of the NAD^+ binding site. C4 of the nicotinamide ring and N5 of the isoalloxazine ring can be approached to around 3.5 Å (Fig. 4*C*) but the ribose-nicotinamide part clashes with the side chains of Ile-β157, Val-β223, and Ser-β226. As demonstrated by spectroscopic characterizations (see next paragraph) NADH reduces β-FAD in the absence of ferredoxin or Bcd and consequently can displace them. This induced displacement by NADH of about 3 Å might significantly affect the conformation of the C-terminal arm of subunit β, the β-meander of subunit α (domain I), and the extended β-hairpin following strand 2:7 of domain III (Fig. 4*C*).

Structure of Bcd_{Af}—The Bcd_{Af} structure was established at 1.9-Å resolution (R/R_{free} = 15.3/18.3%) based on the *M. elsdenii* enzyme (24) as a model for molecular replacement calculations. The architecture of Bcd_{Af} and Bcd of *M. elsdenii* corresponds to each other with a root mean square deviation of 0.6 Å (95% of the C_α atoms) and a sequence identity of 66%. Bcd_{Af} is a homotetramer built up of a dimer of two tightly associated dimers (Fig. 5). Each subunit is composed of an amino-terminal α-helical bundle domain, a medial seven-stranded β-sheet domain, and a second α-helical domain at the carboxyl terminus. Dh-FAD is embedded between the two latter domains and its conformation and polypeptide surrounding is virtually identical in the two enzymes. Although no substrate analog was supplemented to the Bcd_{Af} solution, CoA persulfide (39) was bound to the *re*-side of the isoalloxazine ring.

Modeled Structures of the Etf_{Af}-Ferredoxin and Etf_{Af}-Bcd_{Af} Complexes—The ferredoxin of *C. acidi-urici* (40) (the structure of the closely related ferredoxin of *C. tetanomorphum* used in this work is not known) can be docked to domain III of Etf in a manner that the proximal [4Fe-4S] cluster and the isoalloxazine

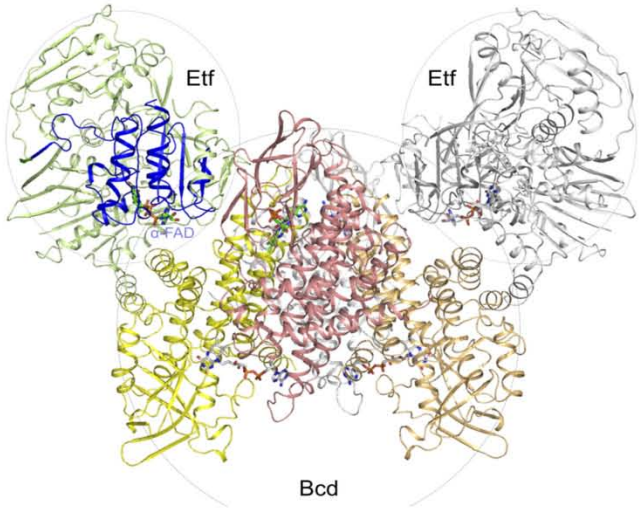

FIGURE 5. **Modeling of the Etf_{Af} and Bcd_{Af} complex.** The Etf_{Af} and Etf_{Af} and Bcd_{Af} structures were separately determined. The first Etf is drawn in *green* (domains I + III) and in *blue* (domain II); the second Etf in *gray*. The subunits of tetrameric Bcd are shown in *yellow*, *orange*, *red*, and *gray*. Docking is based on the structure of the Etf-MCAD structure (PDB code 2A1T). The isoalloxazine rings of α-FAD of Etf_{Af} and Dh-FAD of Bcd_{Af} are more than 30 Å apart from each other. Therefore, a productive electron transfer requires a large-scale conformational change of domain II or a different Etf_{Af}-Bcd_{Af} interface.

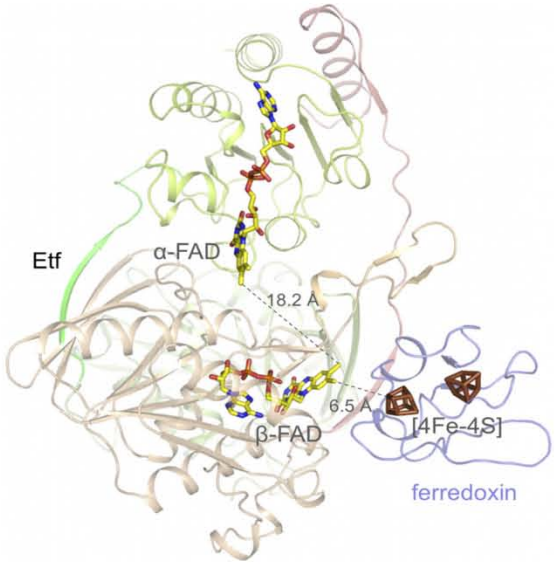

FIGURE 6. **Docking of ferredoxin of *C. acidici-urici* to Etf_{Af}.** Ferredoxin was modeled to domain III in a manner that the distance between its [4Fe-4S] cluster and the isoalloxazine ring of the bifurcating β-FAD is minimal. The resulting edge-to-edge distance at about 6.5 Å allows a rapid electron transfer. It is unclear whether NAD^+ is released to bulk solvent prior to bifurcation. This short distance is adjustable because the isoalloxazine of β-FAD directly sits at the protein surface. Ferredoxin could also be attached to domain II at the Etf_{Af}-Bcd_{Af} interface (not shown) to provide a suitable electron transfer distance between the redox centers. However, the distance between the [4Fe-4S] cluster and α-FAD is about 14 Å significantly longer than that between the [4Fe-4S] cluster and β-FAD and thus the electron transfer is less likely.

ring of β-FAD are below 8 Å apart from each other in the presence of NADH and nearly in van der Waals contact in its absence (Fig. 6).

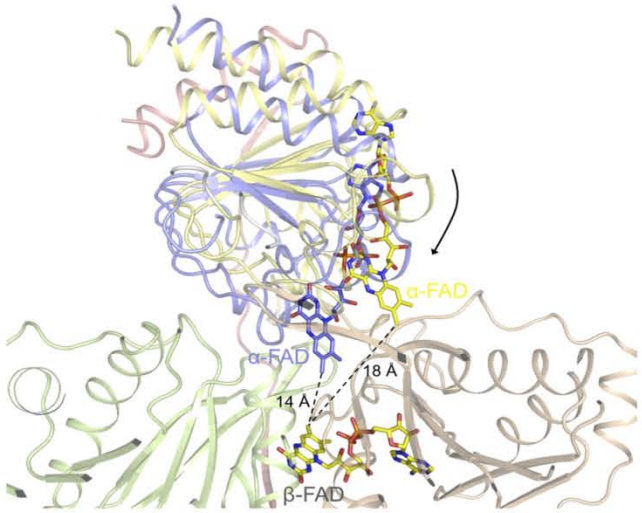

FIGURE 7. **Modeling of domain II of Etf_{Af} in a conformation in that the distance between the isoalloxazine rings of α-FAD and β-FAD are about 14 Å sufficient for an effective electron transfer.** Because of the soft interface between the base of domain II and the domains I + III, a rotation of domain II is not severely restricted. It can also not be excluded that, alternatively, selective electron transfer between α-FAD and β-FAD is provided by fixing them in a distance that the rate is determined by the polypeptide tuned one-electron redox potentials of the isoalloxazine rings.

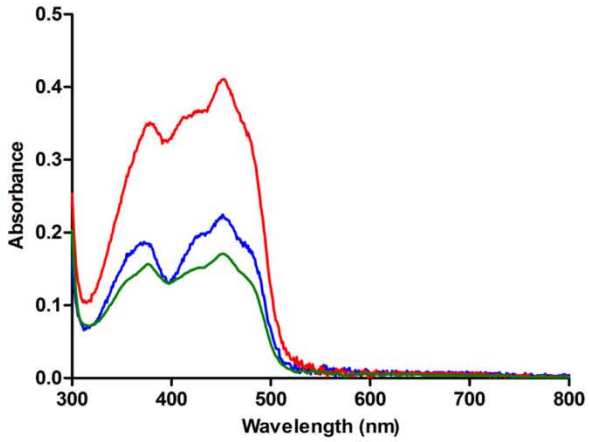

FIGURE 8. **UV-visible absorption spectrum of the electron transferring flavoprotein of *A. fermentans*.** Etf_{Af} as isolated from *E. coli* (*green*), reconstituted Etf_{Af} (*red*), and KBr-treated Etf_{Af} (*blue*).

The Etf_{Af}-Bcd_{Af} complex can be modeled (Fig. 5) on the basis of the MCAD-Etf (medium chain acyl-CoA dehydrogenase-Etf from *Homo sapiens*) complex structures (36, 41). After superposition of Etf_{Af} and Bcd_{Af} onto the MCAD-Etf complex, the distance between α-FAD and Dh-FAD of Bcd_{Af} is more than 30 Å. Different Etf_{Af}-Bcd_{Af} contact areas were tested, but no orientation was found that meets the 14 Å distance criteria for an appropriate electron transfer rate between α-FAD and Dh-FAD (42). Therefore, we suggest a reorientation of domain II analogous to that observed between human Etf in the isolated and in complex with MCAD (43). The distance between the two FAD can thus be shortened to about 10 Å.

Electron Transfer between α-FAD and β-FAD—Based on the described findings, the one-electron transfer steps between

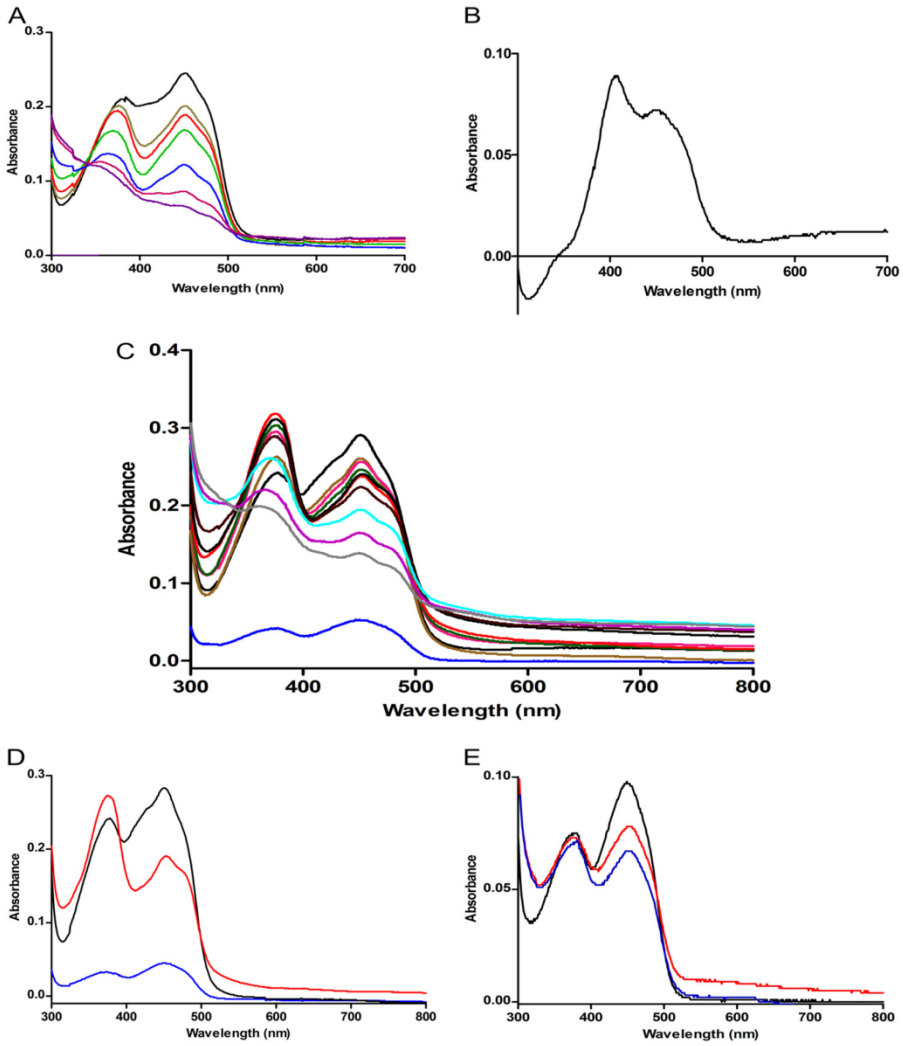

FIGURE 9. **Formation of stable red anionic FAD semiquinones.** *A*, to 10 μM Etf NADH was added stepwise: 0 (*black line*), 4 (*khaki*), 6 (*red*), 10 (*blue*), 14 (*green*), 18 (*pink*), and 20 μM (*magenta*). *B*, difference spectrum between unreduced Etf_{Af} − Etf_{Af} reduced with 10 μM NADH. It shows the UV-visible spectrum of α-FAD bound to Etf_{Af}. *C*, to 10 μM Bcd-subunit (*blue*) and 10 μM Etf, NADH was added stepwise: 0 (*black line*), 2.5 (*brown*), 5 (*pink*), 7.5 (*green*), 10 (*red*), 12.5 (*black*), 15 (*dark brown*), 17.5 (*light blue*), 20 (*magenta*), and 22.5 μM (*gray*). *D*, same as *C* but instead of NADH, 100 μM butyryl-CoA was added. *E*, to 20 μM Bcd-subunit (*black*), 100 μM butyryl-CoA (*red*) or 200 μM butyryl-CoA (*blue*) were added.

β-FAD and α-FAD are a necessary prerequisite to explain the experimentally observed coupling between NADH oxidation at β-FAD and crotonyl-CoA reduction at Bcd mainly attached to domain II carrying α-FAD. However, the isoalloxazine rings of β-FAD and α-FAD have an edge-to-edge distance of 18 Å in the present Etf_{Af} structure (Fig. 3*A*), which appears to be too long for an efficient electron transfer at biologically relevant rates (42). The Etf_{Af} structure offers as solution a rigid-body movement of domain II relative to domains I + III, which reduces the distances between the isoalloxazine rings to about 14 Å (Fig. 7). These conformational changes are realistic because of the soft solvent-mediated domain II-(I + III) interface and their realization in the related Etf-MCAD and Etf-TMADH systems (36, 41). It might be triggered by productive NADH binding conveyed to domain II and/or by Bcd binding (43).

Spectroscopic Characterizations—The UV-visible absorption spectrum of recombinant Etf_{Af} as isolated from *E. coli* containing 0.7 FAD/heterodimer is shown in Fig. 8. Upon overnight incubation at 4 °C with 1 mM FAD and removal of the excess FAD by gel filtration the spectrum changes to a much higher absorption of the two peaks at 375 and 450 nm and a less deep trough between the two peaks (Fig. 8). This reconstituted Etf_{Af} contained 2 FAD/heterodimer. Stepwise addition of NADH in 2.0 μM amounts to 10 μM reconstituted Etf_{Af} (occupied with 20 μM FAD) under anoxic conditions and in the absence of Bcd and ferredoxin (Fig. 9*A*) revealed a shift of the peak at 375 to 370 nm and a decrease of the 450 nm peak resulting in an equal intensity to the 370 nm peak (at 4–6 μM NADH). We attribute this 370 nm peak to a stable red anionic semiquinone (44). After addition of about 10 μM NADH the spectrum corresponds to a

Mechanism of Electron Bifurcation

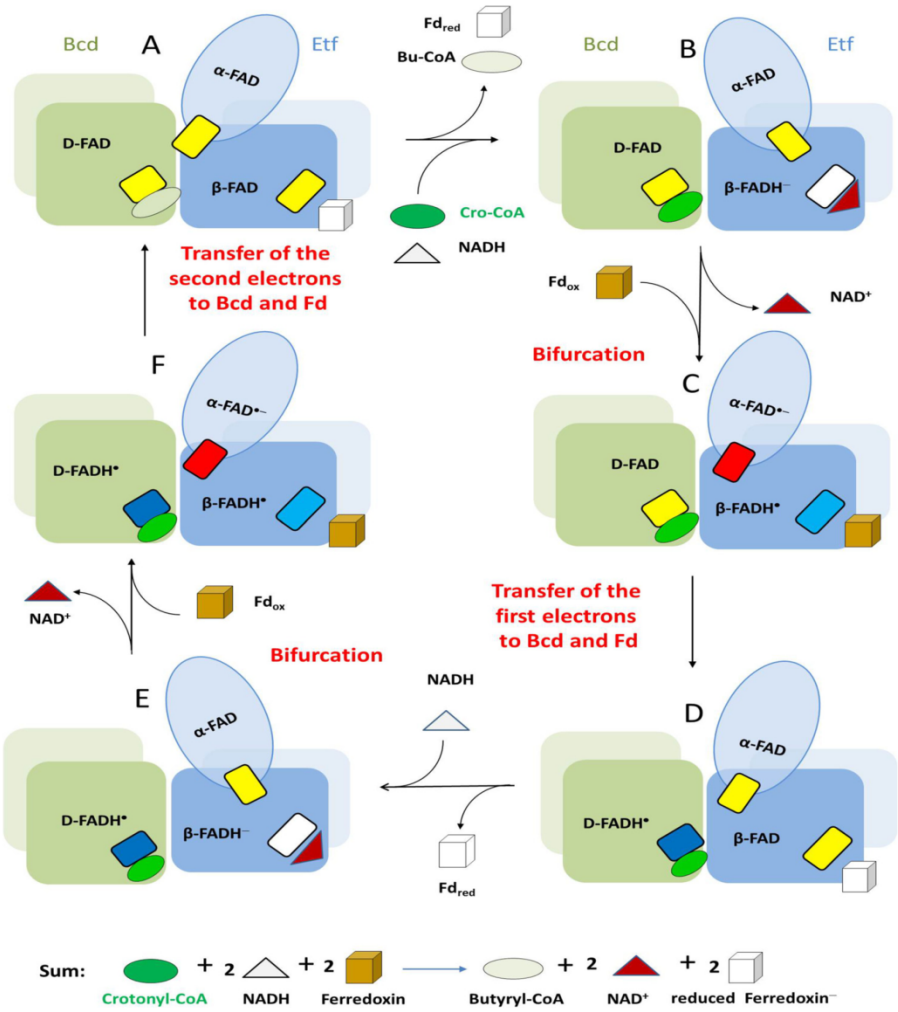

FIGURE 10. **Proposed mechanism of the flavin-based electron bifurcation process of the Etf/Bcd system on a structural ground.** The figure shows the Bcd dimers (*green* and *gray* and *light green*) interacting with Etf (*light blue*, domain I; *medium blue*, domain II; *dark blue*, domain III). We propose that domain II changes its position relative to domains I and III. The *small rectangles* depict FAD in the quinone state (*yellow*), anionic semiquinone state (*red*), neutral semiquinone state (*light blue* in Etf and *dark blue* in Bcd), and hydroquinone state (*white*). For the sake of simplicity addition of one electron to oxidized ferredoxin (*brown*) yields reduced ferredoxin (*white*). The cycle starts with *A* containing three oxidized FAD. Butyryl-CoA and reduced ferredoxin, the products of the last turnover, are exchanged by the substrates crotonyl-CoA and NADH. As soon as bound, NADH immediately reduces β-FAD to β-FADH$^-$ (*B*). The formed NAD$^+$ is released and ferredoxin binds. Bifurcation concomitant with a conformational change of domain II yields β-FADH$^\bullet$ and α-FAD$^{\bullet-}$, which swings to Dh-FAD (*D-FAD*) (*C*). Two one-electron transfers to ferredoxin and to Bcd end the first half of the cycle (*D*). Release of the first reduced ferredoxin and binding of the second NADH starts the second half of the cycle (*E-F-A*), the only difference being the action of Dh-FADH$^\bullet$ rather than Dh-FAD as electron acceptor in Bcd. After the second bifurcation and electron transfers to ferredoxin and Dh-FADH$^\bullet$, the second reduced ferredoxin and butyryl-CoA are formed. It should be noted that only the α-FAD$^{\bullet-}$ has been shown experimentally. The existence of the two neutral semiquinones, β-FADH$^\bullet$ and Dh-FADH$^\bullet$, remains to be established. Also the binding order of NADH, crotonyl-CoA, and ferredoxin is without experimental evidence.

mixture of an oxidized and a reduced FAD. The unusual difference spectrum-oxidized half-reduced Etf_{Af} with maxima at 400 and 450 nm is shown in Fig. 9*B*. Complete reduction of the FAD content was achieved at around 20 μM NADH (NADH/FAD = 1.0). Very similar spectra were recently reported from Etf_{Me} (37, 38).

To remove the weakly bound FAD, the protein was mixed with an equal volume of 2 M KBr and washed in a Centricon (30 kDa cut off) two times with 1 M KBr, followed by 50 mM potassium phosphate, pH 6.8 (38). The KBr-treated Etf exhibited a spectrum with absorbance at 375 and 450 nm of only 50% of that of the reconstituted Etf. Hence one of the two FADs was completely removed. Furthermore, there was a deep trough between the two peaks, like that of free FAD. A very similar behavior has been described for Etf from *M. elsdenii* (Etf_{Me}) (37). Notably, titration of the KBr-treated Etf_{Af} (10 μM) with NADH indicated a progressive reduction of both peaks, without the transient formation of the anionic semiquinone. Complete reduction was achieved with 10 μM NADH.

In context of the structural results we concluded that Etf_{Af} contained a strongly bound β-FAD and a weekly bound α-FAD. Removal of α-FAD with KBr gave an Etf, whose β-FAD was smoothly reduced by NADH to β-FADH$^-$ without semiquinone intermediate. Upon reduction of the reconstituted Etf (2

FAD/Etf) by NADH, one electron of β-FADH$^-$ is further transferred to α-FAD yielding the stable anionic red semiquinone α-FAD$^{\cdot-}$ (44). The remaining electron on the presumably blue neutral semiquinone β-FADH$^{\cdot}$ is not observable at 590 nm (44). We postulate an immediate intermolecular oxidation of the unstable β-FADH$^{\cdot}$ by reducing α-FAD of another oxidized Etf_{Af} molecule to α-FAD$^{\cdot-}$. Hence, the intermolecular electron transfer from β-FADH$^{\cdot}$ to α-FAD should be faster than the intramolecular transfer of the second electron to α-FAD$^{\cdot-}$. The observations that the maximum of the peak at 370 nm was already reached at 0.5 NADH/2 FAD and that both FAD are located at the surface of the Etf_{Af} structure were compatible with an intermolecular electron transfer. Half-reduction of Etf_{Af} and Etf_{Me} (1 NADH/2 FAD) was interpreted as reduced α-FADH$^-$ and oxidized β-FAD (38), whereby the spectrum of α-FAD with a maximum at 400 nm turned out to be untypical for flavoproteins (Fig. 9*B*).

In the presence of 5 μM tetrameric Bcd_{Af} (20 μM Bcd subunit) and 10 μM Etf_{Af} the peak at 370 nm reached its maximum at a ratio of 1 NADH/Etf (Fig. 9*C*) in contrast to 0.5 NADH/Etf in the absence of Bcd. Moreover, the peak of α-FAD$^{\cdot-}$ at 370 nm rose much higher with than without Bcd_{Af}. Apparently, Bcd_{Af} binding (± crotonyl-CoA) to Etf_{Af} increases the concentration of α-FAD$^{\cdot-}$ by suppressing its further reduction to α-FADH$^-$ to some extent and/or changes its surrounding. The rotation of domain II predicted on the basis of the presented structural data would increase the distance between β-FAD and α-FAD and turn α-FAD from an accessible to a more shielded position. This reorientation might also implicate a decrease of the extremely high redox potential $E_0' = +81$ mV of α-FAD/α-FAD$^{\cdot-}$ (for Etf_{Me}) to ensure an electron transfer from α-FAD$^{\cdot-}$ to Dh-FAD and eventually to crotonyl-CoA ($E_0' = -10$ mV). An increased peak at 370 nm was also achieved by adding butyryl-CoA to Etf_{Af} + Bcd_{Af} instead of NADH (Fig. 9*D*). Obviously electrons can also flow in the reverse direction generating α-FAD$^{\cdot-}$. Thus, Etf_{Af} can also act as an electron carrier like the AMP containing Etfs. In a control experiment with Bcd alone no anionic semquinone was observed (Fig. 9*E*).

The additional absorbance increase between 500 and 700 nm (Fig. 9, *C–E*) could be due to an extremely broad band of a neutral semiquinone in Bcd, although the absorption maximum at 590 nm (44) is missing. A similar featureless band was observed with the FAD-containing 4-hydroxybutyryl-CoA dehydratase after addition of the substrate crotonyl-CoA (45). Concomitantly, EPR spectroscopy detected the formation of a neutral semiquinone (46, 47). Reduction of the dehydratase by light or with dithionite, however, gave the "normal" spectrum of a semiquinone with a maximum at 590 nm.

Proposed Mechanism—The reaction starts with a hydride transfer from NADH to the *re*-side of β-FAD of Etf_{Af} forming β-FADH$^-$ (Fig. 10, *A* and *B*). Taking the two-electron redox potential of −280 mV for β-FAD/β-FADH$^-$ (38), bifurcation could lead to estimated one-electron potentials downhill to α-FAD of about −60 mV and uphill to ferredoxin of about −500 mV. The one-electron transfer from β-FADH$^-$ to α-FAD is thermodynamically feasible and presumably requires a reorientation of domain II to reduce the distance between the two isoalloxazine rings from 18 to 14 Å (Fig. 7). Simultaneously or subsequently the remaining β-FADH$^{\cdot}$, whose redox potential has dropped to <-500 mV, donates the other electron to the nearby ferredoxin (Fig. 10, *C* and *D*). See Fig. 6 for the predicted proximity between its [4Fe-4S] cluster and the isoalloxazine of β-FAD.

This electron flow from β-FADH$^{\cdot}$ to ferredoxin is only accomplished if the thermodynamically more favorable electron transfer to α-FAD$^{\cdot-}$ is prevented. Therefore, after the first electron transfer to α-FAD, we postulate a rotation of domain II toward the FAD binding site of Bcd_{Af} based on spectroscopic and structural data. This conformational change, concomitantly, also reduces the distance between α-FAD$^{\cdot-}$ and Dh-FAD from about 30 to about 10 Å according to modeling studies with the determined Etf_{Af} and Bcd_{Af} structures (Fig. 5) on the basis of the reported Etf-MCAD structure (41). Thus, α-FAD embedded into the weakly associated domain II serves as a shuttle between the electron-donating β-FADH$^-$ and the electron-accepting Dh-FAD. How the shuttle process is coordinated remains open. According to the presented data and the well explored Etf/acyl-CoA dehydrogenase systems (48), Bcd binding but also productive NADH, ferredoxin, and crotonyl-CoA binding might trigger domain II rearrangement. Interestingly, the electron transfer between the semiquinone in the bifurcating bc_1 complex to the low potential heme b_L is also ensured by an interruption of the second electron transfer between ubiquinone and the high potential [2Fe-2S] cluster because of a conformational change of the Rieske protein (49).

After reorientation of domain II, α-FAD$^{\cdot-}$ donates an electron to Dh-FAD forming presumably Dh-FADH$^{\cdot}$ (Fig. 10, *C* and *D*) (19). Repetition of this process affords a second reduced ferredoxin (Fd^-) or Fd^{2-} and the generated FADH$^-$ of Bcd transfers a hydride to crotonyl-CoA forming butyryl-CoA (Fig. 10, *E-F-A*).

The mechanism presented for flavin-based electron bifurcation in the Etf_{Af}/Bcd_{Af} system can be extended to the other systems. Most likely, their flavin functions as β-FAD and the low-potential ferredoxin can be closely attached to it. Interestingly, in most cases α-FAD has been replaced by iron-sulfur clusters that should have potentials higher than that of ferredoxin and in the same range than that of the terminal high-potential electron acceptors. It might be difficult to tune a flavin in a way that it works in the other systems. The same arguments may explain the presence of the Rieske iron-sulfur cluster in the bifurcating bc_1 complex of the respiratory chain.

Acknowledgments—We thank Professor Rolf K. Thauer (MPI of terrestrial Microbiology) for helpful discussions, Professor Hartmut Michel (MPI of Biophysics) for continuous support, the Biochemisches Institut, Universität Giessen, for the determination of the N-terminal sequences of Etf, Yvonne Thielmann and Barbara Rathmann of the Core Center (MPI of Biophysics) for performing initial crystallization screenings and the staff of the Swiss-Light-Source, Villigen, for help during data collection, Dr. Seigo Shima (MPI of terrestrial Microbiology) for help in flavin identification. N. P. C. acknowledges Dr. Anutthaman Parthasarathy (Stanford University) and Dr. Ankan Banerjee (MPI of terrestrial Microbiology) for constant encouragement.

REFERENCES

1. Mitchell, P. (1975) The protonmotive Q cycle. A general formulation. *FEBS Lett.* **59,** 137–139
2. Herrmann, G., Jayamani, E., Mai, G., and Buckel, W. (2008) Energy conservation via electron-transferring flavoprotein in anaerobic bacteria. *J. Bacteriol.* **190,** 784–791
3. Li, F., Hinderberger, J., Seedorf, H., Zhang, J., Buckel, W., and Thauer, R. K. (2008) Coupled ferredoxin and crotonyl coenzyme A (CoA) reduction with NADH catalyzed by the butyryl-CoA dehydrogenase/Etf complex from *Clostridium kluyveri*. *J. Bacteriol.* **190,** 843–850
4. Sousa, F. L., Thiergart, T., Landan, G., Nelson-Sathi, S., Pereira, I. A., Allen, J. F., Lane, N., and Martin, W. F. (2013) Early bioenergetic evolution. *Philos. Trans. R. Soc. Lond. B Biol. Sci.* **368,** 20130088
5. Buckel, W., and Thauer, R. K. (2013) Energy conservation via electron bifurcating ferredoxin reduction and proton/Na^+ translocating ferredoxin oxidation. *Biochim. Biophys. Acta* **1827,** 94–113
6. Bertsch, J., Parthasarathy, A., Buckel, W., and Müller, V. (2013) An electron-bifurcating caffeyl-CoA reductase. *J. Biol. Chem.* **288,** 11304–11311
7. Wang, S., Huang, H., Kahnt, J., and Thauer, R. K. (2013) *Clostridium acidurici* electron-bifurcating formate dehydrogenase. *Appl. Environ. Microbiol.* **79,** 6176–6179
8. Thamer, W., Cirpus, I., Hans, M., Pierik, A. J., Selmer, T., Bill, E., Linder, D., and Buckel, W. (2003) A two [4Fe-4S]-cluster-containing ferredoxin as an alternative electron donor for 2-hydroxyglutaryl-CoA dehydratase from *Acidaminococcus fermentans*. *Arch. Microbiol.* **179,** 197–204
9. Boiangiu, C. D., Jayamani, E., Brügel, D., Herrmann, G., Kim, J., Forzi, L., Hedderich, R., Vgenopoulou, I., Pierik, A. J., Steuber, J., and Buckel, W. (2005) Sodium ion pumps and hydrogen production in glutamate fermenting anaerobic bacteria. *J. Mol. Microbiol. Biotechnol.* **10,** 105–119
10. Biegel, E., and Müller, V. (2010) Bacterial Na^+-translocating ferredoxin: NAD^+ oxidoreductase. *Proc. Natl. Acad. Sci. U.S.A.* **107,** 18138–18142
11. Imkamp, F., Biegel, E., Jayamani, E., Buckel, W., and Müller, V. (2007) Dissection of the caffeate respiratory chain in the acetogen *Acetobacterium woodii*. Identification of an Rnf-type NADH dehydrogenase as a potential coupling site. *J. Bacteriol.* **189,** 8145–8153
12. Wohlfarth, G., and Buckel, W. (1985) A sodium ion gradient as energy source for *Peptostreptococcus asaccharolyticus*. *Arch. Microbiol.* **142,** 128–135
13. Parthasarathy, A., Pierik, A. J., Kahnt, J., Zelder, O., and Buckel, W. (2011) Substrate specificity of 2-hydroxyglutaryl-CoA dehydratase from *Clostridium symbiosum.* Toward a Bio-based production of adipic acid. *Biochemistry* **50,** 3540–3550
14. Buckel, W. (1986) Biotin-dependent decarboxylases as bacterial sodium pumps. Purification and reconstitution of glutaconyl-CoA decarboxylase from *Acidaminococcus fermentans*. In *Methods of Enzymology* (Fleischer, S., and Fleischer, B., eds.), Vol. 125, pp. 547–558, Academic Press, New York
15. Hetzel, M., Brock, M., Selmer, T., Pierik, A. J., Golding, B. T., and Buckel, W. (2003) Acryloyl-CoA reductase from *Clostridium propionicum.* An enzyme complex of propionyl-CoA dehydrogenase and electron-transferring flavoprotein. *Eur. J. Biochem.* **270,** 902–910
16. Bradford, M. M. (1976) A rapid and sensitive method for the quantitation of microgram quantities of protein utilizing the principle of protein-dye binding. *Anal. Biochem.* **72,** 248–254
17. Laemmli, U. K. (1970) Cleavage of structural proteins during the assembly of the head of bacteriophage T4. *Nature* **227,** 680–685
18. Mayhew, S. G., and Massey, V. (1969) Purification and Characterization of flavodoxin from *Peptostreptococcus elsdenii*. *J. Biol. Chem.* **244,** 794–802
19. Engel, P. C., and Massey, V. (1971) The purification and properties of butyryl-coenzyme A dehydrogenase from *Peptostreptococcus elsdenii*. *Biochem. J.* **125,** 879–887
20. Nakos, G., and Mortenson, L. (1971) Purification and properties of hydrogenase, an iron sulfur protein, from *Clostridium pasteurianum* W5. *Biochim. Biophys. Acta* **227,** 576–583
21. Lehman, T. C., Hale, D. E., Bhala, A., and Thorpe, C. (1990) An acyl-coenzyme A dehydrogenase assay utilizing the ferricenium ion. *Anal. Biochem.* **186,** 280–284
22. Ziegenhorn, J., Senn, M., and Bücher, T. (1976) Molar absorptivities of β-NADH and β-NADPH. *Clin. Chem.* **22,** 151–160
23. Kabsch, W. (2010) Xds. *Acta Crystallogr. D Biol. Crystallogr.* **66,** 125–132
24. Djordjevic, S., Pace, C. P., Stankovich, M. T., and Kim, J. J. (1995) Three-dimensional structure of butyryl-CoA dehydrogenase from *Megasphaera elsdenii*. *Biochemistry* **34,** 2163–2171
25. Emsley, P., and Cowtan, K. (2004) Coot. Model-building tools for molecular graphics. *Acta Crystallogr. D Biol. Crystallogr.* **60,** 2126–2132
26. Murshudov, G. N., Vagin, A. A., and Dodson, E. J. (1997) Refinement of macromolecular structures by the maximum-likelihood method. *Acta Crystallogr. D Biol. Crystallogr.* **53,** 240–255
27. Chang, Y. J., Pukall, R., Saunders, E., Lapidus, A., Copeland, A., Nolan, M., Glavina Del Rio, T., Lucas, S., Chen, F., Tice, H., Cheng, J. F., Han, C., Detter, J. C., Bruce, D., Goodwin, L., Pitluck, S., Mikhailova, N., Liolios, K., Pati, A., Ivanova, N., Mavromatis, K., Chen, A., Palaniappan, K., Land, M., Hauser, L., Jeffries, C. D., Brettin, T., Rohde, M., Göker, M., Bristow, J., Eisen, J. A., Markowitz, V., Hugenholtz, P., Kyrpides, N. C., and Klenk, H. P. (2010) Complete genome sequence of *Acidaminococcus fermentans* type strain (VR4). *Stand. Genomic. Sci.* **3,** 1–14
28. Whitfield, C. D., and Mayhew, S. G. (1974) Purification and properties of electron-transferring flavoprotein from *Peptostreptococcus elsdenii*. *J. Biol. Chem.* **249,** 2801–2810
29. Dawson, R. M. C., Elliott, D. C., Elliott, H. C., and Jones, K. M. (1986) *Data for Biochemical Research*, 3 Ed., Clarendon Press, Oxford
30. Aboulnaga, el-H., Pinkenburg, O., Schiffels, J., El-Refai, A., Buckel, W., and Selmer, T. (2013) Butyrate production in *Escherichia coli.* Exploitation of an oxygen tolerant bifurcating butyryl-CoA dehydrogenase/electron transferring flavoprotein complex from *Clostridium difficile*. *J. Bacteriol.* **195,** 3704–3713
31. Herrmann, T. G. E. (2008) Enzymes of two clostridial amino-acid fermentation pathways. Ph.D. thesis, Philipps-Universität, Marburg, Germany
32. Kölzer, S. (2008) Aufreiningung und Charakterisierung des butyryl-CoA dehydrogenase/ETF komplexes aus *Clostridium tetanomorphum.* Master thesis, Philipps-Universität, Marburg, Germany
33. Hans, M., Bill, E., Cirpus, I., Pierik, A. J., Hetzel, M., Alber, D., and Buckel, W. (2002) Adenosine triphosphate-induced electron transfer in 2-hydroxyglutaryl-CoA dehydratase from. *Acidaminococcus fermentans*. *Biochemistry* **41,** 5873–5882
34. Roberts, D. L., Frerman, F. E., and Kim, J. J. (1996) Three-dimensional structure of human electron transfer flavoprotein to 2.1-Å resolution. *Proc. Natl. Acad. Sci. U.S.A.* **93,** 14355–14360
35. Roberts, D. L., Salazar, D., Fulmer, J. P., Frerman, F. E., and Kim, J. J. (1999) Crystal structure of *Paracoccus denitrificans* electron transfer flavoprotein. Structural and electrostatic analysis of a conserved flavin binding domain. *Biochemistry* **38,** 1977–1989
36. Leys, D., Basran, J., Talfournier, F., Sutcliffe, M. J., and Scrutton, N. S. (2003) Extensive conformational sampling in a ternary electron transfer complex. *Nat. Struct. Biol.* **10,** 219–225
37. Sato, K., Nishina, Y., and Shiga, K. (2003) Purification of electron-transferring flavoprotein from *Megasphaera elsdenii* and binding of additional FAD with an unusual absorption spectrum. *J. Biochem.* **134,** 719–729
38. Sato, K., Nishina, Y., and Shiga, K. (2013) Interaction between NADH and electron-transferring flavoprotein from *Megasphaera elsdenii*. *J. Biochem.* **153,** 565–572
39. Williamson, G., Engel, P. C., Mizzer, J. P., Thorpe, C., and Massey, V. (1982) Evidence that the greening ligand in native butyryl-CoA dehydrogenase is a CoA persulfide. *J. Biol. Chem.* **257,** 4314–4320
40. Murthy, H. M., Hendrickson, W. A., Orme-Johnson, W. H., Merritt, E. A., and Phizackerley, R. P. (1988) Crystal structure of *Clostridium acidi-urici* ferredoxin at 5-Å resolution based on measurements of anomalous X-ray scattering at multiple wavelengths. *J. Biol. Chem.* **263,** 18430–18436
41. Toogood, H. S., van Thiel, A., Basran, J., Sutcliffe, M. J., Scrutton, N. S., and Leys, D. (2004) Extensive domain motion and electron transfer in the human electron transferring flavoprotein/medium chain acyl-CoA dehydrogenase complex. *J. Biol. Chem.* **279,** 32904–32912
42. Moser, C. C., Keske, J. M., Warncke, K., Farid, R. S., and Dutton, P. L. (1992) Nature of biological electron transfer. *Nature* **355,** 796–802
43. Toogood, H. S., van Thiel, A., Scrutton, N. S., and Leys, D. (2005) Stabili-

zation of non-productive conformations underpins rapid electron transfer to electron-transferring flavoprotein. *J. Biol. Chem.* **280,** 30361–30366
44. Massey, V., and Palmer, G. (1966) On the existence of spectrally distinct classes of flavoprotein semiquinones. A new method for the quantitative production of flavoprotein semiquinones. *Biochemistry* **5,** 3181–3189
45. Müh, U., Cinkaya, I., Albracht, S. P., and Buckel, W. (1996) 4-Hydroxybutyryl-CoA dehydratase from *Clostridium aminobutyricum*. Characterization of FAD and iron-sulfur clusters involved in an overall non-redox reaction. *Biochemistry* **35,** 11710–11718
46. Cinkaya, I., Buckel, W., Medina, M., Gomez-Moreno, C., and Cammack, R. (1997) Electron-nuclear double resonance spectroscopy investigation of 4-hydroxybutyryl-CoA dehydratase from *Clostridium aminobutyricum*. Comparison with other flavin radical enzymes. *Biol. Chem.* **378,** 843–849
47. Näser, U., Pierik, A. J., Scott, R., Cinkaya, I., Buckel, W., and Golding, B. T. (2005) Synthesis of ^{13}C-labeled γ-hydroxybutyrates for EPR studies with 4-hydroxybutyryl-CoA dehydratase. *Bioorg. Chem.* **33,** 53–66
48. Toogood, H. S., Leys, D., and Scrutton, N. S. (2007) Dynamics driving function. New insights from electron transferring flavoproteins and partner complexes. *FEBS J.* **274,** 5481–5504
49. Zhu, J., Egawa, T., Yeh, S. R., Yu, L., and Yu, C. A. (2007) Simultaneous reduction of iron-sulfur protein and cytochrome b_L during ubiquinol oxidation in cytochrome bc_1 complex. *Proc. Natl. Acad. Sci. U.S.A.* **104,** 4864–4869
50. Sheldrick, G. M. (2008) A short history of SHELX. *Acta Crystallogr. A* **64,** 112–122
51. De la Fortelle, E., and Bricogne, G. (1997) Maximum-likelihood heavy-atom parameter refinement for multiple isomorphus replacement and multiwavelength anomalous diffraction method. In *Methods of Enzymology* (Carter, C. W., ed.) Vol. 276, pp. 472–494, Academic Press, San Diego
52. Abrahams, J. P., and Leslie, A. G. (1996) Methods used in the structure determination of bovine mitochondrial F1 ATPase. *Acta Crystallogr. D Biol. Crystallogr.* **52,** 30–42
53. Afonine, P. V., Grosse-Kunstleve, R. W., Chen, V. B., Headd, J. J., Moriarty, N. W., Richardson, J. S., Richardson, D. C., Urzhumtsev, A., Zwart, P. H., and Adams, P. D. (2010) phenix.model_vs_data. A high-level tool for the calculation of crystallographic model and data statistics. *J. Appl. Crystallogr.* **43,** 669–676
54. Langer, G., Cohen, S. X., Lamzin, V. S., and Perrakis, A. (2008) Automated macromolecular model building for X-ray crystallography using ARP/wARP version 7. *Nat. Protoc.* **3,** 1171–1179

Additional experiment

Calibration of Crotonyl-CoA concentration by an enzyme mixture of *Acidaminococcus fermentans*

Crotonyl-CoA concentration can be measured with a coupled assay involving steps 3 and 4 with an enzyme mix of five auxillary enzymes purified together from the soluble fraction of cell-free extract from *A. fermentans*. Crotonyl-CoA is hydrated to (3*S*)-3-hydroxybutyryl-CoA which is oxidized to acetoacetyl-CoA forming NADH.

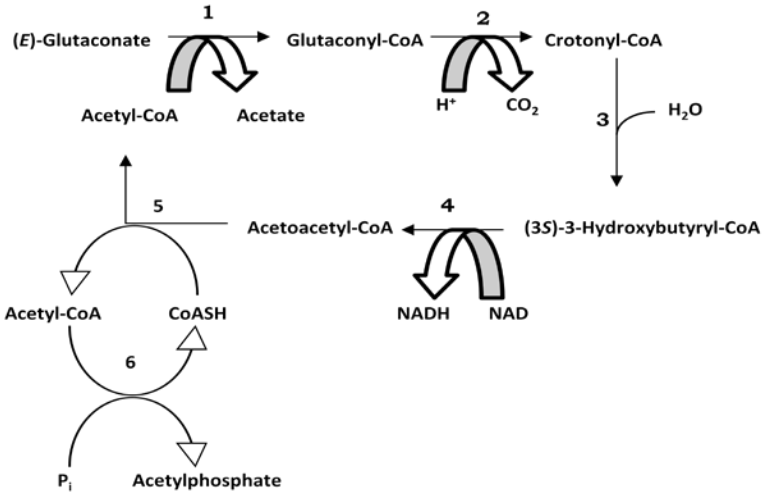

1 Glutaconate-CoA transferase,

2 Glutaconyl-CoA decarboxylase

3 Enoyl-CoA hydratase (crotonase),

4 (3*S*)-3-hydroxybutyryl-CoA dehydrogenase,

5 acetyl-CoA acetyltransferase (thiolase),

6 Phosphate acetyltransferase

The stoichiometry of crotonyl-CoA oxidized to acetoacetyl-CoA formed is 1:1; therefore 1mole of NADH is formed from 1 mole of crotonyl-CoA. Different volume of crotonyl-CoA was incubated with excess NAD^+ and formation of NADH was measured at 340 nm under anoxic condition on addition of enzyme pool.

Reaction volume of 500 µl consisted of 50 µg of enzyme pool mix, 500 µM of NAD^+ and different volume of crotonyl-CoA. A standard curve was plotted, concentration of NADH formed against different volumes of crotonyl-CoA.

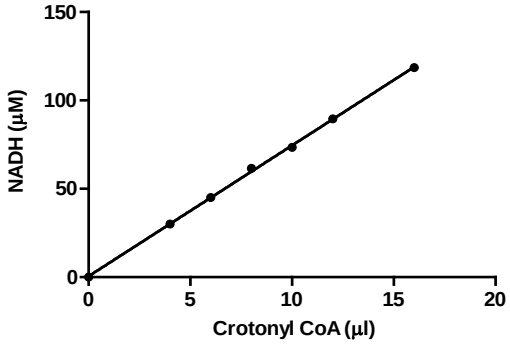

Calibration curve of crotonyl-CoA to NADH formed

Pull down assay

A pull down assay was performed with His-tagged Etf and cell free extracts from *A. fermentans* under aerobic conditions. The objective of the experiment was to investigate whether the interacting ferredoxin can be brought down from the cell free extracts. The final SDS-PAGE of the experiment is shown below.

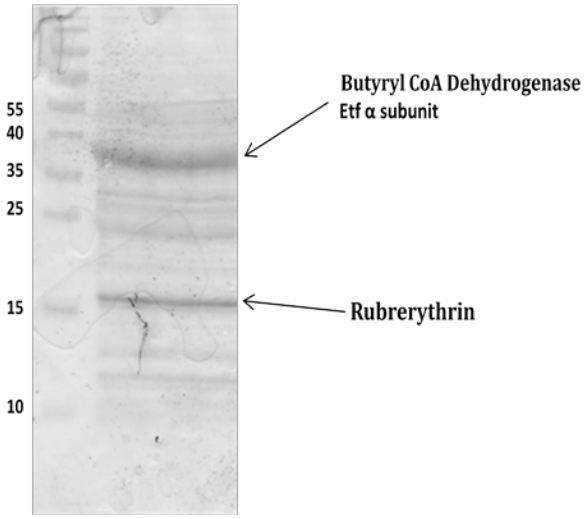

Procedure

0.5 mg of Etf was incubated 500 µl of 8 mg/ml of cell free extract at 4 °C in an Eppendorf 1.5 ml tube. The tube was kept on shaking condition for 5-6 hours for efficient binding. Finally the protein was loaded on to a 500 µl pre-equilibrated His-tag column and washed with 2 ml of 50 mM KPP pH 6.8 buffer supplemented with 0.5 M NaCl. Post washing, all proteins were eluted with 250 µM imidazole in the same buffer. Protein were run in a SDS-PAGE as shown above.

Comments.

The SDS-PAGE revealed 3 major protein bands which were analyzed MALDI-TOF analysis. With the C-terminal His-tag α subunit of Etf came down the butyryl-CoA dehydrogenase which was as expected, since from modeling experiments we found that Bcd interacts with the α subunit of Etf. Surprisingly Rubrerythrin was found as one of the interacting protein. Rubrerythrin has been reported to have NADH peroxidase activity [51] and termed as oxidative stress protein [52]. This observation can be well linked to our results presented in Chapter 3A and further dicussed in the Discussion part.

Flavodoxin and electron bifurcation

Summary

Flavodoxin are known to substitute ferredoxin in most of the metabolic reactions. However growth experiments of *A. fermentans* in low and high iron containing media show an inverse relation between the production of ferredoxin and flavodoxin. In low iron media the growth rate of *A. fermentans* remain unaffected indicating that energy conserved by fermenting glutamate in low iron condition essentially remains the same as in high iron content media. Ferredoxin was found to be an essential component of the electron bifurcation and energy conservation in *A. fermentans*, which should be affected during iron deprivation. Thamer et al. showed that the doubling time of *A. fermentans* remained unaffected even iron content in the media was varied between 7 µM-45 µM. Earlier Hans et al. (2002) identified that the hydroquinone form of flavodoxin can be an in vivo electron donor for 2-hydroxy-glutaryl-CoA dehydratase.

Here in this study we have overproduced and purified the recombinant flavodoxin from *A. fermentans* in *E. coli*. Biochemical experiments show that flavodoxin can replace ferredoxin in bifurcation reactions. Similar to ferredoxin, reduced flavodoxin can reoxidized by the membrane bound Rnf complex to its blue semiquinone form which is again reduced to hydroquinone form by electron bifurcation which has been shown by spectroscopic study. Most probably in vivo the flavodoxin shuttles between the blue semiquinone and the colorless hydroquinone form which supports the observation that flavodoxin purified under anaerobic conditions was always blue.

This chapter has been presented as a draft manuscript which will be submitted shortly.

Flavodoxin and flavin based electron-bifurcation

Nilanjan Pal Chowdhury[1, 2], Katharina Klomann[1] and Wolfgang Buckel[1, 2]

From the [1]Laboratorium for Microbiology, FachbereichBiologie and SYNMIKRO, Philipps-University,35032 Marburg, Germany, the [2]Max-Planck-Insitute for terrestrial Microbiology, Karl-von-Frisch-Str 10, 35043 Marburg, Germany

Introduction:

In the metabolism of acetogenic and fermentative bacteria, both ferredoxin and flavodoxin play central roles as electron acceptors and donors for numerous oxidation-reduction reactions. Flavodoxin was first discovered in *Clostridium pasteurianum* [53, 54], has a molecular mass of approximately 15,000 and contains 1 molecule of non-covalently bound flavin mononucleotide. Flavodoxin has been purified and studied from different organisms and the most extensive studies at the structural level have been carried out with flavodoxins from *Desulfovibrio vulgaris* [55-57], *Clostridium beijerinckii* MP [58, 59] , *Anabena* [60] and *Megasphaera elsdenii* [61]. Flavodoxin was shown to be the substitute for ferredoxin in most of the redox reactions with low redox potentials [62]. Flavodoxins can stabilize the neutral semiquinone of the bound FMN under anaerobic conditions which stays stable for long period. It can be reduced further to two electron reduced state (hydroquinone) which causes large shifts in the redox potentials for the 2nd electron reduced state. It is proposed that for reactions in-vivo, flavodoxin from *M. elsdenii* shuttles between semiquinone and hydroquinone state [61, 63]. Depending on the protein, the 2nd redox potential can vary between -0.368 and -0.518 V for FMN in flavodoxins [64] which makes it as a perfect candidate for electron donor or receiver in redox metabolic processes. However, the redox titration of flavodoxin from *Acidaminococcus fermentans* revealed a midpoint potential of -0.06 V for the semiquinone/benzoquinone couple and -0.43 V for the hydroquinone/semiquinone couple at pH 7.0 [65].

It is well known that under iron limiting conditions in growth medium, flavodoxin production surpasses the production of ferredoxin, as studied in *C. pasteurianum, C. acidiurici, C. formicoaceticum, M. elsdenii* and *A. fermentans* [53, 66-69]. An inverse dependence of ferredoxin/flavodoxin syntheses on iron concentration in the growth medium of *A. fermentans* in range of 7-45µM Fe was reported earlier [65]. The strict anaerobic bacterium *A. fermentans* ferments glutamate via hydroxyglutarate pathway to ammonia, carbon dioxide, acetate, butyrate and hydrogen [16-18]. It was shown that the hydroquinone form of the flavodoxin from *A. fermentans* could replace the reducing agent titanium (III) citrate in the activity assay of 2-hydroxyglutaryl-CoA dehydratase (a key enzyme in the glutamate fermenting pathway) suggesting that reduced flavodoxin might act as an natural electron donor to the dehydratase enzyme [65]. A second most important stage in the same metabolic pathway is the reduction of crotonyl-CoA to butyryl-CoA, which involves electron transferring flavoprotein (Etf), butyryl-CoA dehydrogeanse (Bcd), low redox potential ferredoxin and NADH as reductant [20]. Stepwise electron transfer to the Bcd and ferredoxin is mediated by Etf via flavin-based electron bifurcation [14, 15, 20, 35] which affords reduction of crotonyl-CoA and reduced ferredoxin.

Here, we report the overproduction and purification of flavodoxin from *A. fermentans* in *E. coli*, which is used to replace the ferredoxin in electron bifurcation reaction for the reduction of crotonyl-CoA to butyryl-CoA. Spectrophotometric analysis revealed that reduced flavodoxin can then be reoxidized to the semiquinonic state via the solubilized membrane

extract, mostly probably via the membrane bound Rnf (Rhodobater nitrogen fixation) complex, whereby an electrochemical Na^+-gradient is formed. Experiments in this study show that the flavodoxin shuttles between the semiquinone and the hydroquinone forms in-vivo.

MATERIALS AND METHODS

Growth of microorganism

A. fermentans VR4 (strain DSM 20731) was grown anaerobically on glutamate/yeast extract/biotin medium as described earlier [27]. *E. coli* (strains DH5α, BL21-DE3) was cultured and grown at 37 °C in Standard I nutrient broth (Merck, Darmstadt, Germany) in orbital shaker. The medium was supplemented with carbenicillin (50 µg/ml) for growth of bacteria with inserted plasmid. For overproduction of flavodoxin, 2 litres of Standard I broth, supplemented with carbenicillin, was inoculated with 25 mL of overnight culture of BL21-DE3 that has been transformed with the pASG-IBA3 expression vector (IBA, Gottingen) containing the flavodoxin gene of *A. fermentans*. The culture was grown till it reached an absorbance of O.D = 0.6, then 200 µg/litre AHT (IBA, Gottingen) was added to induce the expression of the recombinant gene during the further growth for next 12 h at room temperature. Post induction and growth, cells were harvested by centrifugation and cell paste stored at -80 °C until use.

Synthesis of CoA esters

Crotonyl-CoA and butyryl-CoA were synthesized by acylation of CoASH in aqueous 1 M $KHCO_3$ using 1 M crotonic anhydride or butyric anhydride in acetonitrile with a slight molar excess. After acidification the CoA-thioesters were purified over C18 columns and stored as lyophilized powders at –80 °C[70]. The concentration of the crotonyl-CoA was calibrated by the NAD^+-dependent β-oxidation to acetyl-CoA and acetylphosphate as described for the assay of glutaconyl-CoA decarboxylase [27]. HPLC of crotonyl-CoA and butyryl-CoA was performed on a C18 Kinetex column (5µm particle size, 100 Å pore size, 250 × 4.6 mm, Phenomenex, Aschaffenburg, Germany) at a flow rate of 1 ml/min in 50 mM KH_2PO_4 pH 5.3 and 5% acetonitrile. During 20 min a linear gradient up to 60% acetonitrile was applied. For detection of respective CoA esters from the assay mixtures, samples were acidified with conc. HCl to a pH 2.0 and centrifuged at around 13000 rpm and filtered to remove the denatured protein. 10µl sample was loaded to the HPLC column for the detection.

Preparation of titanium (III) citrate

Titanium (III) citrate was prepared as decribed by Zehnder and Wuhrmann [71]. Titanium (III) chloride in HCl (12%, 0.5 ml) was added to 5ml of 0.2 M sodium citrate. After 10 min the mixture was neutralized with saturated sodium carbonate solution to pH 7.0. The prepared titanium (III) citrate was stored under anaerobic conditions in air tight bottles.

Recombinant DNA methods

Genomic DNA was isolated from *A. fermentans* cells using genomic DNA preparation kit (Fermentas, Thermo Fischer) as per manufacturer's instruction. The flavodoxin protein from *A. fermentans* was identified earlier by N-terminal sequencing [72]. The gene corresponding to the protein, *Acfer_0269*[73] was amplified by PCR using genomic DNA as the template and forward primer 5'-AAGCTCTTCAATGAGCAAAATCGCAGTG GTGTTCT and reverse primer 5'-AAGCTCTTCACCCTGCCAGCGCCTCTCCC AG. The PCR product was cloned into the p-ENTRY vector and introduced in *E. coli* DH5α by chemical transformation. The cloned gene sequence was confirmed and then transferred to expression vector pASG IBA 3 and the cloned vector finally transferred to *E. coli* BL21-DE3. The colonies harboring the plasmid were used for overproduction of the protein.

Purification of flavodoxin

E. coli cells over-producing the recombinant flavodoxin (10g wet mass) were suspended in 50mM Tris-HCl/150 mM NaCl, pH 7.5 (buffer

A) and disrupted by three passages through a French press at 140 MPa. Cell debris and membranes were separated by centrifugation at 150,000 × g for 45 mins at 4 °C to obtain membrane free extract. The membrane free extract was the filtered using a 45 µM filter and loaded on to a 10ml Strep-tag II column (IBS GmbH, Germany) which was pre-equilibrated with buffer A. All purifications steps were performed at 4 °C, unless otherwise mentioned. The column post loading of the membrane free extract was washed with 10 column volumes of buffer A to remove contaminating proteins. The protein was eluted with 2.5 mM D-desthiobiotin in buffer B. The purified protein was desalted and concentrated; FMN in molar excess was added and incubated overnight in dark at 4 °C. Homogenous protein and excess flavin removal was obtained by loading the incubated protein onto a Superdex 75 pg (GE Healthcare Life Sciences). The protein was stored at -80 °C until use.

Purification of ferredoxin

Ferredoxin was purified from *Clostridium tetanomorphum* (DSM 526). *C. tetanomorphum* cells were grown on the same glutamate media as was used for *A. fermentans* with the exception, biotin was omitted. All purification was done under strict anoxic conditions, under an atmosphere of 95% N_2 and 5% H_2 (Coy Anaerobic Chamber). 10g frozen cells were suspended in 50 mM phosphate buffer pH 6.8 (buffer B) and passed 3 times through the French press at 140 MPa. The supernatant obtained by centrifugation at 150,000 × *g* for 1 h at 4 °C, was loaded on a DEAE column which was pre-equilibrated by buffer B. The column was washed with 2 column volumes of buffer B and the protein was eluted with a gradient of 0-100% 1M NaCl achieved over 10 column volumes (600ml). Active fractions of ferredoxin were identified by the bifurcation assay [15, 35]. Active fractions were pooled together and concentrated with a 3kDa ultrafiltration centricon (Millipore). The concentrated protein sample was loaded on to a Superdex 75 column pre-equilibrated with 150mM NaCl in buffer B. The fractions containing ferredoxin were identified by its dark brown color and was concentrated and stored at -80 °C under anaerobic conditions. The ferredoxin concentration was measured as per [68] and a molecular mass of 6 kDa was used.

Preparation of Hydrogenase

A partial purification of hydrogenase was obtained from *Clostridium pasterianum*. *Clostridium pasteurianum* (DSM 525) was grown on a medium containing 100 mM glucose, 70 mM $NaHCO_3$ and yeast extract (2 g/L). 5gm of frozen cells were re-suspended in 10 ml buffer B and broken through three passages through a French press at 140 MPa (20,000 Psi) under strict anoxic conditions. The broken cells were centrifuged at low speed 7000 x g for 20min. The supernatant was heated at 55-60 °C for 10-15 min under a hydrogen atmosphere. Post heating, the extract was kept in ice for 30 min for rapid cooling. The precipitated proteins and cells were now removed by centrifugation at a higher speed at 20,000 x g for 30 min. The supernatant containing hydrogenase was stored at -80 °C until use [74].

Preparation of Electron transferring flavoprotein and Butyryl CoA dehydrogenase

Etf and Bcdh was prepared as per reported earlier [35]. Both proteins were flavin saturated by incubating the proteins with excess FAD overnight in dark at 4 °C. Excess flavin was removed by using a PD 10 desalting column (**GE** healthcare)**.** Flavin content of the proteins was calculated using an extinction co-efficient, ε_{450} = 11.3 $mM^{-1}cm^{-1}$ at 450 nm

Preparation of membrane extracts

20 g wet packed cells of *A. fermentans* were suspended in buffer B and broken by 4 passages through the French press at 140 MPa under strict anoxic conditions. Cell debris was removed by centrifugation 20,000 x g for 20 min at 4 °C. The crude extract was centrifuged at 150,000 x g for 60 min. The supernatant was stored for further purification of soluble proteins and the membrane extract was collected and washed twice with buffer B by centrifuging at 150,000 x

g for 30 min. The washed membrane was then solubilised with 2% n-dodecyl-β-D-maltoside (DM) in buffer B supplemented with 0.5 M NaCl and homogenized well to further solubilise the membrane proteins. Post homoginization the extract was kept on ice for 30 min. The solubilised membrane was then centrifuged at 150,000 x g for 30 min and the supernatant containing the membrane protein was collected [27].

Analytical methods

Protein concentrations were estimated with the Bradford assay [75] (Biorad-Microassay reagent, Bio-Rad-Laboratories, Munich, Germany). Bovine serum albumin (Sigma, Germany) was used as standard. SDS-PAGE was performed as described by Laemmli [76]

All enzyme assays were done under an atmosphere of 95% N_2 and 5% H_2. The bifurcation assay measurement for the reduction of crotonyl-CoA to butyryl-CoA was done in a 500 µL quartz cuvette (d = 1 cm) using 0.5 µM Etf_{Af}, 1 µM Bcd_{Af},1 µM $ferredoxin_{Ct}$, crude $hydrogenase_{Cp}$ and 250 µM NADH. 100 µM of substrate was used in buffer B. The decrease in NADH concentration was monitored at 340 nm. Stoichiometric amounts of flavodoxin (50 µM) were used in place ferredoxin/hydrogenase to observe oxidation of NADH.

Reduction of flavodoxin for spectrophotometric assays was done by treating the protein with 500 µM titanium (III) citrate under anaerobic condition. Re-oxidation of reduced flavodoxin was done by adding the membrane extract coupled to reduction of NAD^+, change in the absorption spectra of flavodoxin on re-oxidation was done by UV-visible spectroscopy.

Results and Discussion

Isolation and characterization

Recombinant flavodoxin was purified from a cell lysate of *E. coli* BL21 (DE3) harboring the GOI_pASG IBA3 vector as mentioned earlier. The protein as was purified by an affinity Strep-Tag column and subjected to gel filtration to achieve homogeneity.By gel filtration at pH 7.0 2 distinct peaks were observed (Fig. 1), which, when ran on a SDS gel, each showed a single band around the 15 kDa marker. Both proteins from the 2 peaks were identified to be flavodoxin by MALDI-TOF analysis. This hints that the flavodoxin tends to make a mixture of the dimeric and monomeric forms, though the nature and extent of dimerization was not investigated. The molecular mass determined to be approximately 15 kD by SDS-PAGE (Fig. 2) which fits to the calculated value (14,500 + 1,000) based on the amino acid sequence from the protein and the strep-tag.

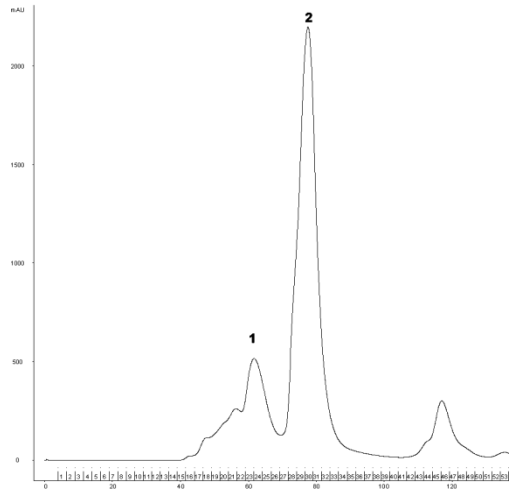

Figure 1. **Gel filtration profile of flavodoxin protein.** *1*, Peak for multimeric flavodoxin; *2*, peak for monomeric flavodoxin

The UV-visible spectrum of the purified protein was measured (see Fig. 2), which revealed two peaks at 375 and 448 nm, characteristic of proteins binding flavin derivatives. Upon heating the flavodoxin at 80 °C and analyzing the supernantant of the precipitated protein with TLC and reverse phase HPLC on C-8 column, the spot and the retention time matched to those of FMN (data not shown). The FMN content of the protein was around 0.2 FMN per monomer which was raised to 0.6 on overnight incubation in the dark at 4 °C after removal of excess FMN by gel filtration. The quantification by absorbancies at $\lambda = 450$ nm ($\varepsilon = 11.3\ mM^{-1}\ cm^{-1}$) and $\lambda = 370$ nm ($\varepsilon = 10.7\ mM^{-1}\ cm^{-1}$) was used [77]. The FMN content of the flavodoxin purified from *A. fermentans* was reported to be 1.0 [72], which suggests that on overproduction

most of the flavodoxin has lost its flavin binding capacity and there exists a mixture of holo and apo-flavodoxin. A ratio of A_{465}/A_{274} = 0.17 was reported to correspond to that of the pure holo-flavodoxin in *Anabena* [78], whereas the ratio of A_{465}/A_{274}, obtained is this study was 0.146.

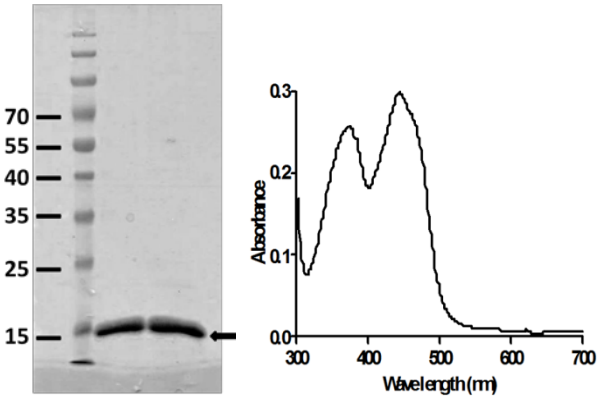

Figure 2. SDS-PAGE of recombinant Strep-tag Flavodoxin (left). UV-vis spectrum of 35 µM flavodoxin (right)

Kinetic characterization

Addition of ferredoxin and hydrogenase to catalytic amounts of Etf_{Af}/Bcd_{Af} with NADH and crotonyl-CoA caused rapid oxidation of NADH [35], which has been established as flavin based electron bifurcation in earlier research. Based on this and the observation that during iron limiting conditions the growth rate of *A. fermentans* was not hampered, we replaced the ferredoxin in the bifurcation reaction with flavodoxin. On incubation of same amounts of Etf_{Af}/Bcd_{Af} with NADH and stoichiometric amounts of flavodoxin, no oxidation of NADH was observed, suggesting no electron transfer to flavodoxin was achieved. However on addition of the substrate (crotonyl-CoA), oxidation of NADH was observed (Fig. 3). The product of the reaction was besides NAD^+, butyryl-CoA (determined by MALDI-TOF mass spectrometry and HPLC). In control experiments, in which crotonyl-CoA was replaced by butyryl-CoA or free CoA, no NADH was oxidized, suggesting that the reduction of flavodoxin was tightly coupled to reduction of crotonyl-CoA.

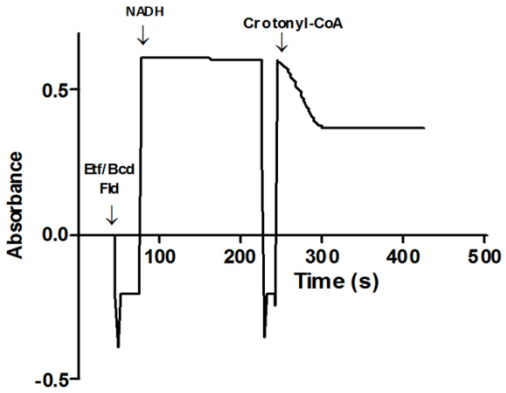

Figure 3. Oxidation of NADH on addition of Crotonyl-CoA

The resulting reaction can be written as in an equation 1,

Crotonyl-CoA + 2NADH + Fld ⟶ Butyryl-CoA + 2 NAD^+ + Fld^{2-}

Increasing concentrations of flavodoxin in the reaction assay increased the rate of NADH oxidation (Fig. 4), which followed Michaelis-Menten kinetics, K_m = 82 µM. As the flavin content of the protein was calculated to be 0.5, the actual K_m has to be considered to be around 40 µM.

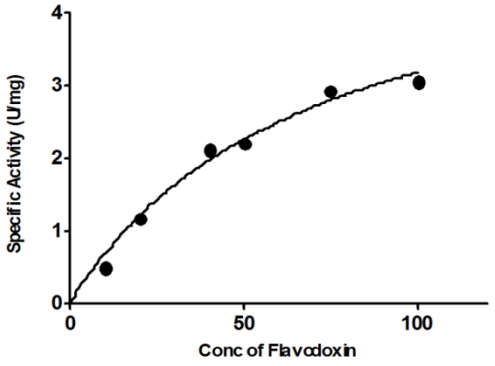

Figure 4. Dependence of the specific activity of NADH oxidation (µmol of NADH/mg of Etf_{Af}) on the concentration of the Fld_{Af}

Spectroscopic characterization

The UV-visible spectrum under anaerobic conditions showed absorption maxima at 375

and 446 nm with a shoulder peak at 464 nm. The protein, when reduced by 1 mM of the synthesized titanium (III) citrate, showed reduced absorbance at 375 and 446 nm and a new peak at 578 nm (Fig. 5) The peak at 578 nm, a characteristic of blue simiquinone, was stable and only after addition of an 5 mM titanium citrate (fig 6), the flavodoxin was completely reduced. Generally the redox potential of the semiquinone-hydroquinone couple of flavodoxins varies with pH andbcomes independent at pH > 7.5 [61, 64]. In the low pH region the potential is more negative than that of hydrogen electrode, so it becomes more difficult to reduce flavodoxin. This correlates with our observation that excess titanium (III) citrate was required to completely reduce the flavodoxin at pH 6.8.

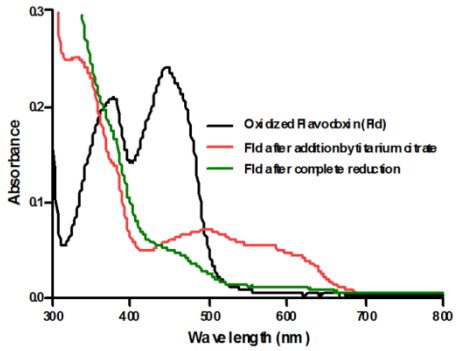

Figure 5. Reduction of flavodoxin by tit (III) citrate. *Black*, oxidized Fld; *Red*, Fld reduced by 1 mM Tit (III) citrate; *Green*, completely reduced Fld by excess Tit (III) citrate.

In the context that the titanium (III) citrate can reduce the flavodoxin$_{Af}$ first to the semiquinone and then to the completely reduced hydroquinone form with a redox potential of -60 mV and -430 mV respectively [72], it was interesting to study the spectral characteristics of the flavodoxin during the electron bifurcation process. To catalytic amounts of Etf/Bcd and 125 µM NADH, 75 µM flavodoxin was added and the spectrum was recorded. Limiting amounts of crotonyl-CoA (30 µM) were added to start the reaction and immediately the spectra were recorded. It was observed that the peak at 446 nm decreased with an increase in the region between 520-660nm. Spectra were again recorded after 1 min which revealed marked decrease in the peak at 446 nm and a stable neutral semiquinone peak at 578 nm (Fig. 6A). On addition of excess crotonyl-CoA (50 µM) the flavin spectrum was completely quenched. As a control, when limiting amounts of flavodoxin (25 µM) were analyzed similarly with an excess crotonyl-CoA (75 µM), the decrease at 446 nm was deeper and the absorption of the region between 520-660 nm was less pronounced (Fig. 6B). Hence the flavodoxin was completely reduced to the hydroquinone form.

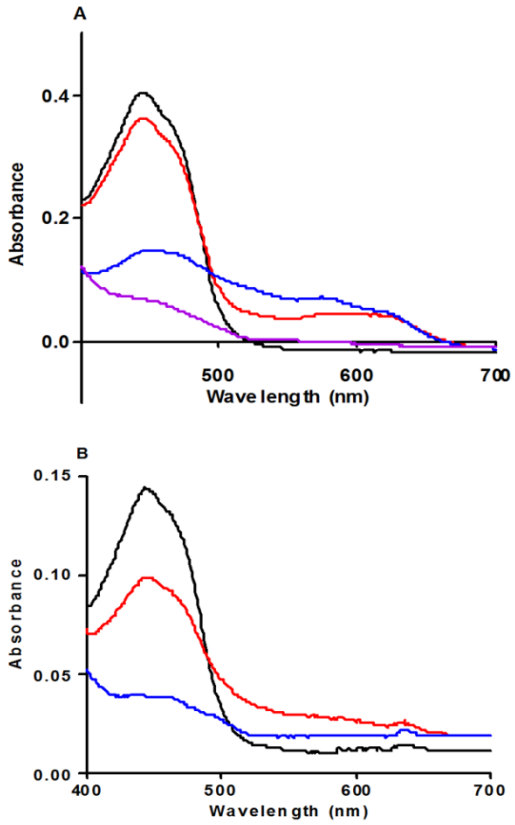

Figure 6(A,B). Flavodoxin UV-vis spectra. (A) Spectra of 75 µM Fld with 30 µM crotonyl-CoA. *Black* oxidized Fld, *Red &Blue*, consecutively spectra recorded; Purple, spectra of Fld on addition of excess crotonyl-CoA. **(B)** Spectra of 25 µM Fld with 75 µM crotonyl-CoA. *Black*, oxidized Fld; *Red*. Spectra recorded after 1min of crotonyl-CoA addition; *Blue*, spectra after 5 min post reaction.

Experiments with membrane fractions

It was observed that the membrane fraction of *Clostridium tetanomorphum* exhibited high NADH-dehydrogenase activities with

ferricyanide [hexacyanoferrate (III)] as an electron acceptor [equation 2], see review [6].

$NADH + 2\ [Fe(CN)_6]^{3-} = NAD^+ + 2\ [Fe(CN)_6]^{4-} + H^+$; (equation 2)
$\Delta E = +740$ mV; $\Delta G^{\circ\prime} = -143$ kJ mol^{-1}

The results led to the proposal that the six deduced Rnf-related proteins detected in the genome of the related organism *Clostridium tetani* might be responsible for this catalytic activity [39]. It was further suggested that, similar to the homologous Na^+-pumping NADH-quinone oxidoreductases (Nqr) from *Vibrio alginolyticus* [79], the Rnf proteins form a membrane complex, which generates an electrochemical H^+ or Na^+-gradient. Later, with inverted membrane vesicle from *Acetobacterium woodii* [8, 45] it was demonstrated that Rnf is an unique primary sodium pump coupling the electron transfer from reduced ferredoxin to NAD^+ with the electrogenic movement of Na^+ out of the cell [6]. The ion gradient thus formed helps in energy conservation by ATP synthesis via the well known Na^+ F_1F_0 ATP synthase.

Earlier observation that the growth rate of *A. fermentans* cells (doubling time 2.5 hr) were independent of the iron concentrations in the media (7-45 µM Fe)[68].Spectroscopic evidence made us believe that flavodoxin actually plays the role of ferredoxin in *A. fermentans*. However, it was interesting to investigate that whether the reduced flavodoxin (hydroquinone form) generated by electron bifurcation can actually be oxidized by NAD^+ mediated by the membrane extract because the genome of *A. fermentans* was also found to encode for the Rnf (*Acfer_0108-0113*) and growth rates were stimulated with 50 mM Na^+ [80].

Spectrophotometric titration of 45 µM flavodoxin at pH 6.8 revealed that the protein can be completely reduced by 5 mM titanium (III) citrate. To the reaction mixture 0.3 mM NAD^+ was added and observed for any rise in absorbance at 340 nm. Rapid increase in the absorbance signifying NADH formation was observed on addition of 150 µg of membrane extract (Fig. 7). This shows that reduced flavodoxin can oxidize NADH catalysed by membrane extracts containing Rnf. Control experiments without flavodoxin, showed a very slow increase of absorbance at 340 nm and omission of titanium (III) citrate from reaction, showed no formation of NADH.

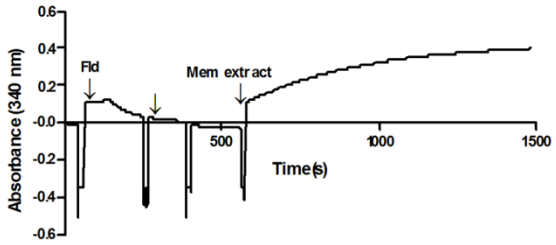

Figure 7. Formation of NADH measured at 340 nm, using reduced flavodoxin, NAD+ and membrane extracts of *A. fermentans*

Alternatively, flavodoxin was completely reduced by electron bifurcation with 2 min as revealed UV-spectroscopy (Fig. 8). After addition of 100 µg membrane extract the blue neutral semiquinonic form of flavodoxin with characteristic absorbance maxima at 500 and 578 nm was observed, which didnot change to the quinone form on addition of excess membrane extract (Fig. 8).

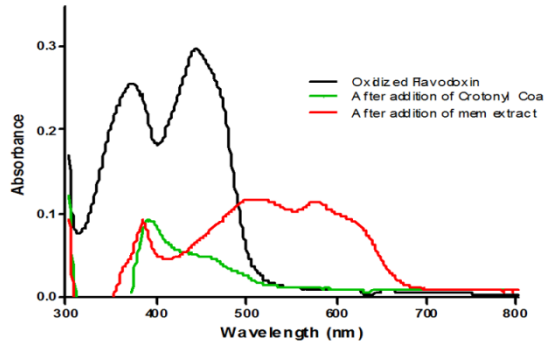

Figure 8. UV-vis absorption spectrum of flavodoxin of *A. fermentans* (reduced and oxidized). *Black*, oxidized Fld; *Green*, Fld after bifurcation reaction; *Red*, reduced Fld after addition of 100 µg of membrane extract.

This is due to the fact that the semiquinone/hydroquinone couple of flavodoxin has a redox potential of -420 mV which allows the electron to be transferred to NAD^+ having a redox potential of -320 mV for the

NADH/NAD^+ couple. Once one electron has been transferred from the hydroquinone form of flavodoxin, the redox potential of the semiquinone falls to -60 mV from which it cannot transfer anymore the electron to the NAD^+. Thus the reduced flavodoxin on re-oxidation with the Rnf is observed in the semiquinone form, the colour of which is blue and can be identified by the naked eye.

Discussion

In summary, this work knits up the story, how under iron limiting conditions bacteria can replace ferredoxin by flavodoxin which has been demonstrated by both biochemical and spectroscopic experiments. Besides the reductive activation of 2-hydroxyglutaryl-CoA dehydratase, we have identified additional steps in the metabolism of glutamate fermentation by *A. fermentans* where flavodoxin can replace ferredoxin. In the reduction of crotonyl-CoA to butyryl-CoA by flavin based electron bifurcation flavodoxin can substitute ferredoxin as electron acceptor. The reduced flavodoxin (hydroquinone form) then transfers one electron for the formation of NADH to the Na^+ pump (Rnf) present in the membrane, which gives rise to the blue semi-oxidized flavodoxin (semiquinone form). We have been able to provide the answer to the question, why flavodoxin purified under anaerobic conditions was found to be blue. Taking the example of our study, flavodoxin once reduced to the hydroquinone form by electron bifurcation is assumed to be oxidized by Rnf to its semiquinone form. Pertaining to its high redox potential of -60 mV, it cannot further be oxidized by NAD^+ due its much lower redox potential of -320 mV. So it becomes clear that the semiquinone form now becomes the electron acceptor for ongoing metabolic processes and then reoxidized again by Rnf. The sodium gradient so formed by the reoxidation of flavodoxin hydroquinone maintains the energy balance by refluxing the Na^+ ions inside the cells for the synthesis of ATP by a chemiosmotic mechanism. Thus we see the energy balance is well maintained and no growth difference in our model system *A. fermentans* during its growth in high and low iron concentrations.

This finding can further be extended to study other bifurcating systems where ferredoxin is an integral part. Unlike ferredoxin, flavodoxin being an oxygen tolerant enzyme is easy to handle. This also opens up the field to further study how electrons are shuttled from NADH to flavodoxin via Etf.

1. Knight, E., Jr., and Hardy, R. W. (1966) *J Biol Chem***241**, 2752-2756
2. Knight, E., Jr., and Hardy, R. W. (1967) *J Biol Chem***242**, 1370-1374
3. Carr, M. C., Curley, G. P., Mayhew, S. G., and Voordouw, G. (1990) *Biochem Int***20**, 1025-1032
4. Curley, G. P., Carr, M. C., Mayhew, S. G., and Voordouw, G. (1991) *Eur J Biochem***202**, 1091-1100
5. O'Farrell, P. A., Walsh, M. A., McCarthy, A. A., Higgins, T. M., Voordouw, G., and Mayhew, S. G. (1998) *Biochemistry***37**, 8405-8416
6. Bradley, L. H., and Swenson, R. P. (1999) *Biochemistry***38**, 12377-12386
7. Chang, F. C., and Swenson, R. P. (1999) *Biochemistry***38**, 7168-7176
8. Lostao, A., Gomez-Moreno, C., Mayhew, S. G., and Sancho, J. (1997) *Biochemistry***36**, 14334-14344
9. Geoghegan, S. M., Mayhew, S. G., Yalloway, G. N., and Butler, G. (2000) *Eur J Biochem***267**, 4434-4444
10. Mortenson, L. E., Valentine, R. C., and Carnahan, J. E. (1962) *Biochem Biophys Res Commun***7**, 448-452
11. Moonen, C. T., and Muller, F. (1984) *Eur J Biochem***140**, 303-309
12. Yalloway, G. N., Mayhew, S. G., Malthouse, J. P., Gallagher, M. E., and Curley, G. P. (1999) *Biochemistry***38**, 3753-3762
13. Hans, M., Bill, E., Cirpus, I., Pierik, A. J., Hetzel, M., Alber, D., and Buckel, W. (2002) *Biochemistry***41**, 5873-5882
14. Schonheit, P., Brandis, A., and Thauer, R. K. (1979) *Arch Microbiol***120**, 73-76
15. Ragsdale, S. W., and Ljungdahl, L. G. (1984) *J Bacteriol***157**, 1-6

16. Thamer, W., Cirpus, I., Hans, M., Pierik, A. J., Selmer, T., Bill, E., Linder, D., and Buckel, W. (2003) *Arch. Microbiol.***179**, 197-204
17. Mayhew, S. G., and Massey, V. (1969) *J. Biol. Chem.***244**, 794-802
18. Buckel, W., and Barker, H. A. (1974) *J Bacteriol***117**, 1248-1260
19. Hartel, U., and Buckel, W. (1996) *Arch Microbiol***166**, 350-356
20. Buckel, W. (2001) *Appl Microbiol Biotechnol***57**, 263-273
21. Buckel, W., and Thauer, R. K. (2013) *Biochim. Biophys. Acta***1827**, 94-113
22. Chowdhury, N. P., Mowafy, A. M., Demmer, J. K., Upadhyay, V., Koelzer, S., Jayamani, E., Kahnt, J., Hornung, M., Demmer, U., Ermler, U., and Buckel, W. (2014) *J. Biol. Chem.***289**, 5145-5157
23. Herrmann, G., Jayamani, E., Mai, G., and Buckel, W. (2008) *J. Bacteriol.***190**, 784-791
24. Li, F., Hinderberger, J., Seedorf, H., Zhang, J., Buckel, W., and Thauer, R. K. (2008) *J. Bacteriol.***190**, 843-850
25. Buckel, W. (1986) in *Meth. Enzymol.* (Sidney Fleischer, B. F., ed) Vol. 125, pp. 547-558, Academic Press
26. Parthasarathy, A., Pierik, A. J., Kahnt, J., Zelder, O., and Buckel, W. (2011) *Biochemistry***50**, 3540-3550
27. Zehnder, A. J. B., and Wuhrmann, K. (1976) *Science***194**, 1165-1166
28. Hans, M., Bill, E., Cirpus, I., Pierik, A. J., Hetzel, M., Alber, D., and Buckel, W. (2002) *Biochemistry***41**, 5873-5882
29. Chang, Y. J., Pukall, R., Saunders, E., Lapidus, A., Copeland, A., Nolan, M., Glavina Del Rio, T., Lucas, S., Chen, F., Tice, H., Cheng, J. F., Han, C., Detter, J. C., Bruce, D., Goodwin, L., Pitluck, S., Mikhailova, N., Liolios, K., Pati, A., Ivanova, N., Mavromatis, K., Chen, A., Palaniappan, K., Land, M., Hauser, L., Jeffries, C. D., Brettin, T., Rohde, M., Goker, M., Bristow, J., Eisen, J. A., Markowitz, V., Hugenholtz, P., Kyrpides, N. C., and Klenk, H. P. (2010) *Stand. Genomic. Sci.***3**, 1-14
30. Nakos, G., and Mortenson, L. (1971) *Biochim. Biophys. Acta***227**, 576-583
31. Bradford, M. M. (1976) *Anal. Biochem.***72**, 248-254
32. Laemmli, U. K. (1970) *Nature***227**, 680-685
33. Dawson, R. M. C., Elliott, D. C., Elliott, H. C., and Jones, K. M. (1986) *Data for Biochemical Research*, 3 Ed., Clarendon Press, Oxford
34. Fillat, M. F., Borrias, W. E., and Weisbeek, P. J. (1991) *Biochem J***280 (Pt 1)**, 187-191
35. Boiangiu, C. D., Jayamani, E., Brügel, D., Herrmann, G., Kim, J., Forzi, L., Hedderich, R., Vgenopoulou, I., Pierik, A. J., Steuber, J., and Buckel, W. (2005) *J. Mol. Microbiol. Biotechnol.***10**, 105-119
36. Bruggemann, H., Baumer, S., Fricke, W. F., Wiezer, A., Liesegang, H., Decker, I., Herzberg, C., Martinez-Arias, R., Merkl, R., Henne, A., and Gottschalk, G. (2003) *Proc Natl Acad Sci U S A***100**, 1316-1321
37. Beattie, P., Tan, K., Bourne, R. M., Leach, D., Rich, P. R., and Ward, F. B. (1994) *FEBS Lett***356**, 333-338
38. Hayashi, M., Nakayama, Y., and Unemoto, T. (1996) *FEBS Lett***381**, 174-176
39. Biegel, E., and Müller, V. (2010) *Proc. Natl. Acad. Sci. U S A***107**, 18138-18142

2.3.1 Electron transferring flavoprotein and reactive oxygen species

Summary

Megasphaera elsdenii a strict anaerobic bacteria uses lactate as a sole energy source for thriving in rumen of homothermic animals. It ferments lactate to propionate, acetate, butyrate and valerate. Butyrate is formed by the reduction of crotonyl-CoA with NADH via the dissociable Etf/Bcd complex. Though the reaction is same as in case of *A. fermentans*, but in older reports the requirement of ferredoxin was not necessary. *M. elsdenii* and *A. fermentans* are very closely related species belonging to the phyla Firmicutes and the Etf from both the species are 50% indentical. In this study we re-examined the characteristics of the Etf-Bcd complex using recombinant protein produced in E. coli.

We found that under anaerobic condition the Etf/Bcd behaves similar to the clostridial bifurcating Etf/Bcd complex which required oxidized ferredoxin to reduce crotonyl-CoA by NADH. However under aerobic condition, oxidation of NADH was observed on addition of crotonyl-CoA and required no ferredoxin. Surprisingly when the substrate was replaced by product (butyryl-CoA), NADH was still oxidized. This strange observation made us to infer that oxygen plays the role of ferredoxin under aerobic condition. However this reaction is not a typical physiological reaction as when limiting amounts of the substrate was added to excess of NADH, a complete oxidation of NADH was achieved. Under aerobic condition a continuous oxidation and reduction of the substrate to the product and vice-versa leads to the complete oxidation of NADH. Reduction of the substrate with NADH under aerobic condition gives rise to reactive oxygen species and finally to hydrogen peroxide. Using superoxide dismutase in the reaction assay mixture we have shown 50% inhibition of the activity can be observed. This indicates the presence of intermediate oxygen radical which can be trapped by the superoxide dismutase, finally slowing down the rate.

The results are presented in as a manuscript draft which will be submitted recently.

Generation of reactive oxygen species by flavin-based electron bifurcation.

Nilanjan Pal Chowdhury[1, 2], Jorg Kahnt[2] and Wolfgang Buckel[1, 2]

From the [1]Laboratorium for Microbiology, Fachbereich Biologie and SYNMIKRO, Philipps-University,35032 Marburg, Germany, the [2]Max-Planck-Insitute for terrestrial Microbiology, Karl-von-Frisch-Str 10, 35043 Marburg, Germany

Introduction

The strictly anaerobic Gram-negative bacterium *Megasphaera elsdenii* ferments lactate to CO_2, H_2, acetate, propionate, butyrate, valerate and traces of caproate [48-50, 81]. Being a member of the ruminal microflora and a model organism for anaerobic metabolism, *M. elsdenii* has been of great interest and its catabolic pathway has been extensively studied [49, 82, 83]. Lactate is oxidized to acetyl-CoA via pyruvate while simultaneously lactyl-CoA is reduced to propionyl-CoA via acrylyl-CoA. Butyrate, valerate and caproate are synthesized by reversed β-oxidation from acetyl-CoA and propionyl-CoA.

Already in 1964, Baldwin and Milligan [84] showed that the electron transferring flavoprotein from *M. elsdenii* (Etf_{Me}) functions in the formation of the short chain fatty acidsby transferring electrons from NADH to butyryl-CoA dehydrogenase (Bcd_{Me}) that catalyzes the reduction of enoyl-CoA to the saturated acyl-CoA derivatives. Since then, Etf_{Me} has been purified and characterized several times [83, 85-87]. The genes encoding the two different subunits (*etfAB*) were also cloned and expressed [88]. The pathway of electron transport has been proposed to occur via equations 1-3:

(1) NADH + 2 Etf$\rightarrow$ NAD^+ + 2 $Etf^{\bullet-}$+ H^+
(2) 2 $Etf^{\bullet-}$+ Bcd$\rightarrow$2 Etf+ Bcd^{2-}
(3) Bcd^{2-} +2 H^+ + crotonyl-CoA$\rightarrow$Bcd+ butyryl-CoA;
(4) Sum (1+3): NADH + H^+ + crotonyl-CoA $\rightarrow$$NAD^+$+ butyryl-CoA.

Recently we characterized Etf_{Af} and Bcd_{Af} from the anaerobic bacterium *Acidaminococcus fermentans* that is related to *M. elsdenii*; both are Gram-negative cocci classified as *Negativicutes* among the order *Clostridiales* [89].We found that Etf_{Af} and Bcd_{Af} coupled the electron transport from NADH to crotonyl-CoA to the simultaneous reduction of ferredoxin by NADH (eqn. 5) [35]. Hence the exergonic reduction of crotonyl-CoA (E_0' = −10 mV) by NADH (E' = −280 mV) drives the endergonic reduction of ferredoxin (E' = −500 mV), a process called flavin-based electron bifurcation [14, 15, 20].

(5) Crotonyl-CoA + 2NADH + 2 $Fd^-$$\rightarrow$Butyryl-CoA+ NAD^+ +2 Fd^{2-}

The crystal structure of Etf_{Af} revealed the presence of two FAD, each in one subunit of the heterodimeric Etf. Spectroscopic and modeling studies led to a mechanistic proposal, in which NADH reduced the FAD of the β-subunit (β-FAD) by a hydride transfer. The FAD of the α-subunit (α-FAD) swings to the β-$FADH^-$ and takes one electron to be reduced to a stabilized α-FAD semiquinone anion (α-$FAD^{\bullet-}$) whereas the other electron at the β-$FADH^{\bullet}$ is not stabilized and immediately reduces ferredoxin. α-$FAD^{\bullet-}$ transfers its electron further to D-FAD of Bcd. After a second electron bifurcation the completely reduced D-$FADH^-$ transfers a hydride to crotonyl-CoA and butyryl-CoA is formed.

The question arose why Etf_{Me}/Bcd_{Me} does not couple the reduction of crotonyl-CoA to the reduction of ferredoxin as does Etf_{Af}/Bcd_{Af}. A closer look revealed, however, that the studies with Etf_{Me}/Bcd_{Me} were all done under aerobic conditions, whereas studies with Etf_{Af}/Bcd_{Af} using the oxygen-sensitive ferredoxin were performed under strict anaerobic conditions. Re-investigation of the Etf_{Me}/Bcd_{Me} system indeed showed that under air reduction of crotonyl-CoA to butyryl-CoA was achieved by NADH alone, but interestingly no activity was found under anaerobic conditions unless ferredoxin was

added. This led us to realize that oxygen serves as the electron acceptor replacing ferredoxin. Like Etf_{Af}/Bcd_{Af}, Etf_{Me}/Bcd_{Me} turnedout to act as an electron bifurcating system which under airgaverise to the reactive oxygen species (ROS) superoxide and hydrogen peroxide.

Materials and Methods

Crotonyl-CoA and butyryl-CoA were synthesized by acylation of CoASH in aqueous 1 M $KHCO_3$ using 1 M crotonic anhydride or butyric anhydride in acetonitrile with a slight molar excess. After acidification the CoA-thioesters were purified over C18 columns and stored as lyophilized powders at −80 °C[70]. The concentration of crotonyl-CoA was calibrated by the NAD^+-dependent β-oxidation to acetyl-CoA and acetylphosphate as described for the assay of glutaconyl-CoA decarboxylase[27]. HPLC of crotonyl-CoA and butyryl-CoA was performed on a C18 Kinetex column (5µm particle size, 100 Å pore size, 250 × 4.6 mm, Phenomenex, Aschaffenburg, Germany) at a flow rate of 1 ml/min in 50 mM KH_2PO_4 pH 5.3 and 5% acetonitrile. During 20 min a linear gradient up to 60% acetonitrile was applied.

The ferricenium (Fc^+) solution for the Bcd assay was prepared in 10 mM HCl to a final concentration of 2 mM set at 617 nm with ε_{617} = 0.41 $mM^{-1}cm^{-1}$ [90].Protein concentrations were estimated with the Bradford assay [75] (Biorad-Microassay reagent, Bio-Rad-Laboratories, Munich, Germany). Bovine serum albumin (Sigma, Germany) was used as standard. SDS-PAGE was performed as described by Laemmli [76].

Detection of Etf_{Me} and Bcd_{Me}

M. elsdenii (DSM 20460) was grown in a 10 L lactate medium under anaerobic conditions at 37 °C as described previously [91]. Wet packed cells (10 g) were suspended in 20 ml 50 mM potassium phosphate pH 7.0 (buffer A) and opened by three passages through at French press. The supernatant, obtained by centrifugation at 150,000 × *g* for 1 h at 4°Cwas loaded on a DEAE column and was fractionated with 10 column volumes of 0-100% 1 M NaCl in buffer A. Etf eluted from the column at around 19% and Bcd at 65% 1 M NaCl. The fractions with the highest activity (INT and ferricenium assays, respectively) were run on SDS-PAGE.

Heterologous production of Etf_{Me}andBcd_{Me}.

Genomic DNA was prepared with the preparation kit of Thermo Scientific, Darmstadt, Germany. By applying the Stargate™ system according to the instructions of IBA, Göttingen, Germany, the genes *Mels_2127* (Etf_β-subunit) and *Mels_2126* (Etf_α-subunit) were cloned in this order as one fragment. *Mels_2128* (Bcd) was cloned as a single gene in a different vector. Genomic DNA of *M. elsdenii* was used as PCR template with forward and reverse primers (see suppl.). The PCR product was cloned into the p-ENTRY vector and introduced into *Escherichia coli* DH5α by chemical transformation. After confirmation of the desired sequence, the genes were transferred from the donor vector to the expression vector pASG IBA3 and further into *E. coli*BL21 (GroEL). The recombinant cells were cultivated in 4 L Standard I nutrient broth (Merck, Darmstadt, Germany) containing ampicillin (100 µg/ml) and chloramphenicol (34 µg/ml). When the O.D. (600 nm) rose to 0.5, both anhydrotetracycline (AHT, 0.2 µg/ml) and 0.1 mM isopropyl thiogalactoside (IPTG) were added to the culture medium to induce the overproduction of Etf and GroEL. The cultures were incubated at room temperature overnight. After harvesting, the cells were stored at −80 °C until purification.

Sequence alignment was done using Clustal W2.

Purification of electron transferring flavoprotein (Etf_{Me}) and butyryl-CoA dehydrogenase (Bcd_{Me})

E. coli cells over-producing $EtfAB_{Me}$ (12gwet mass) were suspended in 50mM Tris-HCl/150 mM NaCl pH 7.5 (buffer B) and disrupted by three passages through a French press at 500 MPa. Cell debris and membranes were removed by centrifugation at 150,000 × *g* for one hour at 4 °C to obtain the cell free extract. All purifications were performed under aerobic conditions at 4 °C, unless mentioned otherwise. The supernatant was applied on a 10 ml Strep-tag column (IBA GmbH, Göttingen, Germany)

which was equilibrated with buffer B. Elution of the protein was done with 2.5 mM D-desthiobiotin in buffer B. The purified protein was concentrated by ultrafiltration and further purified by gelfiltration on Superdex 200, pre-equilibrated with 150 mM NaCl in buffer A, concentrated and stored at −80 °C until use.

The *E. coli* cells over-producing Bcd_{Me} were disrupted and the extract was prepared as mentioned above. The supernatant was directly loaded onto a DEAE column equilibrated with buffer A and fractionated with 10 column volumes of 0-100% 1 M NaCl in buffer A. Bcd eluted at 65 % of NaCl, the fractions containing the protein were analyzed by SDS-PAGE, pooled and dialyzed against buffer A overnight. The dialyzed protein was concentrated by ultrafiltration and mixed with an equal volume of 2 M $(NH_4)_2SO_4$ and loaded onto a phenyl-Sepharose column pre-equilibrated with 1.5 M $(NH_4)_2SO_4$. The protein was fractionated over a gradient of 100-0% 1.5 M $(NH_4)_2SO_4$. The obtained pure green protein was dialyzed, concentrated and stored at –80 °C until use.

Hydrogenase from *Clostridium pasteurianum* and ferredoxin from *Clostridium tetanomorphum* were prepared as previously reported[35].

Enzyme Assays

Etf_{Me} activity was measured in a 500 µL cuvette (d = 1 cm) containing 50 mM potassium phosphate pH 7.0, 250 µM NADH, and 100 µM iodonitrosotetrazolium chloride (INT). The formation of the red formazane was followed at 492 nm, ε = 19.2 mM^{-1} cm^{-1}[80]. Bcd_{Me} activity was measured in 50 mM potassium phosphate pH 7.0 with 0.2 mM ferricenium hexafluorophosphate (Fc^+) and 0.1 mM butyryl-CoA. The decrease of the absorbance was followed at 300 nm, ε = 4.3 mM^{-1} cm^{-1}, because 2 mol Fc^+ are required to oxidize 1 mol butyryl-CoA [ ]. Unless otherwise indicated the anaerobic assay for Etf_{Me}/Bcd_{Me} activity (bifurcation assay) contained 250 µM NADH, 100 µM crotonyl CoA, 0.5 µM Etf_{Me}, 1 µM Bcd_{Me}, 1 µM ferredoxin, crude hydrogenase (30 µg/ml), and 50 mM potassium phosphate pH 7.0 [ ]. The oxidation of NADH was monitored

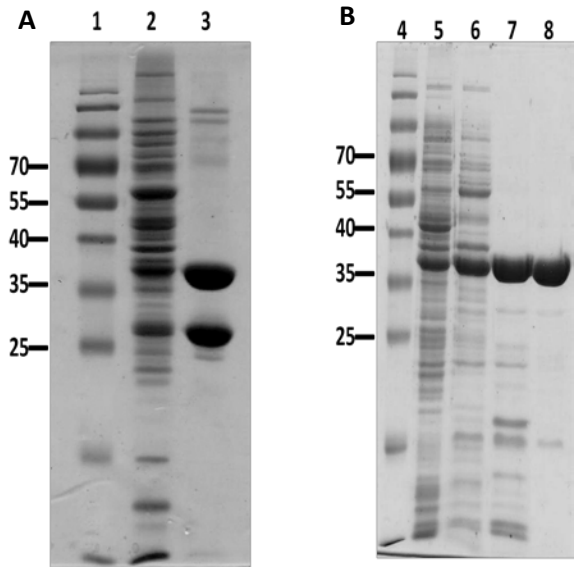

FIGURE 1. SDS-PAGE of recombinant Etf_{Me} (*A, lanes 2-3*) and Bcd_{Me} (B, *lanes 5-8*) at different purification stages. Each contained 10 µg of protein. *Lane 1 & 4*, molecular mass marker. *Lane 2*, cell-free extract of *E.coli*producing Etf_{Me}. *Lane 3*, elute from Strep-tag column. *Lane 5*, cell free extract of *E. coli* producing Bcd_{Me}. *Lane 6*, DEAE-Sepharose eluate. *Lane 7*, Phe-Sepharose eluate. *Lane 8*, purified Bcd_{Me} after gel-filtration.

at 340 nm, ε = 6.3 mM^{-1} cm^{-1}[93]. The aerobic assay (bifurcation assay) was done similar to the anoxic assay, whereby ferredoxin and hydrogenase were omitted. The buffer was well oxygenated by repeated bubbling of oxygen through it.

The H_2O_2 formed by NADH oxidation via bifurcation was determined using the oxidation of 2,2'-azino-bis(3-ethylbenzthiazoline-6-sulfonic acid) (ABTS, Roche Diagnostics, Mannheim, Germany) catalyzed by peroxidase at 412 nm, ε = 45 mM^{-1} cm^{-1} [90]. After the NADH consumption had ceased as measured at 340 nm, 0.2 mM ABTS and 10 µg horseradish peroxidase (Sigma Aldrich, USA) were added. Inhibition of NADH oxidation under aerobic conditions was done using different concentrations of superoxide dismutase (SOD) (Sigma Aldrich, USA). The SOD enzyme was incubated with the reaction mixture for 2 minutes before the start by addition of the CoA-thioester.

Results

Biochemical characterization

To confirm which gene cluster was expressed under the conditions of lactate fermentation by

M. elsdenii (DSM 20460) [94], the soluble proteins of the membrane-free extract were fractionated. Etf_{Me} was kinetically characterized by a formazane producing NADH dependent assay [80] and Bcd_{Me} by the ferricenium assay using butyryl-CoA as the electron donor. The purified proteins were identified by peptide mapping with MALDI-TOF mass spectrometry. Etf_{Me} was found to be encoded by the genes MELS_2126 and MELS_2127 and Bcd_{Me} by MELS_2128 as reported earlier [88, 95]. EtfA and EtfB are composed of 338 and 270 amino acids, respectively, and Bcd_{Me} of 383 amino acids.

We overproduced recombinant Etf_{Me} and Bcd_{Me} with C-terminal Strep-tags (at the alpha-subunit of Etf) in *E.coli* to obtain higher amounts. An earlier report stating the Etf_{Me} to be toxic to the *E.coli* cells when overproduced aerobically [88] was proved to be incorrect in this study. As reported earlier for the untagged native Etf_{Me} [88] the flavin content of was found to be 0.9-1.1 mol FAD/mol protein because the α-FAD was lost during purification. Upon overnight incubation with excess FAD, the flavin content increased to 1.8-1.9 mol FAD/mol protein. A similar observation was reported earlier for Etf from *A. fermentans* [35].

Kinetic characterisation.

Incubation of catalytic amounts of Etf_{Me} and Bcd_{Me} with NADH and crotonyl-CoA under anaerobic conditions caused oxidation of NADH at the very low rate of 0.02 U mg^{-1}Etf (1 U = 1 µmol min^{-1}). Fast oxidation of NADH, up to 0.6 U mg^{-1}, was only observed when catalytic amounts of ferredoxin (1µM) and hydrogenase were added to the reaction mixture (Fig. 2). The products of the reaction were NAD^+, butyryl-CoA (confirmed by HPLC and MALDI-TOF mass spectrometry) and molecular hydrogen. These results were similar to our earlier report with *A. fermentans* [ ].Hence, Etf_{Me} + Bcd_{Me} catalyzed the reduction of crotonyl-CoA to butyryl-CoA coupled to the reduction of ferredoxin (equation 5, see above), whereby hydrogenase recycled the oxidized ferredoxin (equation 6) resulting in equation 7.

(6) $2\ Fd^{2-} + 2\ H^+ \rightleftharpoons 2\ Fd^- + H_2$

(7) Crotonyl-CoA + 2 NADH + 2 $H^+ \rightarrow$ Butyryl-CoA + 2 NAD^+ + H_2

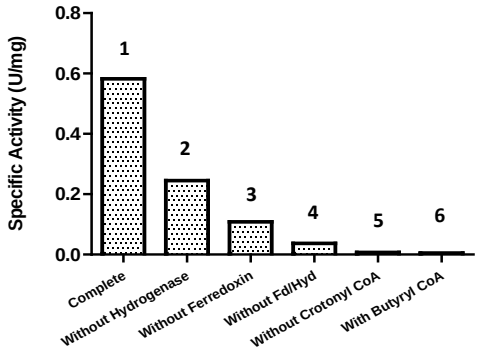

Figure 2. Bifurcation Assay (NADH oxidation assay under anaerobic condition). ***1***, contains 1 µM Etf_{Me}, 0.5 µM Bcd_{Me}, 1 µM $ferredoxin_{Cp}$, 30 µg $hydrogenase_{Ct}$, 250 µM NADH and 100 µM crotonyl-CoA. ***2***, hydrogenase was omitted. ***3***, ferredoxin omitted. ***4***, ferredoxin and hydrogenase were omitted. ***5***, crotonyl-CoA was not added. ***6***, butyryl-CoA added in place of crotonyl-CoA.

Notably omission of Etf_{Me}, Bcd_{Me}, or crotonyl-CoA gave no activity. No reaction was observed when NADH was replaced by NADPH or crotonyl-CoA by butyryl-CoA. The observed stoichiometry of NADH:crotonyl-CoA = 1.8 ± 0.1 was similar to our earlier report with *A. fermentans*. Ttitration of Etf with Bcd increased the rate of NADH oxidation until the optimal ratio of Etf:Bcd (tetramer) = 2:1 was obtained (Fig. 3). The ratio agrees well with that seen in the non-dissociable Bcd-Etf complexes of *C. kluyveri* [ ], *C. difficile* [34], *C. tetanomorphum* [33] and also with the dissociable Bcd-Etf system from *A. fermentans* [35].

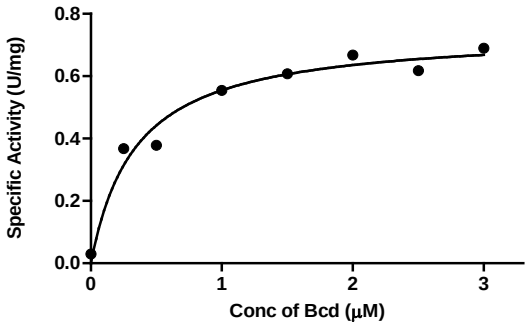

Figure 3. Dependence of the specific activity of NADH oxidation(µmol of NADH/mg of Etf_{Me})on the concentration of the Bcd_{Me} monomer. Each assaycontained 0.5 µM Etf_{Me}, 1 µM ferredoxin and hydrogenase (30 µg/ml).

To prove the tight coupling of ferredoxin reduction with the reduction of crotonyl-CoA, stoichiometric amounts of ferredoxin (15 µM) in the absence of hydrogenase were used. The observed visible spectra in the range of 400-500 nm indicated a complete reduction of the ferredoxin irrespective whether the reduction was performed enzymatically by NADH/crotonyl-CoA mediated by Etf_{Me}/Bcd_{Me} or chemically by dithionite (Fig. 4). These results were similar to those reported for other flavin-based bifurcating systems [, 34, 35, 96].

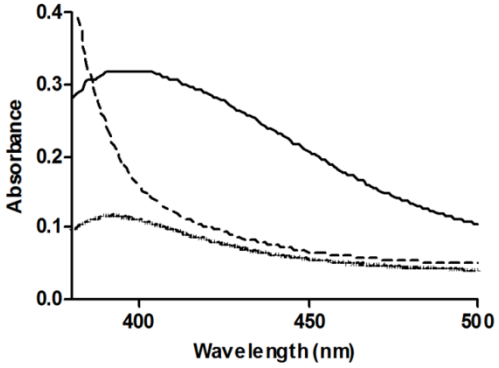

Figure 4. Complete reduction of 15 µM ferredoxin in the bifurcation assay without hydrogenaseSolid line, spectrum of oxidized ferredoxin before starting the bifurcation; **broken line**, excess dithionite added; **dotted line**, after bifurcation terminated due to limiting amounts of ferredoxin

Under aerobic conditions, however, Etf_{Me}/Bcd_{Me} catalyzed the oxidation of NADH in the presence of crotonyl-CoA at an even faster rate (1.0 U mg^{-1}; Fig. 5) than that observed in the absence of oxygen (0.6 U mg^{-1}; Fig. 2). Furthermore, NADH was consumed at the same rate when crotonyl-CoA was exchanged by butyryl-CoA. MALDI-TOF mass spectrometry and HPLC indicated that regardless whether crotonyl-CoA or butyryl-CoA was initially present, always a mixture of both CoA-derivatives was obtained. These experiments match with the older data, which were interpreted as a reduction of crotonyl-CoA by NADH mediated by Etf_{Me}/Bcd_{Me}. In this earlier work, however, the product butyryl-CoA was not identified, nor was crotonyl-CoA replaced by butyryl-CoA [ ].

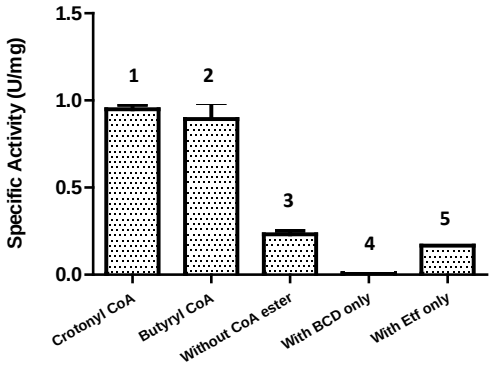

Figure 5.NADH oxidation assay under aerobic condition.*1*, contains 1 µM Etf_{Me}, 5 µM Bcd_{Me},250 µM NADH and 100 µM crotonyl-CoA. ***2***, crotonyl-CoA is replaced by butyryl-CoA. ***3***, CoA ester omitted. ***4***, 5 µM Bcd_{Me} and 250 µM NADH.***5***, 1 µM.$Etf_{Me}$and 250 µM NADH.

We hypothesize that under aerobic conditions oxygen replaces ferredoxin and instead of reduced ferredoxin, H_2O_2 is formed. The overall reaction can be written as shown in equation 8.

(8) Crotonyl-CoA + 2 NADH + 2 H^+ + O_2 → Butyryl-CoA + 2 NAD^+ + H_2O_2.

The formed hydrogen peroxide was analyzed by the peroxidase/ABTS assay (Table 1). The data show that the formed H_2O_2 equals roughly the amount of oxidized NADH. Closer inspection reveals that crotonyl-CoA yields less H_2O_2 than butyryl-CoA, especially at higher concentrations. According to equation 8, however, the oxidation of NADH with crotonyl-CoA via electron bifurcation should yield only ½ H_2O_2 for 1 NADH. Hence, a second source of H_2O_2 must be present in this system, possibly Bcd. After incubation of Bcd with butyryl-CoA for 5 min, ABTS and peroxidase were added (Fig. 6A). There was a very rapid absorbance increase at 412 nm, followed by a slower decline, indicating the formation of H_2O_2 according to equation 9. The immediate absorbance decrease was due to the concomitant action of ABTS as electron acceptor of Bcd.
This was shown under anaerobic conditions by oxidizing ABTS with H_2O_2, followed by addition of Bcd and butyryl-CoA, which resulted in an absorbance decrease at 412 nm (Fig. 6 B).

(9) Butyryl-CoA + O_2 → Crotonyl-CoA+ H_2O_2.

Table 1

	H_2O_2 formed (µM) Butyryl-CoA		Crotonyl-CoA	
CoA ester/NADH (µM)	**250**	**50**	**250**	**50**
25	**250**	**65**	**235**	**39**
50	**260**	**59**	**229**	**37**
75	**256**	**60**	**211**	**34**
100	**263**	**59**	**188**	**35**

Table 1. Concentration of H_2O_2 formed at two different concentration of NADH (250/50 µM). Increasing concentration of CoA ester was added to the assay mixture.

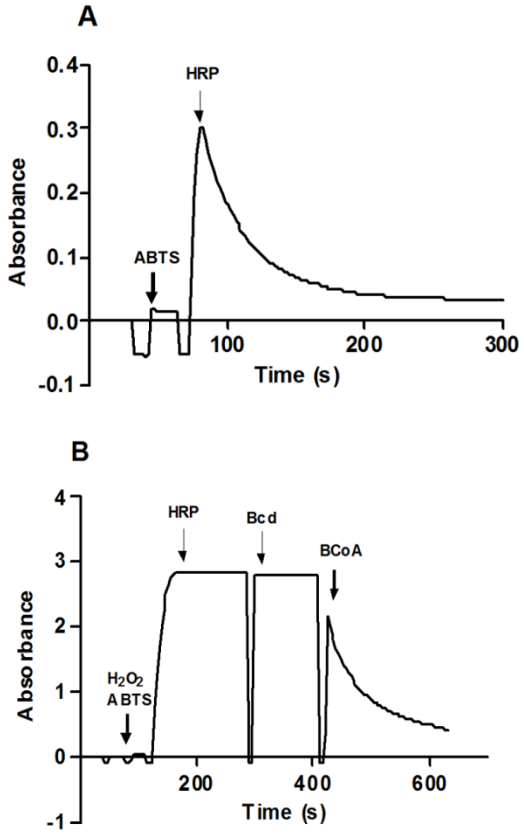

Figure 6. Decolorization of oxidized ABTS. *A*, on incubation of butyryl-CoA with Bcd_{Me}, reaction started by addition of horse radish peroxidase.***B***, color formed by hydrogen peroxide and ABTS/HRP, Bcd_{Me} added after color stabilization, rapid decline in color observed on addition of butyryl-CoA.

If indeed oxygen has replaced ferredoxin, which is reduced by one electron, superoxide must have been an intermediate in the bifurcation of the two electrons from NADH via Etf. To confirm this, we added superoxide dismutase (SOD, equation 10) to the reaction mixture.

(10) 2 $O_2^{\bullet-}$ + 2 H^+ → H_2O_2 + O_2

Catalytic amounts of Etf_{Me} and Bcd_{Me} were incubated with NADH and increasing SOD concentrations. After addition of crotonyl-CoA, the rate of NADH oxidation decreased, maximally by 50% (Fig.7). These results indicate that oxygen is reduced in two steps; one electron is donated to O_2 to give $O_2^{\bullet-}$. In the second round, $O_2^{\bullet-}$ acts as a thermodynamically ($O_2^{\bullet-}/H_2O_2$, E_0' = +940 mV) and presumably also kinetically much better electron acceptor than O_2 ($O_2/O_2^{\bullet-}$, E_0= –330 mV [97] or –160 mV [98]leading to H_2O_2.

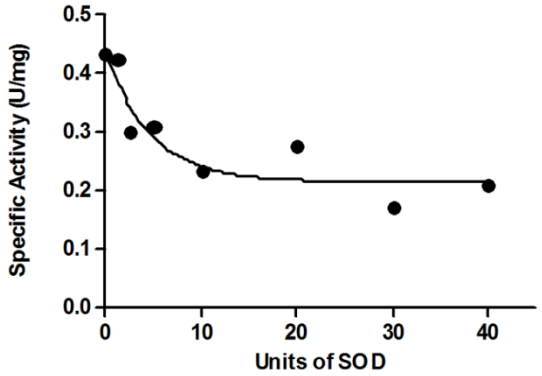

Figure 7.Inhibiton of NADH oxidation by SOD. Maximum 50% decrease in oxidation of NADH under aerobic condition observed with varying concentration of superoxide dismutase

The action of SOD can be described by assuming that the rate of oxygen reduction v_{ox} = k_1 [O_2] is much smaller than the rate of superoxide reduction v_{su} = k_2 [$O_2^{\bullet-}$]. Hence the slow reduction of oxygen is followed by a very fast reduction of superoxide resulting in the total rate v_{tot}' = v_{ox}. Removal of superoxide by SOD decreases v_{su}; when it becomes equal to v_{ox} or lower, the slow oxygen reduction takes over, resulting in v_{tot}'' =½v_{ox} or in an apparent 50% inhibition of the reaction without SOD.

Spectroscopic characterization.

The UV-visible absorption spectrum of Etf_{Me} under aerobic conditions exhibited two peaks at 375 and 450 nm similar to that of FAD. Stepwise addition of 2.5 µM amounts of NADH to 10 µM Etf (containing around 18 µM FAD) under anaerobic conditions and in absence of Bcd (Fig. 8A) revealed a shift in the absorption peak at 375 to 370 nm; similar observations were made with Etf from *A. fermentans* (Etf_{Af}) and Etf_{Me} [35, 86, 87]. Although a pronounced rise in the 370nm peak was observed when holo Etf_{Me} was titrated at pH 6 with NADH [87], only a small rise was observed in this study. An interesting observation was made when Etf was titrated in presence of Bcd. The absorption of the anionic semiquinone at 370 nm was much more pronounced, similar to our earlier report [35] (Fig. 8B). The peak reached its maximum at the ratio NADH/FAD around 1/2.

A titration of Etf/Bcd with butyryl-CoA also showed a stable anionic semiquinone peak at 370 nm with a similar intensity (Fig. 8C) as observed in the titration Etf/Bcd with NADH. This indicates that Etf_{Me} is also able to act as electron acceptor of acyl-CoA dehydrogenases as observed with the FAD and AMP containing Etfs.

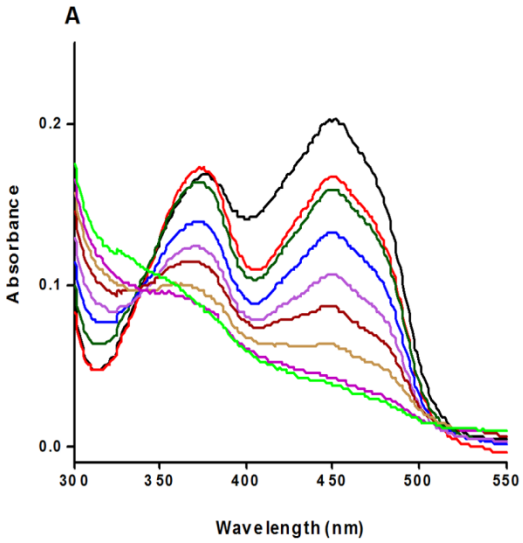

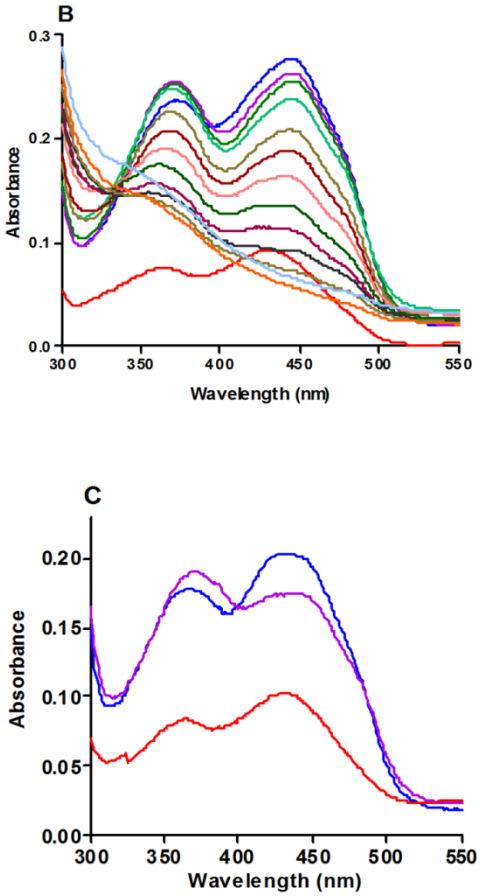

Figure 8 (A,B,C) Formation of stable red anionic FAD semiquinones. A,10 10 µM Etf NADH was added stepwise : 0 (black),2.5 (red),5 (deep green),7.5 (blue),10 (magenta),12.5 (brown),15 (mustard), 17.5 (violet),20 µM (fluorescent green). **B**, 10 µM Bcd subunit (red) and 10 µM Etf, NADH, added stepwise: 0 (blue), 2.5 (violet), 5 (deep green), 7.5 (light green), 10 (grey), 12.5 (brown), 15 (pink), 17.5 (dark green), 20 (magenta), 22.5 (ash), 27.5 (saffron), 32.5 µM (sky blue). **C**, same as B but instead of NADH , 100 µM butyryl-CoA was added.

Sequence alignment

FAD binding in human Etf (Etf_{Hu}) has been extensively studied [99]. As most Etfs from aerobic and facultative bacteria, Etf_{Hu} contains only one FAD which corresponds to α-FAD in Etf_{Me}, whereas at the place of β-FAD only AMP is present in the molecule. The binding of the FAD in Etf_{Hu} involves eighteen residues within hydrogen bonding distances. This α-FAD binding site has been conserved mostly in all the sequenced Etfs, 13 residues are highly conserved (yellow and red highlighted) irrespective of the two FAD or one FAD containing Etfs. The notable differences compared to the human Etf

and *M. elsdenii* is at the residues binding the AMP part of the α-FAD, Lysα226in Etf_{Hu} is replaced by Asnα225. The residues binding the isoalloxazine ring of the FAD remain the same except the human Tyrβ16, which interacts with C8-CH_3, is replaced by Thrβ12in *M. elsdenii* and in all other bifurcating Etfs. In Etf_{Hu} the C2 carbonyl oxygen atom of FAD is H-bonded to Hisα286 which is conserved in *M. elsdenii* (Hisα287) and other Etfs (marked in red).This histidine stabilizes the red anionic semiquinone, visible during titration of Etf-Bcd with NADH. Further stabilization also comes from Argα250 and Thrα267 (highlighted inred)as compared with Etf_{Hu} and Etf_{Af} [35, 99].A close comparison of Etf_{Me} with Etf_{Af} also shows the same arrangement of amino acids around the FAD proving that the architecture of the region around the α-subunit has been conserved across different species.

The crystal structure of Etf_{Af} revealed the second flavin binding site at the β-subunit. Since Etf_{Me} also binds a second FAD, it is worthwhile to find similarities in the binding domains of β-FAD. It was found in Etf_{Af} that the planar tricyclic isoalloxazine ring is flanked from the *si*-face by Thrβ125, Glyβ123, Argα146 and Alaα148 and from the *re*-face by Ileα157, Thrβ221 and Valβ223 [35]. On comparing the sequence of Etf_{Me} with those of other bifurcating Etfs, all of these residues are highly conserved (highlighted in ash). Other identical residues in Etf_{Af} and Etf_{Me} around β-FAD are Leuα127, Alaα148, and Thr-β94, which are also conserved in other bifurcating Etfs. Interestingly, on comparison of the sequence with the structure of the Etf from *Paracoccus dentrificans* [100], Ser-β62, Gly-β120, Lys-β121 interacting with the AMP moiety (highlighted in yellow) were similar to Etf_{Me} were conserved. The Lys-β121 from *P. denitrificans* is replaced by Arg in *A. fermentans* and *C. kluyveri* and *C. difficile* (conservative change). Taking all conserved residues, a specific region within this β domain: -GR(K)QAIDGDTAQVGPE(Q)- arises (highlighted in red) which is specially conserved for 2 FAD containing and bifurcating Etfs. This sequence can be regarded as a signature for the bifurcating Etfs.

A

```
Ckluy          RDLGPRVAGRVFTGLTADCTGLDIDEATKNLMMTRPAFGGNLMATIACEKTRPQMSTVRP 166
Cdiff          RDLAPRVSARIHTGLTADCTGLAVAEDTKLLLMTRPAFGGNIMATIVCKDFRPQMSTVRP 161
Mels           RDLGPRVANSLKTGLTADCTQLGVDDDKKTIVWTRPALGGNIMAEIICPDNRPQMGTVRP 166
Afer           RDLGPRIAARVNTGLCADCTILDAEED-GLIEWTRPAAGGNIMATILCKEHRPQMGTVRP 171
Mmet           LGYASSLASKTGYGFATDVYIVEYQGD--ELVATRGGYNQKVNVEVDFPGKSTVVLTIRP 158
Para           KNVMPRVAALLDVMVLSDVSAILDADT-----FERPIYAGNAIQVVKSKD-AKKVFTIRT 149
Hsap           KNLLPRVAAKLEVAPISDIIAIKSPDT-----FVRTIYAGNALCTVKCDE-KVKVFSVRG 170
                 .  . ::        :*   :            *     :    :        : ::*

Ckluy          GVFNALPRDASRTGKIEKIAANVAKDDIRIEVLEVVKSAGDTIDISEADVIVSGGRGLGG 226
Cdiff          GVMKKNEPDETKEAVINRFKVEFNDADKLVQVVQVIKEAKKQVKIEDAKILVSAGRGMGG 221
Mels           HVFKKPEADPSATGEVIEKKANLSDADFMTKFVELIKLGGEGVKIEDADVIVAGGRGMNS 226
Afer           KTFKAMEPDASRTGEVINYTLKNHVDDRVTCIRREEVVSEGEMAIDDAPFVCSGGRGMKA 231
Mmet           SVFKPLEG---AGSPVVSNVDAPSVQSRSQNKDYVEVGGGNDIDITTVDFIMSIGRGIGE 215
Para           ASFDAAGE---GGTAPVTETAAAADP-GLSSWVADEVAESDRPELTSARRVVSGGRGLGS 205
Hsap           TSFDAAAT---SGGSASSEKASSTSPVEISEWLDQKLTKSDRPELTGAKVVVSGGRGLKS 227
                 :.                                          :   .   : : ***:

Ckluy          PDGFK--VLKELADLLGGTIGGSRATIDAGWIDKSYQVGQTGKTVR-PGLYIACGISGQI 283
Cdiff          KENLD--ILYELAEIIGGEVSGSRATIDAGWLDKARQVGQTGKTVR-PDLYIACGISGAI 278
Mels           EEPFKTGILKECADVLGGAVGASRAAVDAGWIDALHQVGQTGKTVG-PKIYIACAISGAI 285
Afer           KENFS--LLYDLAHALGGAVGGSRAAVDEGFIEHPRQVGQSGKTVT-PKIYFACGISGSV 288
Mmet           ETNVE--QFRELADEAGATLCCSRPIADAGWLPKSRQVGQSGKVVGSCKLYVAMGISGSI 273
Para           KESFA--IIEELADKLGAAVGASRAAVDSGYAPNDWQVGQTGKVVA-PELYVAVGISGAI 262
Hsap           GENFK--LLYDLADQLHAAVGASRAAVDAGFVPNDMQVGQTGKIVA-PELYIAVGISGAI 284
                  .    : : *.   . :  **.  * *:     ****:** *    :*.* .*** :

Ckluy          QHLAGMQDSGFIVAINKDENAPMMQVADLAIVGDLYKVVPEFVEQVKALNL------- 334
Cdiff          QHIAGMEDAEFIVAINKNPEAPIFKYADVGIVGDVHKVLPELISQLSVAKEKGEVLAN 336
Mels           QHLAGMTGSDCIIAINKDEDAPIFKVCDYGIVGDVFKVLPLLTEAIKKQKGIA----- 338
Afer           QHKAGMSKSDTIVCINKDPDAPMFEISKYGIVGDALKILPLLTAKIKAFKES------ 340
Mmet           QHMAGMKHVPTIIAVNTDPGASIFTIAKYGIVADIFDIEEELKAQLAA---------- 321
Para           QHLAGMKDSKVIVAINKDEEAPIFQIADYGLVGDLFSVVPELTGKL------------ 308
Hsap           QHLAGMKDSKTIVAINKDPEAPIFQVADYGIVADLFKVVPEMTEILKKK--------- 333
```

B

```
Afer            GAHVTVITMGPPHAESVLRDCLAVGADEAKLVSDRAFGGA--DTLATSAAMANTIKHFGV 110
Elsdenii        DVKITLLSMGPDQAKDVLREGLAMGADDAYLLSDRKLGGS--DTLATGYALAQAIKKLAA 111
Kluyveri        GGTVTVVSMGPPQAVDALREALAMGADEAILVSDRAFAGA--DTQATSYALAGALKNLEY 110
Difficile       GAHVTVITMGPPQADMALKEALAMGADRGILLTDRAFAGA--DTWATSSALAGALKNIDF 115
Paracoccus      AEEIIAVSIGVKQAAETLRTALAMGADRAILVVAADDVQQDIEPLAVAKILAAVARAEGT 114
Human           VKEVIAVSCGPAQCQETIRTALAMGADRGIHVEVPPAEAERLGPLQVARVLAKLAEKEKV 117
Methylo         DVEVVVVSVGPDRVDESLRKCLAKGADRAVRVWDDAAEGS--DAIVVGRILTEVIKKEAP 113
:  :: *       ::  :* *** .  :           .  ..  ::   .

Afer            P------DLILCGRQAIDGDTAQVGPEIAEHLGLPQVTAALKVQVK--DDTVVVDRDNEQ 162
Elsdenii        DKGIEQFDIILCGKQAIDGDTAQVGPQIACELGIPQITYARDIKVE--GDKVTVQQENEE 169
Kluyveri        D-------LIFAGRQAIDGDTAQVGPQIAEKLGIPQITYVEKVDVD--GDTLTVQRAWED 161
Difficile       D-------IIIAGRQAIDGDTAQVGPQIAEHLNLPSITYAEEIKTE--GEYVLVKRQFED 166
Paracoccus      E-------LIIAGKQAIDNDMNATGQMLAAILGWAQATFASKVEIE--GAKAKVTREVDG 165
Human           D-------LVLLGKQAIDDDCNQTGQMTAGFLDWPQGTFASQVTLE--GDKLKVEREIDG 168
Methylo         D-------MVFAGVQSSDQAYASTGISVASYLNWPHAAVVADLQYKPGDNKAVIRRELEG 166
::: * *: *     .*   *  *. .  :    :  .  .    : :  :
Afer            GKAGSPTQVMKSFTP-KVTQVHGEIFDDEDPAVAVDKLVNKLIEDKIITK 263
Elsdenii        GLSGSPTKVRKIFTPPQRSGGLVLKVEDDNEQAIVDQVMEKLVAQKII-- 270
Kluyveri        GLNGSCTKVKRSHTKEAKGAG---EIVNKPIKEAVAYSISKLREKHVI-- 259
Difficile       GLKGSPTSVFKSFTKSVKPAG---TIYNEDAKTSAGIIIDKLKEKYII-- 265
Paracoccus      VDVAPRLEVVSVREPEGRKAG--------IKVGSVDELVGKLKEAGVI-- 252
Human           VDLTSKLSVISVEDPPQRTAG--------VKVETTEDLVAKLKEIGRI-- 255
Methylo         GAAQSMSRVRRMYIPEKGRAT----MIEGTISEQAAKIIQIINEFKGA— -264
```

Figure 9.*A*, sequence alignment of α-subunit'***s*,** of β subunit across 7 different species

Discussion

Baldwin and Milligan [84] demonstrated that partially purified Etf and Bcd from *M. elsdenii* catalyzed the reduction of crotonyl-CoA by NADH without adding ferredoxin. Since then Etf_{Me} became one of the well-studied Etfs and over a dozen papers [85, 86, 88] have been published on this issue. Whereas all known Etfs act as one-electron acceptors for acyl-CoA dehydrogenase and act as electron carrier to the membrane-bound Etf-quinone oxidoreductase, Etf_{Me} was the only Etf that is reduced by NADH and carries the electron to Bcd. We became interested in this work, when we established the related Etf_{Af} as bifurcating protein [35].This led us to re-investigate Etf_{Me} and Bcd_{Me}.

We cloned the genes encoding Etf_{Me} and Bcd_{Me} and expressed them as Strep-tagged proteins in *E. coli*. The sequence analysis of Etf_{Me} revealed 50% identity to that of Etf_{Af}. This was not surprising since *M. elsdenii* and *A. fermentans* both belong to the *Negativicutes*. But also the sequences of the other bifurcating Etfs from clostridia and *Acetobacterium woodii* exhibited similar close relationships.

Furthermore the sequence analysis showed no significant differences between the free Etfs as are Etf_{Me} and Etf_{Af}, and the clostridial and acetogenic Etfs, which form tight complexes with their corresponding dehydrogenases. [35]. All these bifurcating Etfs contain a second FAD located between the β-subunit (domain III) and domain I of the α-subunit. The amino acid residues of the β-subunit, interacting with the isoalloxazine ring of this β-FAD, form a conserved stretch of ten amino acids, which can be used as a signature for a bifurcating Etf.

The spectroscopic and kinetic characterizations of Etf_{Me} under anaerobic conditions revealed no significant difference to Etf_{Af}. Upon addition of NADH the Etfs transiently form an anionic semiquinone, which is more pronounced in the presence of their cognate butyryl-CoA dehydrogenase (Bcd), whereby the optimum ratio of heterodimeric Etf: tetrameric Bcd has been determined as 2:1. Together with their Bcd, Etfs couple the

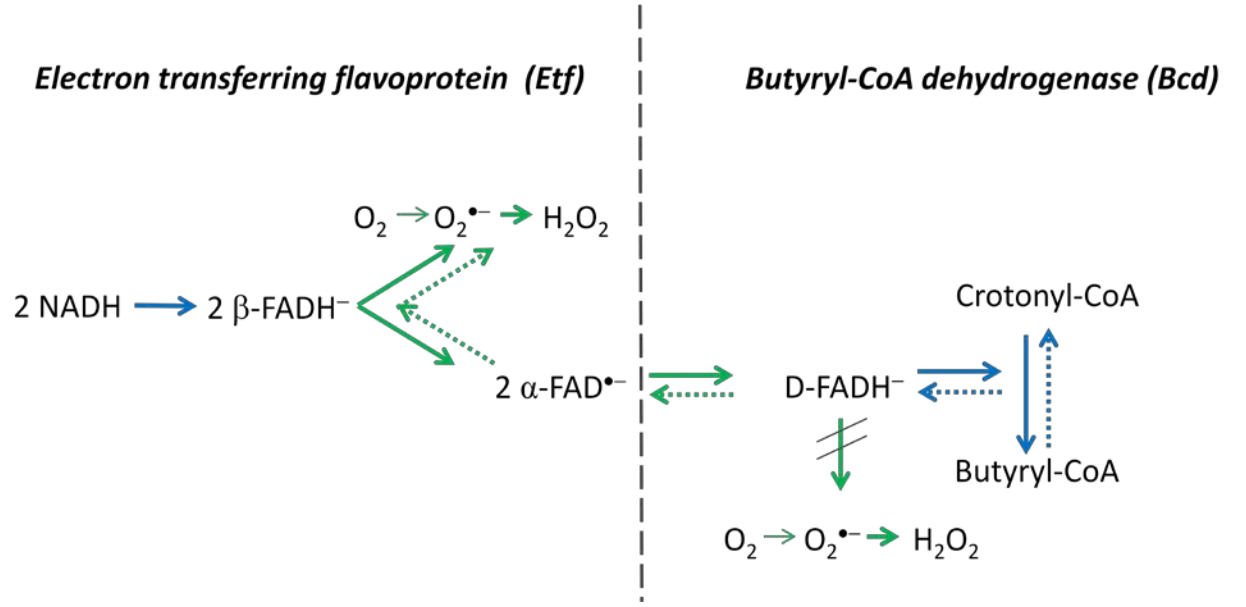

Figure 10. Proposed mechanism of H_2O_2 formation during bifurcation under aerobic conditions (Blue and green arrows represent two electron and once electron transfer)

exergonic reduction of crotonyl-CoA to butyryl-CoA (E_0'= –10 mV) by NADH (E' = –280 mV) to the endergonic reduction of ferredoxin (E_0' = –420 mV) by NADH. Thereby ferredoxin is almost completely reduced and approaches E' = –500 mV. The reduced ferredoxin can be used for formation of hydrogen and for energy conservation via the Na^+-pumping ferredoxin-NAD reductase also called Rnf.

Closer examination of the Etf_{Me} literature revealed that all reductions of crotonyl-CoA by NADH were done under aerobic conditions. Therefore we repeated the bifurcation experiment with Etf_{Me}, Bcd_{Me}, NADH and crotonyl-CoA in air-saturated water and found no requirement for ferredoxin, but we observed the formation of H_2O_2. Addition of increasing amounts of SOD inhibited the oxidation of NADH up to 50% indicating a slow reduction of O_2 to superoxide ($O_2^{\bullet-}$) followed by a fast reduction of the latter to H_2O_2 (see Results section). Replacement of ferredoxin by O_2 in the bifurcation process could explain these data. In reality, the system is more complex, since according to equation 8 the reduction of 25 µM crotonyl-CoA should require 50 µM NADH and yield 25 µM H_2O_2, but 250 µM NADH have been consumed and 250 µM H_2O_2 have been measured. Only the limiting amounts of 50 µM NADH approach the expected stoichiometry of close to 25 µM H_2O_2 (Table 1). Furthermore, the stoichiometry of NADH/H_2O_2 close to 1.0 was observed with butyryl-CoA as substrate. Hence the reaction must go backwards. The formed butyryl-CoA is oxidized again to crotonyl-CoA and the electrons return one by one from D-$FADH^-$ of Bcd to α-FAD of Etf. The obtained α-$FAD^{\bullet-}$transfers its electron via β-FAD to O_2or $O_2^{\bullet-}$. Thus two H_2O_2 are formed per oxidized NADH, one in the forward direction and the other in the reverse reaction, which agrees with our measurements (Table 1). Now crotonyl-CoA is reduced again by NADH and the resulting butyryl-CoA is re-oxidized until all NADH is consumed. Therefore, in the presence of catalytic amounts of crotonyl-CoA or butyryl-CoA, Etf/Bcd can be regarded as a NADH oxidase (H_2O_2 forming; EC 1.6.3.3). The obtained mixtures of crotonyl-CoA and butyryl-CoA after NADH consumption agree well with this concept.

An alternative explanation for the NADH oxidase activity could be the formation of H_2O_2 at D-FAD^- of Bcd (Fig. 10), as observed with butyryl-CoA and ABTS in the absence of Etf and NADH (Fig. Y). There are three arguments

against this explanation. (i) The redox potential of D-FAD is too high for the reduction of $O_2$to $O_2^{\bullet-}$, whereas a direct reduction to H_2O_2 is possible. If β-FADH$^{\bullet}$ would reduce $O_2$to $O_2^{\bullet-}$ and D-FAD^{-}would reduce $O_2$to H_2O_2, the inhibition by SOD should be only 25% rather than 50%. (ii) D-FADH$^{\bullet}$or D-FAD^{-}should also react with O_2 before the electrons reduce crotonyl-CoA, which is not observed. (iii) Etf should protect D-FAD^{-} from the reaction with oxygen, because α-FAD$^{\bullet-}$ of Etf reversibly transfers one electron to D-FAD or to D-FADH$^{\bullet}$.

The use of oxygen as electron acceptor in the bifurcation by Etf/Bcd readily explains the earlier data on the presumed ferredoxin independent reduction of crotonyl-CoA to butyryl-CoA by NADH. As HPLC of CoA thioesters was not well established in these days, the authors never measured whether crotonyl-CoA was indeed reduced to butyryl-CoA. Furthermore, they never tried to use the believed product butyryl-CoA as substrate. In contrast to all other established bifurcating systems, Etf/Bcd has the extraordinary property of being insensitive to oxygen, because it contains no iron-sulfur cluster. Therefore it is an ideal system to study the formation of reactive oxygen species by flavin-based electron bifurcation (FBEB), which can be regarded as an "Achilles' heel" of anaerobic bacteria. Preliminary results with Etf/Bcd from *A. fermentans* indicate that the NADH oxidase activity is not a specialty of *M. elsdenii*. Furthermore, the tight Etf/Bcd complex from *C. difficile* also produces ROS under air.

ROS are well-known to be formed in the mitochondrial respiratory chain. The responsible enzyme complexes also bifurcate, FBEB in complex I and quinone based electron bifurcation (QBEB) in complex III. Hence, electron bifurcation appears to be the main source of ROS in biology.

The results presented in this work have also implications on the pathway of lactate fermentation in *M. elsdenii*, which will be discussed elsewhere.

References

1. Elsden, S. R., Gilchrist, F. M., Lewis, D., and Volcani, B. E. (1956) Properties of a fatty acid forming organism isolated from the rumen of sheep. *J Bacteriol***72**, 681-689
2. Counotte, G. H., Prins, R. A., Janssen, R. H., and Debie, M. J. (1981) Role of *Megasphaera elsdenii* in the Fermentation of dl-[2-^{13}C]lactate in the Rumen of Dairy Cattle. *Appl Environ Microbiol***42**, 649-655
3. Hashizume, K., Tsukahara, T., Yamada, K., Koyama, H., and Ushida, K. (2003) *Megasphaera elsdenii* JCM1772T normalizes hyperlactate production in the large intestine of fructooligosaccharide-fed rats by stimulating butyrate production. *J Nutr***133**, 3187-3190
4. Marounek, M., Fliegrova, K., and Bartos, S. (1989) Metabolism and some characteristics of ruminal strains of *Megasphaera elsdenii*. *Appl Environ Microbiol***55**, 1570-1573
5. Baldwin, R. L., Wood, W. A., and Emery, R. S. (1965) Lactate Metabolism by *Peptostreptococcus Elsdenii*: Evidence for Lactyl Coenzyme a Dehydrase. *Biochim Biophys Acta***97**, 202-213
6. Brockman, H. L., and Wood, W. A. (1975) Electron-transferring flavoprotein of Peptostreptococcus elsdenii that functions in the reduction of acrylyl-coenzyme A. *J Bacteriol***124**, 1447-1453
7. Baldwin, R. L., and Milligan, L. P. (1964) Electron Transport in *Peptostreptococcus Elsdenii*. *Biochim. Biophys. Acta***92**, 421-432
8. Whitfield, C. D., and Mayhew, S. G. (1974) Purification and properties of electron-transferring flavoprotein from *Peptostreptococcus elsdenii*. *J. Biol. Chem.***249**, 2801-2810
9. Sato, K., Nishina, Y., and Shiga, K. (2003) Purification of electron-transferring flavoprotein from *Megasphaera elsdenii* and binding of additional FAD with an unusual

absorption spectrum. *J. Biochem.***134**, 719-729
10. Sato, K., Nishina, Y., and Shiga, K. (2013) Interaction between NADH and electron-transferring flavoprotein from *Megasphaera elsdenii*. *J. Biochem.***153**, 565-572
11. O'Neill, H., Mayhew, S. G., and Butler, G. (1998) Cloning and analysis of the genes for a novel electron-transferring flavoprotein from *Megasphaera elsdenii*. Expression and characterization of the recombinant protein. *J. Biol. Chem.***273**, 21015-21024
12. Marchandin, H., Teyssier, C., Campos, J., Jean-Pierre, H., Roger, F., Gay, B., Carlier, J. P., and Jumas-Bilak, E. (2010) *Negativicoccus succinicivorans* gen. nov., sp. nov., isolated from human clinical samples, emended description of the family *Veillonellaceae* and description of *Negativicutes classis* nov., *Selenomonadales* ord. nov. and *Acidaminococcaceae* fam. nov. in the bacterial phylum *Firmicutes*. *Int. J. Syst. Evol. Microbiol.***60**, 1271-1279
13. Chowdhury, N. P., Mowafy, A. M., Demmer, J. K., Upadhyay, V., Koelzer, S., Jayamani, E., Kahnt, J., Hornung, M., Demmer, U., Ermler, U., and Buckel, W. (2014) Studies on the Mechanism of Electron Bifurcation Catalyzed by Electron Transferring Flavoprotein (Etf) and Butyryl-CoA Dehydrogenase (Bcd) of *Acidaminococcus fermentans*. *J. Biol. Chem.***289**, 5145-5157
14. Herrmann, G., Jayamani, E., Mai, G., and Buckel, W. (2008) Energy conservation via electron-transferring flavoprotein in anaerobic bacteria. *J. Bacteriol.***190**, 784-791
15. Li, F., Hinderberger, J., Seedorf, H., Zhang, J., Buckel, W., and Thauer, R. K. (2008) Coupled ferredoxin and crotonyl coenzyme A (CoA) reduction with NADH catalyzed by the butyryl-CoA dehydrogenase/Etf complex from *Clostridium kluyveri*. *J. Bacteriol.***190**, 843-850
16. Buckel, W., and Thauer, R. K. (2013) Energy conservation via electron bifurcating ferredoxin reduction and proton/Na^+ translocating ferredoxin oxidation. *Biochim. Biophys. Acta***1827**, 94-113
17. Parthasarathy, A., Pierik, A. J., Kahnt, J., Zelder, O., and Buckel, W. (2011) Substrate Specificity of 2-Hydroxyglutaryl-CoA Dehydratase from *Clostridium symbiosum*: Toward a Bio-Based Production of Adipic Acid. *Biochemistry***50**, 3540-3550
18. Buckel, W. (1986) Biotin-dependent decarboxylases as bacterial sodium pumps: Purification and reconstitution of glutaconyl-CoA decarboxylase from *Acidaminococcus fermentans*. in *Meth. Enzymol.* (Sidney Fleischer, B. F. ed.), Academic Press. pp 547-558
19. Hetzel, M., Brock, M., Selmer, T., Pierik, A. J., Golding, B. T., and Buckel, W. (2003) Acryloyl-CoA reductase from *Clostridium propionicum*. An enzyme complex of propionyl-CoA dehydrogenase and electron-transferring flavoprotein. *Eur. J. Biochem.***270**, 902-910
20. Bradford, M. M. (1976) A rapid and sensitive method for the quantitation of microgram quantities of protein utilizing the principle of protein-dye binding. *Anal. Biochem.***72**, 248-254
21. Laemmli, U. K. (1970) Cleavage of structural proteins during the assembly of the head of bacteriophage T4. *Nature***227**, 680-685
22. Prabhu, R., Altman, E., and Eiteman, M. A. (2012) Lactate and acrylate metabolism by *Megasphaera elsdenii* under batch and steady-state conditions. *Appl. Environ. Microbiol.***78**, 8564-8570
23. Wohlfarth, G., and Buckel, W. (1985) A sodium ion gradient as energy source for *Peptostreptococcus asaccharolyticus*. *Arch. Microbiol.***142**, 128-135
24. Lehman, T. C., Hale, D. E., Bhala, A., and Thorpe, C. (1990) An acyl-coenzyme A dehydrogenase assay

utilizing the ferricenium ion. *Anal. Biochem.***186**, 280-284
25. Ziegenhorn, J., Senn, M., and Bücher, T. (1976) Molar absorptivities of beta-NADH and beta-NADPH. *Clin. Chem.***22**, 151-160
26. Marx, H., Graf, A. B., Tatto, N. E., Thallinger, G. G., Mattanovich, D., and Sauer, M. (2011) Genome sequence of the ruminal bacterium Megasphaera elsdenii. *J Bacteriol***193**, 5578-5579
27. Djordjevic, S., Pace, C. P., Stankovich, M. T., and Kim, J. J. (1995) Three-dimensional structure of butyryl-CoA dehydrogenase from *Megasphaera elsdenii*. *Biochemistry* **34**, 2163-2171
28. Aboulnaga, E.-H., Pinkenburg, O., Schiffels, J., El-Refai, A., Buckel, W., and Selmer, T. (2013) Butyrate production in *Escherichia coli*: Exploitation of an oxygen tolerant bifurcating butyryl-CoA dehydrogenase/electron transferring flavoprotein complex from *Clostridium difficile*. *J. Bacteriol.***195**, 3704-3713
29. Kölzer, S. (2008) Aufreiningung und Charakterisierung des Butyryl-CoA Dehydrogenase/ETF Komplexes aus *Clostridium tetanomorphum*. Philipps-Universität, Marburg, Germany
30. Bertsch, J., Parthasarathy, A., Buckel, W., and Müller, V. (2013) An electron-bifurcating caffeyl-CoA reductase. *J. Biol. Chem.***288**, 11304-11311
31. Muir Wood, P. (1974) The redox potential of the system oxygen--superoxide. *FEBS Lett***44**, 22-24
32. Mishra, S., and Imlay, J. (2012) Why do bacteria use so many enzymes to scavenge hydrogen peroxide? *Arch Biochem Biophys***525**, 145-160
33. Roberts, D. L., Frerman, F. E., and Kim, J. J. (1996) Three-dimensional structure of human electron transfer flavoprotein to 2.1-A resolution. *Proc. Natl. Acad. Sci. U S A***93**, 14355-14360
34. Roberts, D. L., Salazar, D., Fulmer, J. P., Frerman, F. E., and Kim, J. J. (1999) Crystal structure of *Paracoccus denitrificans* electron transfer flavoprotein: structural and electrostatic analysis of a conserved flavin binding domain. *Biochemistry***38**, 1977-1989

2.3.2 Lactate dehydrogenase of *Megasphaera elsdenii*

Summary

The first step of lactate to pyruvate oxidation in *M. elsdenii* is done by the enzyme D-lactate dehydrogenase. Here we present initial results of an on-going project, where we have purified the D-lactate dehydrogenase (D-Ldh) from the cell free extracts of *M. elsdenii* and show that the electrons from D-lactate can be transferred to the electron transferring flavoprotein (Etf) by the purified enzyme D-Ldh in a stepwise manner. Etf can then carry single electron one by one to the butyryl-CoA dehydrogenase (Bcd) where crotonyl-CoA is reduced to butyryl-CoA. In the intial results presented we find that the Etf can not only bifurcate electrons as presented earlier but also can shuttle single electrons like classical type Etf to the Bcd. This is however a very short study to draw any final conclusion. The intial results are presented in a manuscript format to keep parity with earlier chapters.

Lactate dehydrogenase and electron transferring flavoprotein of *Megasphaera elsdenii*

Nilanjan Pal Chowdhury[1, 2], Arno Fricke[1] and Wolfgang Buckel[1, 2]

From the [1]Laboratorium for Microbiology, FachbereichBiologie and SYNMIKRO, Philipps-University,35032 Marburg, Germany, the [2]Max-Planck-Insitute for terrestrial Microbiology, Karl-von-Frisch-Str 10, 35043 Marburg, Germany

Background: Lactate dehydrogenase (Ldh) transfers single electron one by one to butyryl-CoA dehydrogenase (Bcd) via electron transferring flavoprotein (Etf)
Results: On receiving an electron from Ldh, Etf stabilizes a red semiquinone which helps in single electron transfer to the Bcd.
Conclusion: Ldh uses Bcd as an electron sink for oxidation of lactate to pyruvate, Etf transfer single electron from Ldh to Bcd and has bifunctional role.
Significance: Explains the dual role-play of Etf in anaerobic metabolism

Introduction

Megasphaera elsdenii, an obligate anaerobic bacterium, ferments D,L-lactate mainly to acetate, propionate, butyrate, valerate and traces of caproate [48]. In the initial steps of the fermentation pathway, D-lactate is oxidized to pyruvate and further to acetate with ATP generation. L-Lactate is converted to D-lactate by a soluble lactate racemase [83, 101]. Using partially purified preparations it has been shown that the electron transferring flavoprotein (Etf_{Me}) acts as oxidant of D-lactate and carries the electrons to the electron sink butyryl-CoA dehydrogenase [83]. Hence, in the oxidation of lactate, Etf_{Me} is proposed to act similar to the Etfs from mammalian sources and bacteria like *Paracoccus denitrificans* [99, 100], which contain one FAD and one AMP per heterodimer of the enzyme. The Etfs from these sources function in shuttling single electron from the interacting acyl-CoA dehydrogenases to the membrane quinone pool. Thus Etf_{Me} should also transport one by one electron from the lactate dehydrogenase to the butyryl-CoA dehydrogenase. In Chapter 3A, however, Etf_{Me} has been shown to be a bifurcating protein with two FAD at different positions. Now the question arises, how Etf_{Me} balances between these dual functions of bifurcation and single electron transfer.

Here we present a short study in which we have purified lactate dehydrogenase from the cell extracts of *M. elsdenii* and using UV-visible spectroscopy we present initial evidences that Etf_{Me} in combination with Ldh transfers single electrons similar to mammalian Etfs.

Results

Purification of lactate dehydrogenase

All purification steps were carried out under aerobic conditions unless mentioned. Ten g of *M. elsdenii* wet cells were dissolved in 100 mM phosphate buffer pH 6.5 and disrupted in a French press. Unbroken cells and membranes were removed by centrifugation of the cell extract at 300,000 × *g* for one hour. The membrane free extract was then filtered and loaded onto a 60 ml DEAE column which was pre-equilibrated with 50 mM phosphate buffer pH 6.5 + 1 mM DTT (Buffer A).After loading, unbound proteins were washed out with 2column volumes (CV) of Buffer A and elution was achieved in 10 CV 0%-100% 1M NaCl in buffer A. The fractions, which showed the highest activity in the ferricenium assay, eluted at 0.35 M NaCl in Buffer A. The active fractions were pooled, concentrated and diluted with 30 mM phosphate buffer pH 6.5 to a final volume of 20 ml.This 20ml protein was mixed with equal volume of 3 M $(NH_4)_2SO_4$ to get a final concentration of 1.5 (M) $(NH_4)_2SO_4$. After the

proteins were bound to the phenyl-Sepharose matrix, it was washed with 2 CV of 1.5 M ammonium sulphate in buffer A. The proteins fractions with the highest activity eluted in a reverse gradient from 100%-0% 1.5 M ammonium sulphate at 1.20 M ammonium sulphate. The protein with highest activity was again concentrated and separated over a 120 ml Superdex 200 gel filtration column to homogeneity. The fractions were loaded into a SDS gel revealing different grades of purity of the protein and were further analyzed via MALDI-TOF mass spectrometry.

Protein detection by ferricenium assay

Lactate dehydrogenase activity was measured with ferricenium hexafluorophosphate ($FcPF_6$) as an artificial electron acceptor (ferricenium assay). The reaction mixture contained 50 mM phosphate buffer pH 7, 0.5 mM $FcPF_6$ and 1 mM D,L-lactate as an electron donor. The $FcPF_6$ was previously prepared in a 10 mM HCl solution to a final concentration of 5 mM set at 617 nm (ε_{617}= 0.1 $mM^{-1}cm^{-1}$) [102]. During the catalysis by the lactate dehydrogenase, ferricenium ions get reduced to ferrocene with a decrease in the absorbance at the more sensitive wavelength at 300 nm (ε_{300}= 4.3 $mM^{-1}cm^{-1}$).

A very high specific activity of 280 U/mg of protein was reported by Brockman and Wood [83, 101] for the Ldh and it was shown that the protein was zinc dependent. However Olson and Massey [103] found with DCIP assay much lower specific activity of 20 U/mg of protein and showed that using EDTA in purification buffer resulted in complete loss of enzyme activity. The role of zinc in this enzyme is still obscure but absolutely necessary as the zinc depleted enzyme is reduced very slowly by D-lactate. In this study we found the specific activity of 2 U/mg protein with the ferricenium assay which can be accounted for the loss of zinc during purification. The protein was reconstituted with FAD before the gel filtration step by incubating the protein with molar excess FAD overnight at 4°C.

Purifications tep	Activity [U]	Protein [mg]	Spec. activity [U/mg]	Purification-factor	Yield [%]
Membrane freeextract	257	3850	0.067	1	100
DEAE Sepharose	59	220	0.27	4	23
Phenyl Sepharose	18	19.8	0.91	14	7
Gelfiltration	18	7.7	2.3	35	7

A 35-fold purification was obtained from *M. elsdenii* cell extracts over 3 different columns as shown below:

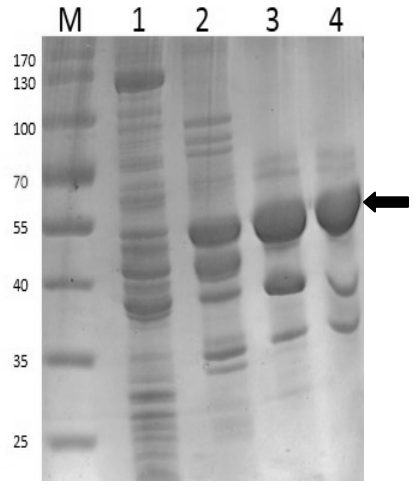

Fig. 1.Purification of D-lactate dehydrogenase from *M. elsdenii*.Lane M: marker proteins, lane 1: membrane-free extract; lane 2: After DEAE-Sepharose column; lane 3: After phenyl-Sepharose column; lane 4: After gel filtration (15µg protein loaded in each well)

Spectroscopic Analysis

UV-visible spectroscopy of the purified protein showed two different peaks at 372 and 446 nm. The flavin content was calculated to be 0.7 using anFAD extinction coefficient of ε = 11.3 $mM^{-1}cm^{-1}$ at 450 nm.

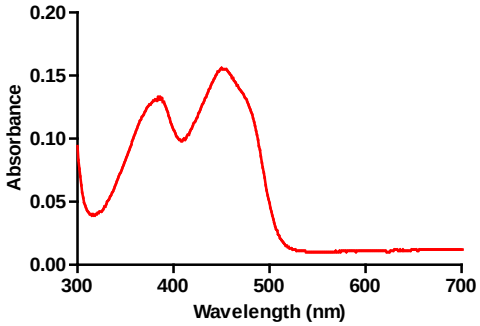

Fig. 2.UV-visible absorption spectrum of 20 µM lactate dehydrogenase of *M. elsdenii*

Titration of Etf_{Me} with NADH revealed that the ratio of NADH to completely reduced Etf is 2:1 (Chapter 3A) and the red anionic semiquinone can only be stabilized onto the α-FAD in the presence of the butyryl-CoA dehydrogenase. In this study we titrated the Etf in presence of both high and catalytic amounts of Ldh_{Me}. In presence of 1 µM Ldh_{Me} and 10 µM Etf_{Me}, the peak at 370 nm reached maxima at 16 µM D,L-lactate which hints that the red semiquinone form of the Etf_{Me} has been reached which is not quenched even upon further addition of 200 µM D,L -lactate in excess (Fig. 3A). A similar observation was obtained when equimolar amounts of 10 µM Ldh_{Me} and 10 µM Etf_{Me} were titrated with D,L–lactate. Even addition of 200µM D,L -lactate did not completely reduce the flavin spectrum (Fig. 3B). Whereas in our earlier observations when 10 µM Bcd and 10 µM Etf_{Me} was titrated with NADH, a molar excess of NADH completely reduced the flavin spectra unlike in this case. We speculate that since lactate/pyruvate couple has a redox potential of -190 mV, a single electron transfer to the α-FAD of Etf somehow decreases the redox potential of the $\alpha\text{-FAD}^{\bullet-}/\text{FADH}^{-}$ couple to much lower than -200 mV, which inhibits the second electron transfer to completely reduce the α-FAD to $\alpha\text{-FADH}^{-}$.

Now the single electron at the $\alpha\text{-FAD}^{\bullet-}$ is further transferred to the Bcd. After arrival of the second $Etf^{\bullet-}$the crotonyl-CoA is reduced tobutyryl-CoA. We have initial results determined by MALDI-TOF analysis (data not shown) which needs further investigation. Hereby the oxidation of lactate to pyruvate uses Bcd as an electron sink. Brockman & Wood showed with their experiments that 3.5 mg of Bcd could be reduced completely with 0.078 units of D-lactate dehydrogenase, 0.2 mM of D-lactate and 0.9 µg of Etf [83]. This supports our initial MALDI-TOF data that indeed a single electron transfer in achieved via the Etf which finds the Bcd as an electron acceptor for the reduction of crotonyl-CoA to butyryl-CoA.

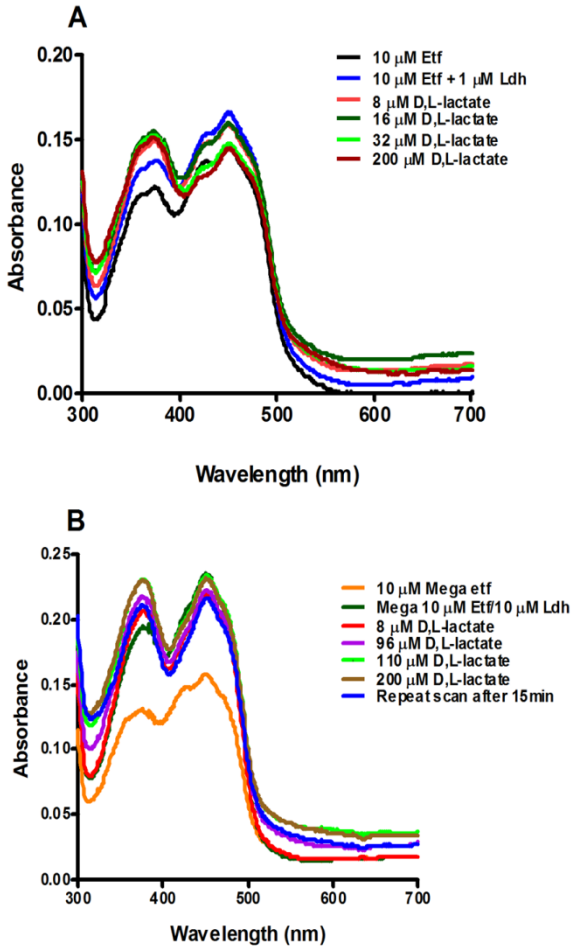

Fig.3. Formation of stable anionic semiquinones. A,to 10 µM of Etf and 10 µM Ldh, D,L-lactate was added stepwise. (orange) 10 µM Etf, (deep green) 10 µM + 10µM Ldh, (red) 8 µM lactate, (purple) 96, (fluorescent green) 110, (brown) 200, (blue) spectra recorded after 15 min post addition. B, (black) 10 µM Etf, (deep blue) 10 µM + 1µM Ldh, (red) 8 µM D,L-lactate, (deep green) 16µM, (fl. green) 32 µM, (brown) 200µM.

Discussion

Flavin based electron bifurcation has recently been established in clostridia, archaea and acetogens. The crystal structure of the two-flavin-containing Etf from *Acidaminococcus fermentans* revealed an NADH binding site in the smaller subunit (β) of the heterodimer. With docking and modeling predictions Bcd was proposed to interact with the bigger subunit (α). Recently the redox potential of *M. elsdenii* has been reported; the benzoquinone/semiquinone couple for the α-FAD is +81 mV and the semiquinone/hydroquinone couple of -136 mV. The redox potential of the completely reduced β-FAD was found to be -279 mV [87]which is reduced by NADH (E_0'= -320 mV). During bifurcation, electrons move to two different redox potential, one towards more positive redox potential crotonyl-CoA (-10 mV) and the other to the more negative redox potential ferredoxin (-420 mV). Etfs of this class can stabilize a red anionic semiquinone which upon further reduction is converted to its hydroquinone form. This red semiquinone resides on the α-$FAD^{\bullet-}$ which is stabilized by the Bcd_{Me} whereas the 2nd electron on β-$FAD^{\bullet-}$is passed onto ferredoxin during an active bifurcation process. Repetition of the process results in reduction of crotonyl-CoA and completely reduced ferredoxin. However complete reduction of Bcd_{Me} was achieved on addition of D-lactate when excess Bcd_{Me} was incubated with catalytic amounts of Ldh and Etf [83, 101].

Recently lactate dehydrogenase from *Acetobacterium woodii* has been reported to form a tight complex with the Etf and it exhibits NAD^+ reduction only when reduced ferredoxin (Fd^{2-}) is present[45]. The complex apparently uses flavin-based electron confurcation for energetic coupling [14, 20]. The exergonic electron flow from reduced ferredoxin to NAD^+ drives the endergonic electron flow from lactate to NAD^+. In *M. elsdenii* the electron transport from lactate to Bcd_{Me} also requires Etf. But the electrons can flow without bifurcation because Bcd_{Me} has a much higher redox potential than NAD^+. Further investigation with UV-visible spectrophotometry and biochemical experiments we found that indeed Ldh uses Bcd_{Me} as an electron sink for oxidation of D-lactate to pyruvate via Etf_{Me}. But an expection to bifurcation, electron are transferred to Bcd_{Me} by the Etf only via the α-FAD, the β-FAD is probably not involved in this process. During oxidation of lactate ($E°'$= -190 mV), single electron is transferred on to the α-FAD of the Etf which is at much positive redox potential ($E°'$= +81 mV). This red semiquinone can be observed in UV-visible spectrum which is not quenched on addition of excess lactate (Fig 3). This hints that on receiving single electron, the semiquinone/hydroquinone couple of α-FAD falls much lower than the reported value of -136 mV. It can be assumed that the redox potential reaches a more negative value than -200 mV, which inhibits the second electron transfer from lactate. We propose that the Etf_{Me} in this case acts like a mammalian Etfs by transferring single electron to the Bcd_{Me} in two steps then finally reducing crotonyl-CoA to butyryl-CoA.

However this is study is under progress and final results are awaited.

To summarize, we have purified the lactate dehydrogenase from *M. elsdenii* to re-investigate and understand the mode of electron transfer from the Ldh_{Me} to the Etf_{Me} during lactate fermentation. From the initial spectroscopic data we can infer that the lactate dehydrogenase can transfer single electron from the lactate to the Etf_{Me}, which is accepted by the α-FAD of the Etf_{Me}. This electron is transferred to the electron sink (Bcd_{Me}) where the electron is stored. In the second round one more electron is taken away from the lactate and transferred via Etf_{Me} to the Bcd_{Me} which affords reduction of crotonyl-CoA to butyryl-CoA and formation of pyruvate from lactate. We can conclude that the bifurcating Etf from *M. elsdenii* has two functions; in presence of Ldh it acts like a classical Etf , transferring single electron. In presence of NADH and ferredoxin, Etf_{Me} bifurcate two electrons to two different redox potential via electron bifurcation.

It is very interesting to investigate the conditions in which the Etf_{Me} accepts electron directly from Ldh_{Me} or goes via electron bifurcation to reduce crotonyl-CoA. The metabolic pathway of lactate fermentation is still not well understood by *M. elsdenii* and we target to understand the pathway in near future

References

1. Elsden, S. R., Gilchrist, F. M., Lewis, D. & Volcani, B. E. (1956) Properties of a fatty acid forming organism isolated from the rumen of sheep, *Journal of bacteriology*. **72**, 681-9.

2. Brockman, H. L. & Wood, W. A. (1975) Electron-transferring flavoprotein of Peptostreptococcus elsdenii that functions in the reduction of acrylyl-coenzyme A, *Journal of bacteriology*. **124**, 1447-53.

3. Brockman, H. L. & Wood, W. A. (1975) D-Lactate dehydrogenase of Peptostreptococcus elsdenii, *Journal of bacteriology*. **124**, 1454-61.

4. Roberts, D. L., Salazar, D., Fulmer, J. P., Frerman, F. E. & Kim, J. J. (1999) Crystal structure of *Paracoccus denitrificans* electron transfer flavoprotein: structural and electrostatic analysis of a conserved flavin binding domain, *Biochemistry*. **38**, 1977-89.

5. Roberts, D. L., Frerman, F. E. & Kim, J. J. (1996) Three-dimensional structure of human electron transfer flavoprotein to 2.1-A resolution, *Proc Natl Acad Sci U S A*. **93**, 14355-60.

6. Lehman, T. C., Hale, D. E., Bhala, A. & Thorpe, C. (1990) An acyl-coenzyme A dehydrogenase assay utilizing the ferricenium ion, *Analytical biochemistry*. **186**, 280-4.

7. Olson, S. T. & Massey, V. (1979) Purification and properties of the flavoenzyme D-lactate dehydrogenase from Megasphaera elsdenii, *Biochemistry*. **18**, 4714-24.

8. Sato, K., Nishina, Y. & Shiga, K. (2013) Interaction between NADH and electron-transferring flavoprotein from *Megasphaera elsdenii*, *J Biochem.* **153**, 565-72.

9. Weghoff, M. C., Bertsch, J. & Muller, V. (2014) A novel mode of lactate metabolism in strictly anaerobic bacteria, *Environmental microbiology*.

10. Buckel, W. & Thauer, R. K. (2013) Energy conservation via electron bifurcating ferredoxin reduction and proton/Na^+ translocating ferredoxin oxidation, *Biochim Biophys Acta.* **1827**, 94-113.

11. Herrmann, G., Jayamani, E., Mai, G. & Buckel, W. (2008) Energy conservation via electron-transferring flavoprotein in anaerobic bacteria, *J Bacteriol.* **190**, 784-791.

3. Discussion

3.1 Closing gaps in glutamate fermentation by *Acidaminococcus fermentans*

The hydroxyglutarate pathway of glutamate fermentation to ammonia, CO_2, acetate and butyrate was well understood and studied in *A. fermentans*. Each intermediate and their corresponding enzymes were purified and have been well studied [17, 20]. Energy conservation in anaerobic bacteria was always thought to be mediated by substrate level phosphorylation since it lacked an electron transport chain as in higher domains of life. However a very interesting observation that the growth of amino acid fermenting bacteria (e.g *C. symbosium*, *A. fermentans*, *P. asaccharolyticus* etc.) was highly dependent on Na^+, at 2 mM Na^+ no growth was observed in *A. fermentans* and *P. asaccharolyticus* [104] whereas when the Na^+ concentration was increased to 3 mM Na^+ both organisms grew almost at their maximum rate. However on decreasing the Na^+ concentration the lag-phase increased in these organisms. It was found that biotin-dependent decarboxylations of organic acids like glutaconyl-CoA liberate a considerable amount of free energy ($\Delta G°'$ ca. - 30 kJ/mol) which is used to pump sodium ions through bacterial membranes [28, 104-106]. This generates a Na^+ gradient within the cell which is used as an additional source of energy when Na^+ is pumped in through the membrane bound ATPase. Higher energy conservation is accounted for the decarboxylation coupled Na^+ transport. Decarboxylation of glutaconyl-CoA generates crotonyl-CoA which is an essential step in fermentation of glutamate by *A. fermentans*. With inverted membrane vesicles prepared from *A. fermentans* it was shown that the organism can accumulate Na^+ if this reaction occurred and on addition of monensin the accumulation of Na^+ was completely abolished [105].

Though the Na^+ dependence could be explained, one observation that remained obscure was the generation of H_2 during the fermentation of glutamate. It was thought that reducing equivalents generated in 3-hydroxybutyryl-CoA dehydrogenase reaction were not used to reduce crotonyl-CoA but liberated as molecular hydrogen [104] driven by the Na^+ gradient [18]. In addition the membrane fraction from *P. asaccharolyticus* contained hydrogenase which generates hydrogen reducing protons. The donor of reducing equivalent to the hydrogenase remained elusive. It was in 2008 that Herrmann et al. proposed for the first time, that reduction of crotonyl-CoA to butyryl-CoA with NADH, could be used for additional energy conservation. The reduction of crotonyl-CoA ($E_0' = -10$ mV) by NADH ($E_0' = -320$ mV) is highly exergonic and irreversible under physiological conditions. However when assayed in-vitro, no oxidation of NADH detected when electron transferring flavoprotein/butyryl-CoA dehydrogenase, crotonyl-CoA and NADH was added together. In a path-breaking hypothesis it was proposed reduction of crotonyl-CoA to butyryl-CoA by NADH also drives reduction of ferredoxin [14]. In a subsequent study from *C. kluyveri* it was shown Etf-Bcd are able to bifurcate the two electrons from NADH ($E_0' = -320$ mV), one electron proceeds to the more positive electron acceptor Bcd and finally to crotonyl-CoA ($E_0' = -10$ mV) and the other electron is transferred to a more negative electron acceptor ferredoxin ($E_0' = -420$ mV) [15]. The reduced ferredoxin (Fd^{2-}), which is generated, reduces protons to hydrogen via the hydrogenase and gets

reoxidized. An enzymatic assay in which Etf/Bcd, catalytic amounts of ferredoxin and hydrogenase was incubated with NADH and the reaction was started with addition of crotonyl-CoA, hydrogen formation could be detected by gas-chromatography. This actually explains the generation of H_2 during glutamate fermentation by *A. fermentans*.

In chapter 2.1, we characterized the dissociating Etf/Bcd complex from *A. fermentans*. Biochemical experiments revealed that under standard conditions, the stoichiometry of ferredoxin: Etf: Bcd in presence of hydrogenase was found to be 2:0.5:1. This suggested that during steady state ferredoxin takes one electron and hands it over to the hydrogenase. It can be inferred that most likely the ferredoxin shuttles between Fd^{-} and Fd^{2-}, the electron acceptor is the semi-reduced Fd^{-} which is reduced to Fd^{2-} by electron-bifurcation. The Fd^{2-} donates the reducing equivalents to hydrogenase which reduces protons to molecular H_2.

3.2 Energy conservation and glutamate fermentation by *Acidaminococcus fermentans*

The complete overview of the glutamate fermented at stoichiometric amounts will give an exact idea of the energy conservation in *A. fermentans*. According to the balanced fermentation equation, fewer molecules are consumed than produced during glutamate fermentation.

$$5\ \text{Glutamate}^- + 6\ H_2O + 2H^+ \longrightarrow 5\ NH_4^+ + 5\ CO_2 + H_2 + 6\ \text{Acetate}^- + 2\ \text{Butyrate}^-$$

Therefore the free energy change $\Delta G'$ becomes more negative at lower concentrations. The calculated $\Delta G'$ decreases to -450kJ/mol H_2, when the physiological concentrations of glutamate, acetate, butyrate and ammonia were assumed to be 1mM each. Via the hydroxyglutarate pathway 5 glutamate are transformed to 5 ammonia, after which 5 x (*R*)-2-hydroxyglutarate are activated 5 x acetyl-CoA to 5 x 2-hydroxyglutaryl-CoA. The subsequent dehydration step forms 5 x glutaconyl-CoA which is decarboxylated to 5 x crotonyl-CoA catalyzed by the membrane bound enzyme glutaconyl-CoA decarboxylase (Gcd) that converts the free energy of decarboxylation to an electrochemical Na^+ gradient resulting the expulsion of 10 Na^+ out of the cell.

Out of the 5 crotonyl-CoA, three are oxidized to 6 acetyl-CoA with the formation of 3 NADH, which together with a fourth NADH are consumed in reduction of the remaining 2 crotonyl-CoA to 2 butyryl-CoA by flavin-based electron bifurcation leading to the formation of 2 Fd_{red}^{2-}. One ferredoxin (Fd_{red}^{2-}) re-cycles the fourth NADH via Rnf resulting in expulsion of 2 Na^+ out of the cell which adds up to the Na^+ ion gradient deficit inside the cell. With 10 Na^+ expelled via ***Gcd*** and 2 Na^+ via ***Rnf***, a sum total of $12\Delta\mu Na^+$ is obtained. For the import of 5 glutamate probably 5 $\Delta\mu Na^+$ are consumed [39], leaving 7 $\Delta\mu Na^+$ for the synthesis of ATP via F_1F_0- ATP synthase. Generally to synthesize 1 ATP via the ATP-synthase, 4 Na^+ ions need to be pumped inside the cell, so when 7 Na^+ is pumped into the cell, an additional 1.75 ATP is synthesized. The remaining Fd_{red}^{2-} reduces2 H^+ to H_2 by the [Fe-Fe] hydrogenase present inside the cell. This explains how hydrogen was formed when *A. fermentans* was grown on glutamate, the reduced ferredoxin once reoxidized, forms hydrogen which is released.

Finally, out of 6 acetyl-CoA formed 5 acetyl-CoA is used to form (R)-2-hydroxyglutaryl-CoA from (R)-hydroxyglutarate, 1 acetyl-CoA gives rise to 1 ATP via acetyl phosphate to form acetate. The 2 butyryl-CoA gives rise to butyrate and 2 ATP via acetyl phosphate. So 3 ATP is conserved by SLP and the extra 1.75 ATP from 7 $\Delta\mu Na^+$. All together, 0.95ATP/glutamate with the high efficiency of 67 kJ/mol ATP under standard conditions is obtanined. At lower concentrations the efficiency decreases, at the assumed 1mM physiological concentrations, it reaches 96 kJ/mol ATP. The thermodynamic efficiency of about 100 kJ/mol ATP which apparently is quite low, therefore it can be predicted that *A. fermentans* increase its efficiency by changing the pathway such that the H_2 production is increased at low concentrations of substrates and products as found in natural environments where the organisms thrive. A simple overview of the pathway in *A. fermentans* is given below.

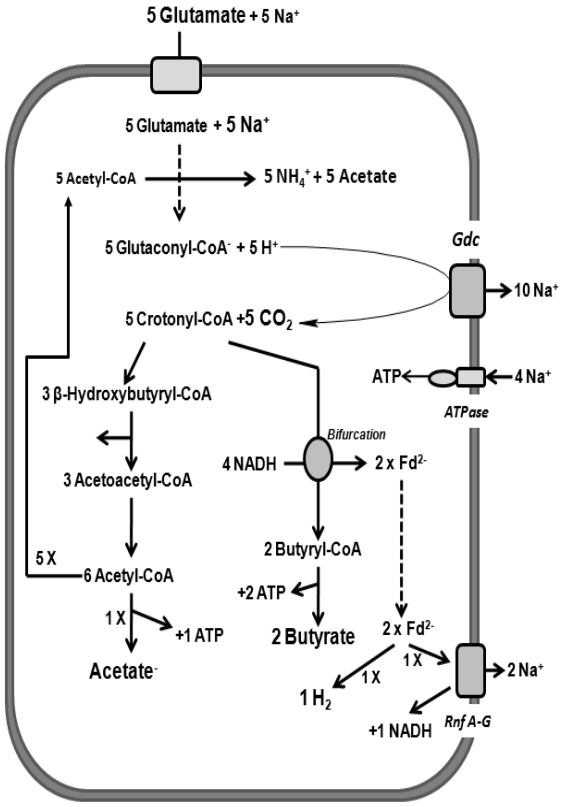

Figure: Fermentation of glutamate in *A. fermentans* by the hydroxyglutaratepathway. Gcd = Na^+translocatingglutaconyl-CoA decarboxylase, F_1F_0 ATPase and the glutamate Na^+-symporter are deduced from the genome of *A. fermentans*

3.3 Electron transferring flavoprotein and electron-bifurcation

Electron transferring flavoprotein (Etf) and butyryl-CoA dehydrogenase are both FAD containing proteins which have a significant role in anaerobic bacterial-metabolism. Etf was first identified by Crane and Beinert [107] as yellow fluorescent component required to mediate the transfer of reducing equivalents from mammalian fatty acyl-CoA dehydrogenases to various electron acceptors. Etf from

mammalian sources like human [99], pig [108] and even bacteria like *Paracocccus denitrificans* [100] and *Methylophilus methylotrophus* [109] belongs to Class I type of Etf which contains only one FAD molecule per heterodimer and does not oxidize NADH. This class of Etf in addition to its role in β-oxidation, serves a series of other mitochondrial flavoprotein dehydrogenases like isovaleryl-CoA dehydrogenase [110], 2-methyl-branched chain-acyl-CoA dehydrogenase [111] involved in amino acid degradation and various short, medium and long chain acyl-CoA dehydrogenases. It shuttles one electron from the dehydrogenases to the matrix side of the inner mitochondrial membrane by reducing ETF-ubiquinone oxidoreductase (ETF-QO) [112]. Another characteristic feature to this class of Etf is that it contains an AMP molecule buried deep into the smaller (β) subunit which helps in keeping the correct architecture of the enzyme [99, 100]

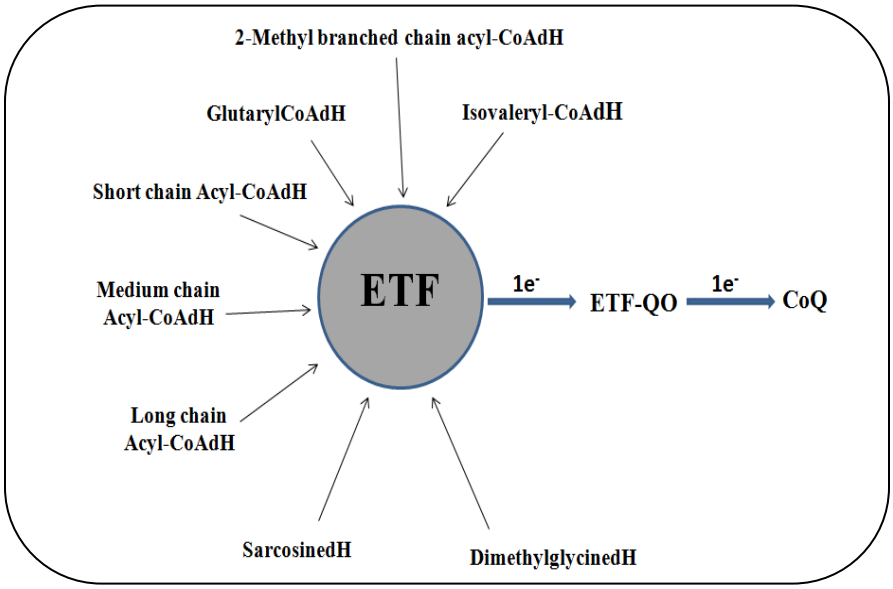

Figure : Classical type Etf (FAD and AMP) containing shuttles electrons from dehydrogenase to membrane bound quinone-oxidoreductase

Etf from *A. fermentans* and *M. elsdenii* belongs to Class II type of Etf where it contains two non-covalently bound FADs. The α-FAD is found in a stretched condition [35] similar to the Class I Etf family members. As depicted in the scheme the α-FAD is reduced by 1e- from the corresponding dehydrogenase which is reflected in high redox potentials of α-FAD/α-FAD$^{\bullet-}$couple (E_0' = +81 mV for Etf_{Me}) [86, 87] that enables a smooth electron transfer to the α-FAD. In Class II type of Etfs, the AMP part in human part is replaced by a second non-covalently bound FAD molecule which binds to the C-terminal side of the β-subunit. The binding domain is well discussed in the Chapter 1, which agrees with the earlier finding of a low redox potential (E_0' = -280 mV for Etf_{Me}) of the β-FAD/ β-FADH$^-$couple and a stronger binding of β-FAD than α-FAD. Co-crystallization experiments of Etf_{Af} with NAD^+ revealed binding of NAD^+ to the β-subunit, though the electron density for ADP moiety and not the nicotinamide part could be detected. Gathering all the observations and the measured redox potential of Etf from *M. elsdenii* fits perfectly to our current model of flavin-based electron bifurcation. The physiological redox

potential of NADH is believed to be around -300 mV which allows a downhill movement of electrons to the β-FAD. The β-FAD/ β-FADH$^-$redox potential of -280 mV and a structural rearrangement probably makes 1e- transfer to the α-FAD feasible which has a redox potential of -60 mV. The red anionic semiquinone that can be trapped on Bcd/Etf titration with NADH suggests one electron reduction of the α-FAD. The electron residing on the β-FAD$^\bullet$ is probably highly unstable and attains a very low redox potential around -500 mV which is sufficient to immediately reduce a ferredoxin (-420 mV) which could be modeled around the β-FAD. Repetition of the process allows a completely reduced ferredoxin (Fd^{2-}) and reduced substrate (crotonyl-CoA) via the butyryl-CoA dehydrogeanse.

Additional to these two classes, a subclass of Etf belonging to Class II has been recently discovered from the acetogenic bacteria, *Acetobacterium woodii*. 2 different complexes has been purified, caffeyl-CoA reductase [96] and lactate dehydrogenase [45] in which Etf forms a tight complex to its dehydrogenases. The unique feature of both these complexes is that they have an additional [Fe-S] cluster bound to the N-terminal region of the α-subunit and unlike Etf_{Af}/Etf_{Me} are highly oxygen sensitive. The LDH/Etf complex has 3 predicted FAD and 1 [4Fe-4S] cluster whereas the flavin content of the caffeyl-CoA reductase is not clear, but 9 mol of iron and 9 mol of sulfur was determined from the complex. In this subclass of Etf the N-terminal extension contains two times the conserved sequence (CX2CX2CX3CP) responsible for the binding of [4Fe-4S] in several ferredoxins [96, 113, 114]. The function of the presence of the [Fe-S] is still unclear but is predicted to play a role in the intramolecular electron transfer from the Etf to the dehydrogenase.

3.4 Ferredoxin, flavodoxin, electron-bifurcation and more…

The role of ferredoxin and flavodoxin in flavin based bifurcation and energy conservation has been discussed in Chapters 1 and 2. Generally clostridial type ferredoxins contain two iron sulfur clusters, which are highly oxygen sensitive, are reduced by one-electron generally at a redox potential more negative than -400 mV. These types of ferredoxins are required in metabolism of anaerobic bacteria and archaea, for reduction of CO_2 to CO in acetogens, of CO_2 to formyl-methanofurane in methanogens, of CO_2 and acetyl-CoA reduction to pyruvate, of protons H^+ to H_2 and with the recent finding lactate to pyruvate in acetogenic bacteria. In these reactions, flavin-based electron bifurcation/confurcation provides the reducing power for the forward reaction. Reduced ferredoxin produced by oxidation of pyruvate and other substrates functions as the main electron source for H_2 formation in most fermentative bacteria. The main purpose of H_2 formation is to release an excess of reducing equivalents generated during fermentation and also to increase the substrate level phosphorylation leading to energy conservation. The role of ferredoxin is immense in both as an electron acceptor and donor in anaerobic metabolisms. As glutamate fermentation via the hydroxyglutarate pathway is concerned, flavin-based electron bifurcation leading to reduced ferredoxin is the only way to give rise to molecular hydrogen which balances the ATP synthesis via SLP.

The balance between the ferredoxin and flavodoxin that is controlled under iron limiting conditions have been well described by earlier researchers (see chapter 2). The interesting observation in *A. fermentans* was that the growth rate (doubling time 2.5 h) was unaffected by varying iron concentrations in the growth medium. The acetate to butyrate ratio was also unaffected by the iron limitations which led us to speculate that flavodoxin must play the role of ferredoxin under these conditions.

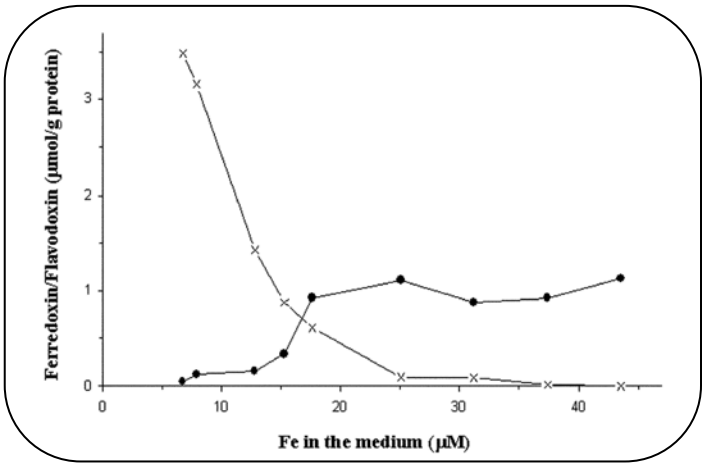

Amounts of flavodoxin and ferredoxin present in A. fermentans cells grown on media with increasing iron concentrations. (×) Flavodoxin, (•) ferredoxin [adapted from Thamer et al. 2003]

As expected, heterologously produced flavodoxin indeed replaced ferredoxin in the electron bifurcation reaction (reduction of crotonyl-CoA to butyryl-CoA). UV-visible spectroscopic experiments revealed that flavodoxin can be reoxidized by membrane extracts containing the Rnf complex to its semiquinone form, which is obvious since the hydroquinone/semiquinone couple for flavodoxin has a redox potential of -430 mV whereas the semiquinone/benzoquinone couple of -60 mV. NAD+/NADH has a physiological redox potential of -300 mV, so the electron flow from completely reduced flavodoxin via the Rnf to NAD+ is possible since its downhill electron movement, whereas when it reaches the semiquinone form it is an uphill electron movement to NAD+ and is not possible. It appears that flavodoxin purified from native cells is always blue in color since it only shuttles between the hydroquinone and semiquinone form.

3.5 Flavin based electron bifurcation and oxygen

Electron transferring flavoprotein was partially purified from *M. elsdenii* and demonstrated by Baldwin and Milligan [84] that Etf functions in formation of butyryl-CoA by coupling the oxidation of NADH via reduction of the Bcd. Later Mayhew and colleagues characterized the protein and showed that indeed the Etf in combination with butyryl-CoA dehydrogenase oxidizes NADH for reduction of crotonyl-CoA [115]. This group of Etf was characterized as the class II type of Etf which contains two FAD per hetero-dimer of the protein. However their study found modified FADs like 8-OH and 6-OH FAD in preparations of the protein which was not investigated in this thesis. Since then Etf from *M. elsdenii* has been well studied over the years [83, 85-88, 91, 116-118]. With the finding of electron bifurcation in Etfs

from *C. kluyveri* [15] , *C. dffici*le [34] and *A. fermentans* [35], it was confusing that whether the closely related *M. elsdenii* Etf was an apparent exception from the bifurcating Etfs. According to the older literature, oxidation of NADH was evident; however, none of the reports mentioned the actual assay conditions. To investigate the confusion, we cloned the genes and overproduced the protein in *E. coli* and successfully purified both Etf and Bcd using affinity chromatography. However no oxidation of NADH was observed when Etf/Bcd, NADH and crotonyl-CoA were incubated under anaerobic conditions. Rapid oxidation of NADH was achieved when ferredoxin/hydrogenase was added to the same reaction mixture. This hinted that most probably the *M. elsdenii* Etf is not different from the related bifurcating Etfs. Now we repeated the same assay under aerobic condition where ferredoxin was omitted. Surprisingly oxidation of NADH was observed when Etf/Bcd was incubated with NADH and the reaction was started with addition of the substrate crotonyl-CoA. However when crotonyl-CoA was replaced by butyryl-CoA, NADH was still oxidized. This led us to think that under aerobic conditions O_2 plays a significant role in this anomalous observation. An earlier report of a similar protein complex, acryloyl-CoA reductase (complex of Etf and propionyl-CoA dehydrogenase) from *Clostridium propionicum* that produced H_2O_2upon oxidation of NADH under aerobic conditions [90] led us to analyze, whether the similar condition applied in this case. Indeed formation of $H_2O_2$was confirmed by the ABTS assay which showed that oxygen was the electron acceptor when NADH was oxidized and uncouples the reaction. A MALDI-TOF analysis of individual reaction mixtures with either crotonyl-CoA or butyryl-CoA as substrates always revealed butyryl-CoA and crotonyl-CoA as products. This was much more confusing as even if crotonyl-CoA is reduced to butyryl-CoA, it was practically impossible to oxidize butyryl-CoA along with oxidizing NADH. An interesting observation was that no oxidation of NADH was observed until either of butyryl-CoA or crotonyl-CoA was added.

We speculated that on addition of either substrate or product a conformational change might expose the reduced FADs to oxygen and NADH was completely oxidized, but this did not explain the observation of the formation of their respective products crotonyl-CoA to butyryl-CoA and vice-versa. Finally a MALDI analysis of a reaction mixture with Bcd and butyryl-CoA under aerobic condition revealed the formation of crotonyl-CoA explained the strange observation. We can explain that under aerobic condition, Bcd on incubation with butyryl-CoA uses molecular oxygen as an electron acceptor which results in formation of crotonyl-CoA. Therefore on incubation of Etf/Bcd, NADH and butyryl-CoA, first crotonyl-CoA is formed using O_2 as electron acceptor and then the reactions runs similarly to the forward reaction of reducing crotonyl-CoA with NADH using O_2 in place of ferredoxin. We propose that the oxygen takes the part of ferredoxin under aerobic condition which now fits the older research which was contradictory to the recently discovered electron bifurcation in Etfs. During a forward reaction using crotonyl-CoA, NADH first reduces the β-FAD and similarly to bifurcation under anaerobic condition a stepwise electron transfer results in reduction of crotonyl-CoA. However, a stepwise electron transfer to O_2 and finally formation of H_2O_2 should result to a superoxide radical intermediate. On incubation of the reaction mixture with varying concentration of superoxide dismutase resulted to a 50% inhibition of the NADH oxidation rate. This showed that in fact an intermediate of oxygen radical which forms H_2O_2on receiving the 2^{nd} electron

by complete bifurcation process. The 50% inhibition can be explained that the rate of formation of H_2O_2 from $O_2^{\bullet-}$ (k_2) should be much higher compared to the rate of O_2 to $O_2^{\bullet-}$ (k_1) and SOD inhibiting the k_2 would result in double working of the k_1 step resulting in slowing down the reaction by half and hence the observation.

Though the reaction might not be relevant with respect to in-vivo condition to anaerobic bacteria, it however has biological interest which explains how electron bifurcation can lead to the formation of reactive oxygen species on exposure to oxygen. However there are a set of protein and enzymes that protect anaerobic bacteria from oxidative stress on exposure to oxygen [119-121]. Pull down experiments with His-tagged Etf from *A. fermentans* and membrane-free extracts showed the presence of the protein rubrerythrinalong with the Etf. Rubrerythrin has been reported to have superoxide dismutase activity and plays a role in detoxification of oxygen radicals in *Clostridium perfringens* [122] and rubrerythrin mutant strains of *Porphyromonas gingivalis* were more dioxygen- and hydrogen-peroxide-sensitive than the wild type [52]. However the role of rubrerythrin in *A. fermentans* requires further scrutiny.

4. Outlook

Within the scope of this thesis we have established the probable working mechanism of the flavin-based electron bifurcation using Etf-Bcd complex. However, mutational studies in the electron transferring flavoprotein will further clear our understanding that how electrons are transferred stepwise within the Etf which remains obscure. Titration of of the Etf/Bcd complex with NADH did not reveal the semiquinone on the β-FAD which needs further investigation. We have designed an experiment which will be excuted shortly in some days. The predicted conformational change needs actual experimental evidences which can only be elucidated by mutational studies. The redox potential measurement of the wild type as well as the mutated protein will answer how the active site modulates the electron movement within the protein.

Using the Etf/Bcd system the activation of oxygen by electron bifurcation will be further studied in coming time. Using flavodoxin we intend to study the Na^+ transport via *Rnf* with inverted vesicles of *A. fermentans*, since flavodoxin can be produced in large amount and is easy to handle.

Recently we have crystallized the Etf/Bcd complex from *Clostridium difficile* in collaboration with Dr. Ulrich Ermler (MPI Frankfurt). Further characterization and redox potential measurement of the complex will help us re-evaluate the observation found in the dissociable Etf/Bcd complex. A co-crystallization trial with NAD^+ has been successful and the results are due to be published.

5. References

1. Thauer, R. K., Jungermann, K. & Decker, K. (1977) Energy conservation in chemotrophic anaerobic bacteria, *Bacteriological reviews.* **41**, 100-80.
2. Ishimoto, M., Umeyama, M. & Chiba, S. (1974) Alteration of fermentation products from butyrate to acetate by nitrate reduction in Clostridium perfringens, *Zeitschrift fur allgemeine Mikrobiologie.* **14**, 115-21.
3. Hasan, S. M. & Hall, J. B. (1975) The physiological function of nitrate reduction in Clostridium perfringens, *Journal of general microbiology.* **87**, 120-8.
4. Hasan, M. & Hall, J. B. (1977) Dissimilatory nitrate reduction in Clostridium tertium, *Zeitschrift fur allgemeine Mikrobiologie.* **17**, 501-6.
5. Kaneko, M. & Ishimoto, M. (1977) Effect of nitrate reduction on metabolic products and growth of Propionibacterium acidi-propionici, *Zeitschrift fur allgemeine Mikrobiologie.* **17**, 211-20.
6. Boiangiu, C. D., Jayamani, E., Brügel, D., Herrmann, G., Kim, J., Forzi, L., Hedderich, R., Vgenopoulou, I., Pierik, A. J., Steuber, J. & Buckel, W. (2005) Sodium ion pumps and hydrogen production in glutamate fermenting anaerobic bacteria, *J Mol Microbiol Biotechnol.* **10**, 105-119.
7. Imkamp, F., Biegel, E., Jayamani, E., Buckel, W. & Müller, V. (2007) Dissection of the caffeate respiratory chain in the acetogen *Acetobacterium woodii*: identification of an Rnf-type NADH dehydrogenase as a potential coupling site, *J Bacteriol.* **189**, 8145-8153.
8. Biegel, E. & Müller, V. (2010) Bacterial Na^+-translocating ferredoxin:NAD^+ oxidoreductase, *Proc Natl Acad Sci U S A.* **107**, 18138-18142.
9. Thauer, R. K., Kaster, A. K., Seedorf, H., Buckel, W. & Hedderich, R. (2008) Methanogenic archaea: ecologically relevant differences in energy conservation, *Nat Rev Microbiol.* **6**, 579-91.
10. Garrity, G. (2001) Bergey's manual of systematic bacteriology, *Berlin Heidelberg New York: Springer*. **2nd edition**.
11. Jackins, H. C. & Barker, H. A. (1951) Fermentative processes of the fusiform bacteria, *Journal of bacteriology.* **61**, 101-14.
12. Barker, H. A. (1981) Amino acid degradation by anaerobic bacteria, *Annual review of biochemistry.* **50**, 23-40.
13. Stickland, L. H. (1935) Studies in the metabolism of the strict anaerobes (Genus Clostridium): The reduction of proline by Cl. sporogenes, *The Biochemical journal.* **29**, 288-90.
14. Herrmann, G., Jayamani, E., Mai, G. & Buckel, W. (2008) Energy conservation via electron-transferring flavoprotein in anaerobic bacteria, *J Bacteriol.* **190**, 784-791.
15. Li, F., Hinderberger, J., Seedorf, H., Zhang, J., Buckel, W. & Thauer, R. K. (2008) Coupled ferredoxin and crotonyl coenzyme A (CoA) reduction with NADH catalyzed by the butyryl-CoA dehydrogenase/Etf complex from *Clostridium kluyveri*, *J Bacteriol.* **190**, 843-50.
16. Buckel, W. (2001) Unusual enzymes involved in five pathways of glutamate fermentation, *Applied microbiology and biotechnology.* **57**, 263-73.
17. Buckel, W. & Barker, H. A. (1974) Two pathways of glutamate fermentation by anaerobic bacteria, *Journal of bacteriology.* **117**, 1248-60.
18. Hartel, U. & Buckel, W. (1996) Sodium ion-dependent hydrogen production in Acidaminococcus fermentans, *Archives of microbiology.* **166**, 350-6.
19. Reitzer, R., Gruber, K., Jogl, G., Wagner, U. G., Bothe, H., Buckel, W. & Kratky, C. (1999) Glutamate mutase from Clostridium cochlearium: the structure of a coenzyme B12-dependent enzyme provides new mechanistic insights, *Structure.* **7**, 891-902.
20. Buckel, W. & Thauer, R. K. (2013) Energy conservation via electron bifurcating ferredoxin reduction and proton/Na^+ translocating ferredoxin oxidation, *Biochim Biophys Acta.* **1827**, 94-113.
21. Buckel, W. (1980) Analysis of the fermentation pathways of clostridia using double labelled glutamade, *Archives of microbiology.* **127**, 167-9.

22. Buckel, W. (1980) The reversible dehydration of (R)-2-hydroxyglutarate to (E)-glutaconate, *European journal of biochemistry / FEBS.* **106**, 439-47.
23. Schweiger, G., Dutscho, R. & Buckel, W. (1987) Purification of 2-hydroxyglutaryl-CoA dehydratase from Acidaminococcus fermentans. An iron-sulfur protein, *European journal of biochemistry / FEBS.* **169**, 441-8.
24. Hans, M., Buckel, W. & Bill, E. (2000) The iron-sulfur clusters in 2-hydroxyglutaryl-CoA dehydratase from Acidaminococcus fermentans. Biochemical and spectroscopic investigations, *European journal of biochemistry / FEBS.* **267**, 7082-93.
25. Buckel, W. & Liedtke, H. (1986) The sodium pump glutaconyl-CoA decarboxylase from Acidaminococcus fermentans. Specific cleavage by n-alkanols, *European journal of biochemistry / FEBS.* **156**, 251-7.
26. Buckel, W. (1986) Substrate stereochemistry of the biotin-dependent sodium pump glutaconyl-CoA decarboxylase from Acidaminococcus fermentans, *European journal of biochemistry / FEBS.* **156**, 259-63.
27. Buckel, W. (1986) Biotin-dependent decarboxylases as bacterial sodium pumps: Purification and reconstitution of glutaconyl-CoA decarboxylase from *Acidaminococcus fermentans* in *Meth Enzymol* (Sidney Fleischer, B. F., ed) pp. 547-558, Academic Press.
28. Dimroth, P. (1980) A new sodium-transport system energized by the decarboxylation of oxaloacetate, *FEBS letters.* **122**, 234-6.
29. Bott, M., Pfister, K., Burda, P., Kalbermatter, O., Woehlke, G. & Dimroth, P. (1997) Methylmalonyl-CoA decarboxylase from Propionigenium modestum--cloning and sequencing of the structural genes and purification of the enzyme complex, *European journal of biochemistry / FEBS.* **250**, 590-9.
30. Braune, A., Bendrat, K., Rospert, S. & Buckel, W. (1999) The sodium ion translocating glutaconyl-CoA decarboxylase from Acidaminococcus fermentans: cloning and function of the genes forming a second operon, *Molecular microbiology.* **31**, 473-87.
31. Wendt, K. S., Schall, I., Huber, R., Buckel, W. & Jacob, U. (2003) Crystal structure of the carboxyltransferase subunit of the bacterial sodium ion pump glutaconyl-coenzyme A decarboxylase, *The EMBO journal.* **22**, 3493-502.
32. Buckel, W. (2001) Sodium ion-translocating decarboxylases, *Biochimica et biophysica acta.* **1505**, 15-27.
33. Kölzer, S. (2008) *Aufreiningung und Charakterisierung des Butyryl-CoA Dehydrogenase/ETF Komplexes aus Clostridium tetanomorphum*, Philipps-Universität, Marburg, Germany.
34. Aboulnaga, E.-H., Pinkenburg, O., Schiffels, J., El-Refai, A., Buckel, W. & Selmer, T. (2013) Butyrate production in *Escherichia coli*: Exploitation of an oxygen tolerant bifurcating butyryl-CoA dehydrogenase/electron transferring flavoprotein complex from *Clostridium difficile*., *J Bacteriol.* **195**, 3704-13.
35. Chowdhury, N. P., Mowafy, A. M., Demmer, J. K., Upadhyay, V., Koelzer, S., Jayamani, E., Kahnt, J., Hornung, M., Demmer, U., Ermler, U. & Buckel, W. (2014) Studies on the Mechanism of Electron Bifurcation Catalyzed by Electron Transferring Flavoprotein (Etf) and Butyryl-CoA Dehydrogenase (Bcd) of *Acidaminococcus fermentans*, *J Biol Chem.* **289**, 5145-57.
36. Schmehl, M., Jahn, A., Meyer zu Vilsendorf, A., Hennecke, S., Masepohl, B., Schuppler, M., Marxer, M., Oelze, J. & Klipp, W. (1993) Identification of a new class of nitrogen fixation genes in Rhodobacter capsulatus: a putative membrane complex involved in electron transport to nitrogenase, *Molecular & general genetics : MGG.* **241**, 602-15.
37. Saeki, K. & Kumagai, H. (1998) The rnf gene products in rhodobacter capsulatus play an essential role in nitrogen fixation during anaerobic DMSO-dependent growth in the dark, *Archives of microbiology.* **169**, 464-7.
38. Biegel, E., Schmidt, S., Gonzalez, J. M. & Muller, V. (2011) Biochemistry, evolution and physiological function of the Rnf complex, a novel ion-motive electron transport complex in prokaryotes, *Cellular and molecular life sciences : CMLS.* **68**, 613-34.

39. Bruggemann, H., Baumer, S., Fricke, W. F., Wiezer, A., Liesegang, H., Decker, I., Herzberg, C., Martinez-Arias, R., Merkl, R., Henne, A. & Gottschalk, G. (2003) The genome sequence of Clostridium tetani, the causative agent of tetanus disease, *Proceedings of the National Academy of Sciences of the United States of America.* **100**, 1316-21.
40. Schut, G. J. & Adams, M. W. (2009) The iron-hydrogenase of *Thermotoga maritima* utilizes ferredoxin and NADH synergistically: a new perspective on anaerobic hydrogen production, *J Bacteriol.* **191**, 4451-4457.
41. Schuchmann, K. & Müller, V. (2012) A bacterial electron-bifurcating hydrogenase, *J Biol Chem.* **287**, 31165-31171.
42. Kaster, A. K., Moll, J., Parey, K. & Thauer, R. K. (2011) Coupling of ferredoxin and heterodisulfide reduction via electron bifurcation in hydrogenotrophic methanogenic archaea, *Proc Natl Acad Sci U S A.* **108**, 2981-6.
43. Huang, H., Wang, S., Moll, J. & Thauer, R. K. (2012) Electron bifurcation involved in the energy metabolism of the acetogenic bacterium Moorella thermoacetica growing on glucose or H2 plus CO2, *Journal of bacteriology.* **194**, 3689-99.
44. Wang, S., Huang, H., Kahnt, J. & Thauer, R. K. (2013) Clostridium acidurici electron-bifurcating formate dehydrogenase, *Applied and environmental microbiology.* **79**, 6176-9.
45. Weghoff, M. C., Bertsch, J. & Muller, V. (2014) A novel mode of lactate metabolism in strictly anaerobic bacteria, *Environmental microbiology*.
46. Fuller, R. (1966) Some morphological and physiological characteristics of gram negative anaerobic bacteria isolated from the alimentary tract of the pig, *The Journal of applied bacteriology.* **29**, 375-9.
47. Rogosa, M. (1969) Acidaminococcus gen. n., Acidaminococcus fermentans sp. n., anaerobic gram-negative diplococci using amino acids as the sole energy source for growth, *Journal of bacteriology.* **98**, 756-66.
48. Elsden, S. R., Gilchrist, F. M., Lewis, D. & Volcani, B. E. (1956) Properties of a fatty acid forming organism isolated from the rumen of sheep, *Journal of bacteriology.* **72**, 681-9.
49. Counotte, G. H., Prins, R. A., Janssen, R. H. & Debie, M. J. (1981) Role of Megasphaera elsdenii in the Fermentation of dl-[2-C]lactate in the Rumen of Dairy Cattle, *Applied and environmental microbiology.* **42**, 649-55.
50. Marounek, M., Fliegrova, K. & Bartos, S. (1989) Metabolism and some characteristics of ruminal strains of Megasphaera elsdenii, *Applied and environmental microbiology.* **55**, 1570-3.
51. Coulter, E. D., Shenvi, N. V. & Kurtz, D. M., Jr. (1999) NADH peroxidase activity of rubrerythrin, *Biochemical and biophysical research communications.* **255**, 317-23.
52. Sztukowska, M., Bugno, M., Potempa, J., Travis, J. & Kurtz, D. M., Jr. (2002) Role of rubrerythrin in the oxidative stress response of Porphyromonas gingivalis, *Molecular microbiology.* **44**, 479-88.
53. Knight, E., Jr. & Hardy, R. W. (1966) Isolation and characteristics of flavodoxin from nitrogen-fixing Clostridium pasteurianum, *The Journal of biological chemistry.* **241**, 2752-6.
54. Knight, E., Jr. & Hardy, R. W. (1967) Flavodoxin. Chemical and biological properties, *The Journal of biological chemistry.* **242**, 1370-4.
55. Carr, M. C., Curley, G. P., Mayhew, S. G. & Voordouw, G. (1990) Effects of substituting asparagine for glycine-61 in flavodoxin from Desulfovibrio vulgaris (Hildenborough), *Biochem Int.* **20**, 1025-32.
56. Curley, G. P., Carr, M. C., Mayhew, S. G. & Voordouw, G. (1991) Redox and flavin-binding properties of recombinant flavodoxin from Desulfovibrio vulgaris (Hildenborough), *European journal of biochemistry / FEBS.* **202**, 1091-100.
57. O'Farrell, P. A., Walsh, M. A., McCarthy, A. A., Higgins, T. M., Voordouw, G. & Mayhew, S. G. (1998) Modulation of the redox potentials of FMN in Desulfovibrio vulgaris flavodoxin: thermodynamic properties and crystal structures of glycine-61 mutants, *Biochemistry.* **37**, 8405-16.
58. Bradley, L. H. & Swenson, R. P. (1999) Role of glutamate-59 hydrogen bonded to N(3)H of the flavin mononucleotide cofactor in the modulation of the redox potentials of the Clostridium beijerinckii

flavodoxin. Glutamate-59 is not responsible for the pH dependency but contributes to the stabilization of the flavin semiquinone, *Biochemistry.* **38**, 12377-86.
59. Chang, F. C. & Swenson, R. P. (1999) The midpoint potentials for the oxidized-semiquinone couple for Gly57 mutants of the Clostridium beijerinckii flavodoxin correlate with changes in the hydrogen-bonding interaction with the proton on N(5) of the reduced flavin mononucleotide cofactor as measured by NMR chemical shift temperature dependencies, *Biochemistry.* **38**, 7168-76.
60. Lostao, A., Gomez-Moreno, C., Mayhew, S. G. & Sancho, J. (1997) Differential stabilization of the three FMN redox forms by tyrosine 94 and tryptophan 57 in flavodoxin from Anabaena and its influence on the redox potentials, *Biochemistry.* **36**, 14334-44.
61. Geoghegan, S. M., Mayhew, S. G., Yalloway, G. N. & Butler, G. (2000) Cloning, sequencing and expression of the gene for flavodoxin from Megasphaera elsdenii and the effects of removing the protein negative charge that is closest to N(1) of the bound FMN, *European journal of biochemistry / FEBS.* **267**, 4434-44.
62. Mortenson, L. E., Valentine, R. C. & Carnahan, J. E. (1962) An electron transport factor from Clostridium pasteurianum, *Biochemical and biophysical research communications.* **7**, 448-52.
63. Moonen, C. T. & Muller, F. (1984) On the intermolecular electron transfer between different redox states of flavodoxin from Megasphaera elsdenii. A 500-MHz 1H NMR study, *European journal of biochemistry / FEBS.* **140**, 303-9.
64. Yalloway, G. N., Mayhew, S. G., Malthouse, J. P., Gallagher, M. E. & Curley, G. P. (1999) pH-dependent spectroscopic changes associated with the hydroquinone of FMN in flavodoxins, *Biochemistry.* **38**, 3753-62.
65. Hans, M., Bill, E., Cirpus, I., Pierik, A. J., Hetzel, M., Alber, D. & Buckel, W. (2002) Adenosine triphosphate-induced electron transfer in 2-hydroxyglutaryl-CoA dehydratase from Acidaminococcus fermentans, *Biochemistry.* **41**, 5873-82.
66. Schonheit, P., Brandis, A. & Thauer, R. K. (1979) Ferredoxin degradation in growing Clostridium pasteurianum during periods of iron deprivation, *Archives of microbiology.* **120**, 73-6.
67. Ragsdale, S. W. & Ljungdahl, L. G. (1984) Characterization of ferredoxin, flavodoxin, and rubredoxin from Clostridium formicoaceticum grown in media with high and low iron contents, *Journal of bacteriology.* **157**, 1-6.
68. Thamer, W., Cirpus, I., Hans, M., Pierik, A. J., Selmer, T., Bill, E., Linder, D. & Buckel, W. (2003) A two [4Fe-4S]-cluster-containing ferredoxin as an alternative electron donor for 2-hydroxyglutaryl-CoA dehydratase from *Acidaminococcus fermentans*, *Arch Microbiol.* **179**, 197-204.
69. Mayhew, S. G. & Massey, V. (1969) Purification and Characterization of Flavodoxin from *Peptostreptococcus elsdenii*, *J Biol Chem.* **244**, 794-802.
70. Parthasarathy, A., Pierik, A. J., Kahnt, J., Zelder, O. & Buckel, W. (2011) Substrate Specificity of 2-Hydroxyglutaryl-CoA Dehydratase from *Clostridium symbiosum*: Toward a Bio-Based Production of Adipic Acid, *Biochemistry.* **50**, 3540-3550.
71. Zehnder, A. J. B. & Wuhrmann, K. (1976) Titanium(III) citrate as a nontoxic oxidation-reduction buffering system for the culture of obligate anaerobes, *Science.* **194**, 1165-1166.
72. Hans, M., Bill, E., Cirpus, I., Pierik, A. J., Hetzel, M., Alber, D. & Buckel, W. (2002) Adenosine triphosphate-induced electron transfer in 2-hydroxyglutaryl-CoA dehydratase from *Acidaminococcus fermentans.*, *Biochemistry.* **41**, 5873-82.
73. Chang, Y. J., Pukall, R., Saunders, E., Lapidus, A., Copeland, A., Nolan, M., Glavina Del Rio, T., Lucas, S., Chen, F., Tice, H., Cheng, J. F., Han, C., Detter, J. C., Bruce, D., Goodwin, L., Pitluck, S., Mikhailova, N., Liolios, K., Pati, A., Ivanova, N., Mavromatis, K., Chen, A., Palaniappan, K., Land, M., Hauser, L., Jeffries, C. D., Brettin, T., Rohde, M., Goker, M., Bristow, J., Eisen, J. A., Markowitz, V., Hugenholtz, P., Kyrpides, N. C. & Klenk, H. P. (2010) Complete genome sequence of *Acidaminococcus fermentans* type strain (VR4), *Stand Genomic Sci.* **3**, 1-14.
74. Nakos, G. & Mortenson, L. (1971) Purification and properties of hydrogenase, an iron sulfur protein, from *Clostridium pasteurianum* W5, *Biochim Biophys Acta.* **227**, 576-83.

75. Bradford, M. M. (1976) A rapid and sensitive method for the quantitation of microgram quantities of protein utilizing the principle of protein-dye binding, *Anal Biochem.* **72**, 248-54.
76. Laemmli, U. K. (1970) Cleavage of structural proteins during the assembly of the head of bacteriophage T4, *Nature.* **227**, 680-685.
77. Dawson, R. M. C., Elliott, D. C., Elliott, H. C. & Jones, K. M. (1986) *Data for Biochemical Research*, 3 edn, Clarendon Press, Oxford
78. Fillat, M. F., Borrias, W. E. & Weisbeek, P. J. (1991) Isolation and overexpression in Escherichia coli of the flavodoxin gene from Anabaena PCC 7119, *The Biochemical journal.* **280 (Pt 1)**, 187-91.
79. Beattie, P., Tan, K., Bourne, R. M., Leach, D., Rich, P. R. & Ward, F. B. (1994) Cloning and sequencing of four structural genes for the Na(+)-translocating NADH-ubiquinone oxidoreductase of Vibrio alginolyticus, *FEBS letters.* **356**, 333-8.
80. Wohlfarth, G. & Buckel, W. (1985) A sodium ion gradient as energy source for *Peptostreptococcus asaccharolyticus*, *Arch Microbiol.* **142**, 128-135.
81. Hashizume, K., Tsukahara, T., Yamada, K., Koyama, H. & Ushida, K. (2003) Megasphaera elsdenii JCM1772T normalizes hyperlactate production in the large intestine of fructooligosaccharide-fed rats by stimulating butyrate production, *J Nutr.* **133**, 3187-90.
82. Baldwin, R. L., Wood, W. A. & Emery, R. S. (1965) Lactate Metabolism by Peptostreptococcus Elsdenii: Evidence for Lactyl Coenzyme a Dehydrase, *Biochimica et biophysica acta.* **97**, 202-13.
83. Brockman, H. L. & Wood, W. A. (1975) Electron-transferring flavoprotein of Peptostreptococcus elsdenii that functions in the reduction of acrylyl-coenzyme A, *Journal of bacteriology.* **124**, 1447-53.
84. Baldwin, R. L. & Milligan, L. P. (1964) Electron Transport in *Peptostreptococcus Elsdenii*, *Biochim Biophys Acta.* **92**, 421-432.
85. Whitfield, C. D. & Mayhew, S. G. (1974) Purification and properties of electron-transferring flavoprotein from *Peptostreptococcus elsdenii*, *J Biol Chem.* **249**, 2801-10.
86. Sato, K., Nishina, Y. & Shiga, K. (2003) Purification of electron-transferring flavoprotein from *Megasphaera elsdenii* and binding of additional FAD with an unusual absorption spectrum, *J Biochem.* **134**, 719-729.
87. Sato, K., Nishina, Y. & Shiga, K. (2013) Interaction between NADH and electron-transferring flavoprotein from *Megasphaera elsdenii*, *J Biochem.* **153**, 565-72.
88. O'Neill, H., Mayhew, S. G. & Butler, G. (1998) Cloning and analysis of the genes for a novel electron-transferring flavoprotein from Megasphaera elsdenii. Expression and characterization of the recombinant protein, *The Journal of biological chemistry.* **273**, 21015-24.
89. Marchandin, H., Teyssier, C., Campos, J., Jean-Pierre, H., Roger, F., Gay, B., Carlier, J. P. & Jumas-Bilak, E. (2010) *Negativicoccus succinicivorans* gen. nov., sp. nov., isolated from human clinical samples, emended description of the family *Veillonellaceae* and description of *Negativicutes classis* nov., *Selenomonadales* ord. nov. and *Acidaminococcaceae* fam. nov. in the bacterial phylum *Firmicutes*, *Int J Syst Evol Microbiol.* **60**, 1271-1279.
90. Hetzel, M., Brock, M., Selmer, T., Pierik, A. J., Golding, B. T. & Buckel, W. (2003) Acryloyl-CoA reductase from *Clostridium propionicum*. An enzyme complex of propionyl-CoA dehydrogenase and electron-transferring flavoprotein, *Eur J Biochem.* **270**, 902-10.
91. Prabhu, R., Altman, E. & Eiteman, M. A. (2012) Lactate and acrylate metabolism by Megasphaera elsdenii under batch and steady-state conditions, *Applied and environmental microbiology.* **78**, 8564-70.
92. Lehman, T. C., Hale, D. E., Bhala, A. & Thorpe, C. (1990) An acyl-coenzyme A dehydrogenase assay utilizing the ferricenium ion, *Anal Biochem.* **186**, 280-284.
93. Ziegenhorn, J., Senn, M. & Bücher, T. (1976) Molar absorptivities of beta-NADH and beta-NADPH, *Clin Chem.* **22**, 151-160.
94. Marx, H., Graf, A. B., Tatto, N. E., Thallinger, G. G., Mattanovich, D. & Sauer, M. (2011) Genome sequence of the ruminal bacterium Megasphaera elsdenii, *Journal of bacteriology.* **193**, 5578-9.
95. Djordjevic, S., Pace, C. P., Stankovich, M. T. & Kim, J. J. (1995) Three-dimensional structure of butyryl-CoA dehydrogenase from *Megasphaera elsdenii*, *Biochemistry.* **34**, 2163-71.

96. Bertsch, J., Parthasarathy, A., Buckel, W. & Müller, V. (2013) An electron-bifurcating caffeyl-CoA reductase, *J Biol Chem.* **288**, 11304-11.
97. Muir Wood, P. (1974) The redox potential of the system oxygen--superoxide, *FEBS Lett.* **44**, 22-4.
98. Mishra, S. & Imlay, J. (2012) Why do bacteria use so many enzymes to scavenge hydrogen peroxide?, *Arch Biochem Biophys.* **525**, 145-60.
99. Roberts, D. L., Frerman, F. E. & Kim, J. J. (1996) Three-dimensional structure of human electron transfer flavoprotein to 2.1-A resolution, *Proc Natl Acad Sci U S A.* **93**, 14355-60.
100. Roberts, D. L., Salazar, D., Fulmer, J. P., Frerman, F. E. & Kim, J. J. (1999) Crystal structure of *Paracoccus denitrificans* electron transfer flavoprotein: structural and electrostatic analysis of a conserved flavin binding domain, *Biochemistry.* **38**, 1977-89.
101. Brockman, H. L. & Wood, W. A. (1975) D-Lactate dehydrogenase of Peptostreptococcus elsdenii, *Journal of bacteriology.* **124**, 1454-61.
102. Lehman, T. C., Hale, D. E., Bhala, A. & Thorpe, C. (1990) An acyl-coenzyme A dehydrogenase assay utilizing the ferricenium ion, *Analytical biochemistry.* **186**, 280-4.
103. Olson, S. T. & Massey, V. (1979) Purification and properties of the flavoenzyme D-lactate dehydrogenase from Megasphaera elsdenii, *Biochemistry.* **18**, 4714-24.
104. Wohlfarth, G. & Buckel, W. (1985) A sodium ion gradient as energy source for Peptostreptococcus asaccharolyticus, *Archives of microbiology.* **142**, 128-35.
105. Buckel, W. & Semmler, R. (1982) A biotin-dependent sodium pump: glutaconyl-CoA decarboxylase from Acidaminococcus fermentans, *FEBS letters.* **148**, 35-8.
106. Buckel, W. & Semmler, R. (1983) Purification, characterisation and reconstitution of glutaconyl-CoA decarboxylase, a biotin-dependent sodium pump from anaerobic bacteria, *European journal of biochemistry / FEBS.* **136**, 427-34.
107. Crane, F. L. & Beinert, H. (1956) On the mechanism of dehydrogenation of fatty acyl derivatives of coenzyme A. II. The electron-transferring flavoprotein, *The Journal of biological chemistry.* **218**, 717-31.
108. Husain, M. & Steenkamp, D. J. (1983) Electron transfer flavoprotein from pig liver mitochondria. A simple purification and re-evaluation of some of the molecular properties, *Biochem J.* **209**, 541-5.
109. Chen, D. & Swenson, R. P. (1994) Cloning, sequence analysis, and expression of the genes encoding the two subunits of the methylotrophic bacterium W3A1 electron transfer flavoprotein, *The Journal of biological chemistry.* **269**, 32120-30.
110. Ikeda, Y. & Tanaka, K. (1983) Purification and characterization of isovaleryl coenzyme A dehydrogenase from rat liver mitochondria, *The Journal of biological chemistry.* **258**, 1077-85.
111. Ikeda, Y. & Tanaka, K. (1983) Purification and characterization of 2-methyl-branched chain acyl coenzyme A dehydrogenase, an enzyme involved in the isoleucine and valine metabolism, from rat liver mitochondria, *The Journal of biological chemistry.* **258**, 9477-87.
112. Ruzicka, F. J. & Beinert, H. (1977) A new iron-sulfur flavoprotein of the respiratory chain. A component of the fatty acid beta oxidation pathway, *The Journal of biological chemistry.* **252**, 8440-5.
113. Bertini, I., Donaire, A., Feinberg, B. A., Luchinat, C., Piccioli, M. & Yuan, H. (1995) Solution structure of the oxidized 2[4Fe-4S] ferredoxin from Clostridium pasteurianum, *European journal of biochemistry / FEBS.* **232**, 192-205.
114. Duee, E. D., Fanchon, E., Vicat, J., Sieker, L. C., Meyer, J. & Moulis, J. M. (1994) Refined crystal structure of the 2[4Fe-4S] ferredoxin from Clostridium acidurici at 1.84 A resolution, *Journal of molecular biology.* **243**, 683-95.
115. Whitfield, C. D. & Mayhew, S. G. (1974) Purification and properties of electron-transferring flavoprotein from Peptostreptococcus elsdenii, *The Journal of biological chemistry.* **249**, 2801-10.
116. Pace, C. P. & Stankovich, M. T. (1987) Redox properties of electron-transferring flavoprotein from *Megasphaera elsdenii*, *Biochim Biophys Acta.* **911**, 267-76.
117. Sato, K., Nishina, Y. & Shiga, K. (2013) Decomposition of the Fluorescence Spectra of Two FAD Molecules in Electron-Transferring Flavoprotein from *Megasphaera elsdenii*, *J Biochem.*

118. Ghisla, S. & Mayhew, S. G. (1976) Identification and properties of 8-hydroxyflavin--adenine dinucleotide in electron-transferring flavoprotein from Peptostreptococcus elsdenii, *European journal of biochemistry / FEBS.* **63**, 373-90.
119. Riebe, O., Fischer, R. J., Wampler, D. A., Kurtz, D. M., Jr. & Bahl, H. (2009) Pathway for H2O2 and O2 detoxification in Clostridium acetobutylicum, *Microbiology.* **155**, 16-24.
120. Hillmann, F., Riebe, O., Fischer, R. J., Mot, A., Caranto, J. D., Kurtz, D. M., Jr. & Bahl, H. (2009) Reductive dioxygen scavenging by flavo-diiron proteins of Clostridium acetobutylicum, *FEBS letters.* **583**, 241-5.
121. Riebe, O., Fischer, R. J. & Bahl, H. (2007) Desulfoferrodoxin of Clostridium acetobutylicum functions as a superoxide reductase, *FEBS letters.* **581**, 5605-10.
122. Lehmann, Y., Meile, L. & Teuber, M. (1996) Rubrerythrin from Clostridium perfringens: cloning of the gene, purification of the protein, and characterization of its superoxide dismutase function, *Journal of bacteriology.* **178**, 7152-8.

Annex

Phenylalanine catabolism in *Archaeoglobus fulgidus* VC-16

Anutthaman Parthasarathy · Jörg Kahnt ·Nilanjan Pal Chowdhury · Wolfgang Buckel

Arch Microbiol (2013) 195:781–797, DOI 10.1007/s00203-013-0925-3

Arch Microbiol (2013) 195:781–797
DOI 10.1007/s00203-013-0925-3

ORIGINAL PAPER

Phenylalanine catabolism in *Archaeoglobus fulgidus* VC-16

Anutthaman Parthasarathy · Jörg Kahnt · Nilanjan Pal Chowdhury · Wolfgang Buckel

Received: 21 May 2013 / Revised: 29 August 2013 / Accepted: 31 August 2013 / Published online: 6 October 2013

Abstract Evidence is presented for a pathway of phenylalanine catabolism in the hyperthermophilic archaeon *Archaeoglobus fulgidus* involving the following enzymes—phenylalanine:2-oxoglutarate aminotransferase, phenyllactate dehydrogenase, radical iron–sulphur 3-phenyllactyl-CoA dehydratase, phenylpropionyl-CoA dehydrogenase, aryl pyruvate ferredoxin oxidoreductase, ADP-forming acetyl-CoA synthetase and family III CoA-transferase. Hitherto amino acid degradation pathways involving radical iron–sulphur dehydratases have been characterised only in mesophilic clostridia and related bacteria. The difference here is that the pathway is not fermentative but coupled to sulphate reduction. Initial experiments also show the utilisation of tryptophan as a growth substrate and the decarboxylation of caffeate by cell extracts, suggesting the potential to catabolise different classes of aromatic compounds.

Communicated by Michael Rother.

Electronic supplementary material The online version of this article (doi:10.1007/s00203-013-0925-3) contains supplementary material, which is available to authorized users.

A. Parthasarathy (✉) · J. Kahnt · N. P. Chowdhury · W. Buckel
Max-Planck-Institut für terrestrische Mikrobiologie,
35043 Marburg, Germany
e-mail: anuttham@stanford.edu; parthasa@staff.uni-marburg.de

Present Address:
A. Parthasarathy
Civil and Environmental Engineering, Stanford University, Clark Center E-250, 318 Campus Drive, Stanford, CA 94305, USA

N. P. Chowdhury · W. Buckel
Laboratorium für Mikrobiologie, Fachbereich Biologie,
Philipps-Universität, 35032 Marburg, Germany

Keywords Phenylalanine · Hyperthermophile · Archaeoglobus

Introduction

Fermentations of 12 of the 20 proteinogenic amino acids by clostridia and related bacteria via the 2-hydroxyacid pathways begin with the deamination of the amino groups yielding the 2-oxoacids. Subsequent reduction leads to the formation of the corresponding (*R*)-2-hydroxyacids. Radical iron–sulphur (*R*)-2-hydroxyacyl-CoA dehydratases catalyse the chemically difficult dehydration reactions involving the removal of protons at unactivated β-positions of the 2-hydroxyacid CoA thioesters derived from the 2-hydroxyacids. The mechanisms of those reactions were predicted to proceed via ketyl radicals generated by iron–sulphur clusters (Buckel and Keese 1995). The involvement of ketyl radicals was later demonstrated using spectroscopic methods (Kim et al. 2008). The unsaturated CoA thioesters produced from these dehydrations then undergo reduction to the corresponding saturated acyl-CoAs and ultimately to the saturated carboxylic acids. Some of those enoyl-CoA reductases were shown to be involved in energy conservation via flavin- and ferredoxin-dependent electron bifurcation (Li et al. 2008; Herrmann et al. 2008).

The following (*R*)-2-hydroxyacyl-CoA dehydratases act as key enzymes of their respective amino acid fermenting pathways: 2-hydroxyglutaryl-CoA dehydratase in glutamate fermentation, lactyl-CoA/2-hydroxybutyryl-CoA dehydratase in the fermentations of alanine, serine, and threonine, 2-hydroxyisocaproyl-CoA dehydratase in leucine fermentation and 3-phenyllactyl-CoA dehydratase in phenylalanine fermentation (Buckel 1980a, b; Buckel and Barker 1974; Buckel et al. 2011; Hans et al. 1999; Kim et al. 2004; Dickert 2001; Dickert

et al. 2000, 2002). These enzymes are also of considerable biotechnological interest due to their involvement in the formation of valuable organic acids such as propionate (Kandasamy et al. 2013), 3-hydroxypropionate (Gokarn et al. 2004), glutaconate and glutarate (Djurdjevic et al. 2010, 2011), adipate (Parthasarathy et al. 2011) and phenylpropionate (this work).

Archaeoglobus fulgidus is a hyperthermophilic, sulphate reducer thriving between 80 and 85 °C. The archaeon was isolated and characterised by Stetter et al. (1987), Stetter (1988). It grows heterotrophically on sulphate with lactate, pyruvate, methanol, ethanol, 1-propanol or formate as carbon and energy sources or lithoautotrophically on H_2, $S_2O_3^{2-}$ and CO_2. Growth with proteins/peptides or sugars with sulphate, sulphite or thiosulphate as electron acceptors has been reported (Stetter et al. 1990). The question remained whether individual amino acids could serve as sole carbon and energy sources. In *A. fulgidus*, the genes AF1957-1959 or *hgdABC* were predicted to encode for 2-hydroxyglutaryl-CoA dehydratase and its activator (Hans et al. 1999, Fig. A1). Another gene was predicted to encode a homologue (50 % amino acid sequence identity) of the hydrophobic β-subunit of the Na^+-translocating glutaconyl-CoA decarboxylase, GcdB of *Acidaminococcus fermentans* (Gerhardt et al. 2000) which belongs to the 2-hydroxyglutarate pathway of glutamate fermentation. Apart from these, two distinct ADP-forming acetyl-CoA synthetase isoenzymes (ACDs) from *A. fulgidus* have been characterised. ACD I (acetyl-CoA synthetase) could be involved in aliphatic amino acid degradation, whereas ACD II (phenylacetyl-CoA synthetase) could be involved in aromatic amino acid degradation (Musfeldt and Schönheit 2002). Owing to the presence of homologues of several clostridial enzymes, *A. fulgidus* has been described as an 'honorary clostridium' (Gerhardt et al. 2000) and it is plausible that degradation of either glutamate or aromatic amino acids occurs, although no growth experiments have been published.

Homologues of 2-hydroxyacyl-CoA dehydratases (HgdAB) are rare in archaea including archaeoglobi other than *A. fulgidus*. About two-thirds of the conserved but not functionally characterised proteins in *A. fulgidus* are also present in the archaeon *Methanocaldococcus jannaschii* (Bult et al. 1996; Klenk et al. 1997). In the latter, glutamate has been proposed to be converted first to 2-oxoglutarate and then 2-hydroxyglutarate. Subsequently, 2-hydroxyglutaryl-CoA is dehydrated to glutaconyl-CoA (catalysed by an HgdAB homologue). Instead of decarboxylating glutaconyl-CoA to crotonyl-CoA as reported in the clostridia (Buckel 2001; Buckel and Semmler 1983), *M. jannaschii* aminates it to β-glutamyl-CoA via an ammonia lyase (Graupner et al. 2005). In methanogenic archaea, β-glutamate is an osmoprotectant (Ciulla and Roberts 1999; Graupner et al. 2005). Since *A. fulgidus* shares a large part of its genome with *M. jannaschii*, similar glutamate fermentation via an ammonia lyase might be possible. The genomes of *Methanopyrus kandleri* and *Ferroglobus placidus* also encode HgdAB homologues, although the latter is known to be a benzoyl-CoA reductase (Holmes et al. 2011).

The hyperthermophile *Pyrococcus furiosus* couples elemental sulphur reduction to incomplete phenylalanine or tryptophan oxidation via the following enzymes: aromatic aminotransferase, indolepyruvate decarboxylase, arylacetaldehyde dehydrogenase, indolepyruvate ferredoxin oxidoreductase, arylacetyl-CoA oxidoreductase and arylglyoxylate oxidoreductase (Mai and Adams 1994). The sulphate reducer *Desulfobacula toluolica* Tol2 was proposed to degrade phenylalanine as follows (Wöhlbrand et al. 2013): Initial non-oxidative deamination yields cinnamate with the liberated ammonium being transferred to α-ketoglutarate. Subsequent degradation of cinnamate proceeds via oxidation to phenylpyruvate. Finally, phenylpyruvate is decarboxylated to phenylacetate, which is in turn activated to phenylacetyl-CoA.

In contrast, we hypothesised that *A. fulgidus* catabolises phenylalanine in the same way as *C. sporogenes,* and the enzymes expected in the reductive branch would be phenylalanine:2-oxoglutarate aminotransferase, phenyllactate dehydrogenase, phenyllactyl-CoA dehydratase, family III CoA-transferase, and cinnamate or cinnamoyl-CoA reductase. The oxidative branch would involve aryl pyruvate ferredoxin oxidoreductase and acetyl-CoA synthetase, whereby ATP is conserved (Fig. 1). An NADP-dependent glutamate dehydrogenase (GDH) from the oilfield strain *A. fulgidus* 7324 has been characterised via purification to apparent homogeneity; however, GDH is absent in *A. fulgidus* VC-16 (Steen et al. 2001). Since the VC-16 genome encodes for an NADPH-dependent glutamate synthase, glutamate is probably converted to glutamine and 2-oxoglutarate.

In cell extracts of *A. fulgidus,* we have measured the activities of all the enzymes postulated to be involved in phenylalanine fermentation, identified the putative genes encoding these enzymes, partially purified and identified the phenylpropionyl-CoA dehydrogenase/cinnamoyl-CoA reductase and purified the electron-transferring flavoprotein (Etf) to apparent homogeneity to test the possibility of electron bifurcation. We could also detect the presence of key intermediates in culture supernatants. Moreover, *A. fulgidus* did not grow on glutamate nor could we measure any enzyme activities in cell extracts of *A. fulgidus* pertaining to glutamate fermentation either via the β-glutamyl-CoA ammonia lyase pathway or via the classical clostridial pathway.

Materials and methods

Chemicals

All chemicals including NMR solvents, labelled compounds, ^{18}O-enriched water and media components were

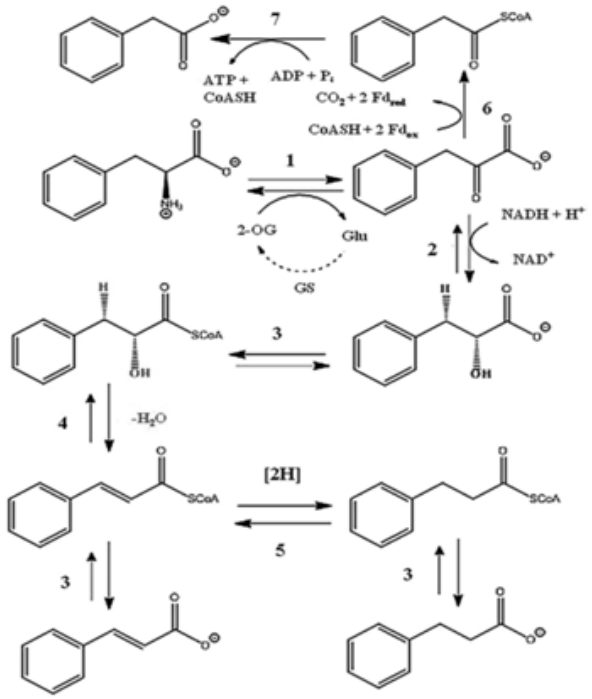

Fig. 1 Putative pathway for phenylalanine metabolism in *A. fulgidus*: *1* = phenylalanine:2-oxoglutarate aminotransferase contains PLP (pyridoxal-5′-phosphate) and NAD-dependent glutamate dehydrogenase, *2* = phenyllactate dehydrogenase, *3* = phenyllactate CoA-transferase (family III), *4* = phenyllactyl-CoA dehydratase and activator: ATP and reduced ferredoxin are needed for activation, *5* = cinnamoyl-CoA reductase/phenylpropionyl-CoA dehydrogenase, *6* = arylpyruvate ferredoxin oxidoreductase and *7* = ADP-forming acetyl-CoA synthetase. *2-OG* = 2-oxoglutarate, *Glu* = L-glutamate and *Fd* = ferredoxin (*ox* = oxidised, *red* = reduced). Note: reaction 5 may involve Etf (electron-transferring flavoprotein), ferredoxin and menaquinone. The red H and OH are lost during the enzymatic *syn*-elimination of water. Phenylalanine oxidation can be coupled to sulphate reduction via reactions 6 and 7, which also conserve ATP and generate reducing equivalents. *GS* stands for NADP-dependent glutamate synthase which generates 2-oxoglutarate and glutamine from glutamate

purchased from Sigma-Aldrich. Syntheses of CoA thioesters from the respective carboxylic acids were accomplished according to published methods (Kawaguchi et al.1981; Parthasarathy et al. 2011; Simon and Shemin 1953). Briefly, 50 μmol of (*R*)-3-phenyllactic acid, phenylpropionic acid, cinnamic acid or phenylacetic acid were dissolved in 0.5 ml acetonitrile and mixed with 40 μmol 1,1′-carbonyldiimidazole. CoA (40 μmol) dissolved in 0.5 ml of 0.1 M $NaHCO_3$ was added to the acetonitrile phase. The two phases were mixed thoroughly and incubated at room temperature for 30 min, after which the volume was increased to 5 ml. The mixture was acidified to pH 2, and the samples were purified to obtain the CoA thioesters of the aromatic acids listed earlier. Glutaconyl-CoA was synthesised from glutaconic acid and acetyl-CoA by an enzymatic method (Parthasarathy et al. 2010), while acetyl-CoA was synthesised from acetic anhydride and CoA (Simon and Shemin 1953; Parthasarathy et al. 2011). 2-Hydroxyglutaryl-CoA was synthesised by a chemical method (Parthasarathy et al. 2010). All the CoA thioesters were purified by passages through reverse phase Sep-Pak C_{18} cartridges (Waters, Massachusetts, USA) in the gravity flow mode. Sample loading and washing were performed using 0.1 % trifluoroacetic acid (aqueous v/v), while elution required 0.1 % trifluoroacetic acid containing 50 % acetonitrile (aqueous v/v). The eluted fractions were frozen at -80 °C and freed from acetonitrile by centrifugation on a Speed-Vac concentrator (Bachofer, Germany). They were then refrozen and vacuum-dried on a lyophiliser (Alpha1-4, Christ Instruments, USA). The lyophilised powders were stored at -80 °C until further use.

Protein concentrations were estimated with the Biorad-Microassay reagent (Bio-Rad-Laboratories, Munich, Germany). Bovine serum albumin (Sigma, Germany) was used as a standard. 3-Phenyl[2-^{2}H]lactate was synthesised by reducing commercial phenylpyruvic acid with a fourfold molar excess of NaB^2H_4 in an ethanol/^2H_2O (1:1 v/v) mixture. After 2 h, the ethanol was removed under vacuum, and the crude product was acidified with trifluoroacetic acid to pH 2. The deuterated product was purified by a passage through a C_{18} column and lyophilised. The purity was confirmed by ^{2}H and ^{1}H NMR.

Cultures

A. fulgidus VC-16 was grown in 50, 100 or 1,000 ml volumes without shaking, under anoxic conditions at 80–85 °C for 6–10 days with sulphate–mineral mixture (Stetter et al. 1987) modified to contain 0.7 mM $FeSO_4.7H_2O$ and 0.5 M NaCl. Larger quantities of cells were obtained from 40-L cultures grown by Dr. Harald Huber, Archaeenzentrum, Universität Regensburg, Germany. The gas phase consisted of N_2/CO_2 = 80/20, and the starting pH was 6.5. The following media containing sulphate minerals including $FeSO_4$ and NaCl were used: medium 1 = 11 mM DL-lactate and 0.5 % yeast extract; medium 2 = 11 mM DL-lactate and Wolfe's vitamins (Atlas 1993; Hartzell and Reed 2006) 10 ml L^{-1}; medium 3 = 0.5 % yeast extract; medium 4 = 11 mM DL-lactate, 6 mM phenylalanine and vitamins (10 ml L^{-1}); medium 5 = 6 mM phenylalanine and vitamins (10 ml L^{-1}). All the assays were performed from extracts of cells grown in media 1 and 2. LC–MS analyses of media after growth were performed in all cases. Total sulphate concentration was 36 mM for all experiments, except for the low sulphate medium 6 (6 mM phenylalanine, vitamins (10 ml L^{-1}) and 0.7 mM $FeSO_4$). The

tryptophan medium contained 36 mM sulphate, 5 mM tryptophan and vitamins (10 ml L^{-1}).

Preparation of cell extracts

Cells were suspended in 100 mM 3-(N-morpholino)propanesulfonic acid (MOPS) pH 7.5 and lysed by ultrasonication. The cell extract was clarified by centrifugation at 100,000×*g* for 1 h at 4 °C on an Optima L-90 K Ultracentrifuge (Beckman Coulter, Germany). For protein purification, ~10 g frozen cells were thawed overnight at 4 °C, suspended in 30 ml 20 mM MOPS, pH 7.0 containing 20 mM $MgCl_2$ (buffer A) and passed through a French pressure cell three times. Unbroken cells were removed by centrifugation at 50,000×*g* for 30 min at 4 °C, and cell membranes were removed by spinning the collected supernatant at 180,000×*g* for 1 h at 4 °C.

Assays for enzyme activity

All assays were performed at 65 °C with crude cell extracts of *A. fulgidus* pre-equilibrated at this temperature. All anoxic operations were done in a glove box (Coy Labs, Ann Arbor, USA) under an atmosphere of 95 % N_2 and 5 % H_2. Buffers were degassed several times under vacuum, flushed with N_2 and reduced with 2 mM dithiothreitol (DTT). Spectrophotometric assays were performed on Ultrospec 1100 *pro* spectrophotometers from Amersham Biosciences installed under anoxic conditions, or an Uvikon 943 double beam spectrophotometer from Kontron Instruments, Switzerland for aerobic measurements.

Phenylalanine:2-oxoglutarate aminotransferase

The cell extract was incubated with 0.2 mM NADH, 5 mM 2-oxoglutarate, 0.5 mM pyridoxal-5′-phosphate (PLP), 5 mM dithiothreitol (DTT) and 10 mM EDTA in 50 mM potassium phosphate pH 8.0. After the absorbance at 340 nm became constant (ca. 3 min), 10 mM L-phenylalanine was added and the activity was monitored at 340 nm, $\varepsilon_{340} = 6.3\ mM^{-1}cm^{-1}$ (Ziegenhorn et al. 1976). This assay is dependent on the initial conversion of phenylalanine into phenylpyruvate, followed by the reduction of the latter compound by NADH to yield 3-phenyllactate.

Phenylalanine ammonia lyase

In a 3.00 ml reaction mix containing cell extract, the final concentrations were 150 mM Tris/HCl pH 8.0 and 2 mM L-phenylalanine. The assay is based on the increase in absorption at 270 nm during the conversion of L-phenylalanine to (*E*)-cinnamate and ammonia, $\varepsilon_{270} = 19.73\ mM^{-1}\ cm^{-1}$ (Havir and Hanson 1970; Hodgins 1971).

Phenyllactate dehydrogenase

The cell extract was incubated with 0.2 mM NADH in 100 mM potassium phosphate pH 8.0. The assay was started by addition of 5 mM 3-phenylpyruvate. Assays were also performed in the reverse direction using 0.2 mM NAD^+ (Steen et al. 2001) and 5 mM 3-phenyllactate. In both cases, the absorbance changes at 340 nm were measured with $\varepsilon_{340} = 6.3\ mM^{-1}cm^{-1}$ (Ziegenhorn et al. 1976).

Phenyllactate CoA-transferase

Cell extracts were incubated with 1 mM phenylpropionyl-CoA in 100 mM potassium phosphate pH 7.5 at 65 °C for 5 min. After addition of 20 mM cinnamate, the formation of cinnamoyl-CoA was monitored at 309 nm, $\varepsilon_{309} = 18.7\ mM^{-1}\ cm^{-1}$ (D'Ordine et al. 1994).

Phenyllactyl-CoA dehydratase

The activity was measured under strictly anoxic conditions ($d = 1$ cm, total volume 0.5 ml) at 65 °C with 50 mM Tris/HCl, pH 8.0, 5 mM $MgCl_2$, 5 mM dithiothreitol, 0.4 mM ATP and 0.1 mM dithionite. After incubation of the cell extract with this mixture for 5 min, the reaction was started by addition of 0.2 mM (*R*)-3-phenyllactyl-CoA. The formation of (*E*)-cinnamoyl-CoA was measured at 309 nm, $\varepsilon_{309} = 18.7\ mM^{-1}\ cm^{-1}$ (D'Ordine et al. 1994). For the ^{18}O-labelling experiment, the same conditions were used, except that the enzyme was incubated in $H_2^{18}O$ (50 % ^{18}O) for 5 h at 65 °C prior to the enzymatic reaction and that 1 mM cinnamoyl-CoA was used as substrate.

Cinnamoyl-CoA reductase

Cinnamoyl-CoA reductase activity was measured in the reverse direction with 0.2 mM phenylpropionyl-CoA as substrate and 0.2 mM ferrocenium hexafluorophosphate($FcPF_6$) as artificial electron acceptor in 50 mM potassium phosphate pH 7.5 (Lehman and Thorpe 1990). The assay measured the decrease in absorbance at 300 nm ($\varepsilon_{300} = 8.6\ mM^{-1}cm^{-1}$). The redox indicator ferrocenium hexafluorophosphate was previously prepared in 10 mM HCl solution to a final concentration of 2 mM set at 617 nm with $\varepsilon_{617} = 0.41\ mM^{-1}cm^{-1}$ (Hetzel et al. 2003).

ACD II assay with phenylacetyl-CoA

The assay was performed by monitoring the ADP-dependent and P_i-dependent release of CoA from phenylacetyl-CoA with DTNB [5,5′-dithiobis(2-nitrobenzoic acid)] (Riddles et al. 1979). The assay mixture (1 ml) contained 200 mM Tris–HCl, pH 8.0, 5 mM $MgCl_2$, 5 mM KH_2PO_4,

0.5 mM ADP, 0.2 mM phenylacetyl-CoA and 0.1 mM DTNB. The reaction was started by the addition of the cell extract, and the formation of the thiophenolate anion was monitored at 412 nm ($\varepsilon_{412} = 14.2$ mM^{-1} cm^{-1}).

Phenylpyruvate ferredoxin oxidoreductase

The activity was determined under anoxic conditions by the phenylpyruvate-dependent reduction of methyl viologen at 604 nm. The standard assay mixture contained 5 mM phenylpyruvate, 2.5 mM $MgCl_2$, 0.4 mM thiamine diphosphate, 0.1 mM free CoA (CoASH) and 1 mM methyl viologen in 50 mM HEPPS (3-[4-(2-hydroxyethyl)-1-piperazinyl]propanesulfonic acid), pH 8.4. Activity was calculated based on an extinction coefficient of $\varepsilon_{604} = 27.2$ mM^{-1}cm^{-1} (Mayhew 1978).

INT assay for Etf

Iodonitrotetrazolium chloride (INT) was used as a coloured indicator to follow the NADH mediated transfer reaction of reducing equivalents. In the assay, the enzyme fraction was added to 50 μM INT and 100 μM NADH in 50 mM potassium phosphate pH 7.5. The formation of formazan was followed at 496 nm using the extinction coefficient $\varepsilon_{496} = 19.2$ mM^{-1}cm^{-1} (Möllering et al. 1974).

Caffeate decarboxylase assay

The assay was performed by incubating extracts of yeast extract–lactate–sulphate grown cells containing about 20 mg of protein in 50 mM Tris–HCl pH 8.0 at 65 ºC with 0.5 mM of caffeate or 0.5 mM cinnamate in a sealed Falcon tube for 1 h. Then, the small molecule fraction was harvested from the flow through of a 3-kDa Centricon filter. The filtrate was acidified to pH 2, saturated with NaCl and extracted three times with ethylacetate. After solvent removal under vacuum, the residue was analysed by LC–MS.

β-Glutamyl-CoA ammonia lyase

The activity was measured by incubating cell extracts with 2 mM glutaconyl-CoA and 100 mM NH_4Cl at 290 nm (Herrmann et al. 2005) in 50 mM Tris HCl pH 8.0. We further tested the activity by subjecting the acidified assay mixture to MALDI-TOF mass spectrometry to detect the addition of ammonia to glutaconyl-CoA, which is unique to the *β*-glutamate pathway known from *M. jannaschii.*

Other enzymes of glutamate fermentation

Published methods were used to measure the activities of the following enzymes of the glutamate fermentation pathway: 2-hydroxyglutarate dehydrogenase (Martins et al. 2005), glutaconate CoA-transferase (Buckel 1980b), 2-hydroxyglutaryl-CoA dehydratase (Parthasarathy et al. 2011) and glutaconyl-CoA decarboxylase (Buckel and Semmler 1983). Except for the glutaconyl-CoA decarboxylase, the other enzymes could either be part of a clostridial-type glutamate fermentation pathway or the β-glutamate pathway.

Electron bifurcation assay

NADH oxidation catalysed by a putative phenylpropionyl-CoA-dehydrogenase/Etf complex was assayed spectrophotometrically ($\varepsilon_{340} = 6.2$ mM^{-1} cm^{-1}) at 25 °C. Each 1 ml assay mixture contained 50 mM Tris–HCl pH 7.5, 2 mM DTT, 0.1 mM NADH, 0.1 mM cinnamoyl-CoA, 5 μM FAD, phenylpropionyl-CoA dehydrogenase (partially purified) and Etf (purified to apparent homogeneity). Twenty micromolar of ferredoxin from *Clostridium tetanomorphum* and 0.4 U hydrogenase from *C. pasteurianum* prepared according to established procedures (Jayamani 2008) were added. The reaction was started by the addition of cinnamoyl-CoA. One unit was defined as the oxidation of 1 μmol NADH per min. The assay was performed separately at 37 and 65 °C.

Sulphate determination

Samples of culture media were centrifuged at 5,000×*g* for 5 min to remove the cells. Samples were prepared during each day of the culture growth and made up to different dilutions to stay within the range of the standards (50–1.000 ppm). The estimation is based on the formation of insoluble Ba(II) sulphate in the presence of EDTA and has been described elsewhere (MacKellar et al. 1978).

Sulphide determination

The concentration of dissolved sulphide was determined by using the absorption of methylene blue at 670 nm (Cline 1969; Çinkaya 2002). To account for precipitated sulphides, the medium was acidified to pH 5 in sealed bottles, whereby most sulphides were solubilised. Several dilutions of each sample were prepared in order to keep the measured concentrations within the range of the standards.

Determination of phenylalanine and other aromatic metabolites

The concentrations of the following aromatic analytes were determined by HPLC (detection at 215 nm): phenylalanine, phenylacetate, phenylpropionate, cinnamate and phenyllactate. Estimations based on the peak areas were performed by calibration against a series of standards from 0 to 8 mM in 0.5 mM steps and 0–0.8 mM in steps of 0.1 mM. For

tryptophan, indoleacetate, indolepropionate, indoleacrylate, caffeate and 3,4-dihydroxystyrene no concentrations were estimated, but their presence confirmed by comparison with authentic standards.

Purification and identification of phenylpropionyl-CoA dehydrogenase and electron-transferring flavoprotein (Etf)

All buffers were sterilised using a 0.45-μm filter. Soluble extracts were prepared in 20 mM MOPS, pH 7.0 containing 20 mM $MgCl_2$ (buffer A). The collected supernatant was filtered through a 0.2-μm filter and was loaded onto a DEAE-Sepharose column (1.25 × 10 cm) equilibrated with buffer A. After loading, the column was washed with 2 column volumes of buffer A and then fractionated with 10 column volumes of a 0–100 % gradient of buffer B (1 M NaCl in buffer A). Fractions with the highest activity were pooled, concentrated and loaded onto a phenyl Sepharose column (0.5 × 20 cm). Elution was performed with five column volumes of a 100–0 % gradient of buffer C (1.5 M $(NH_4)_2SO_4$ in buffer A). The fractions with highest phenylpropionyl-CoA dehydrogenase activity were again pooled, dialysed against 50 mM MOPS pH 7.0 containing 20 mM $MgCl_2$, concentrated and loaded on to a hydroxyl apatite column (0.5 × 15 cm), and proteins were fractionated with a five column volume gradient from 0 to 100 % or 50 to 500 mM buffer D (potassium phosphate pH 7.0). The Etf was purified by applying two chromatographic steps: DEAE-Sepharose (co-elution with Acd-8 at 0.63 M NaCl or 63 % in a gradient from 0 to 1 M) and phenyl Sepharose (elution at 0.9 M $(NH_4)_2SO_4$ or 60 % in a gradient from 1.5 to 0 M). The fractions were pooled, concentrated and run on SDS-PAGE performed by the method of Laemmli (Laemmli 1970) using 12 % polyacrylamide gels.

Bioinformatics

All amino acid sequences were downloaded from the NCBI Pubmed Server (http://www.ncbi.nlm.nih.gov/pubmed/). NCBI gene names were used wherever known; in other cases, NCBI gene IDs or locus tags were used. All the phylogenetic trees were created in the MAFFT ClustalW (Katoh et al. 2005) mode using the default settings of the Trex Online webpage (Boc et al. 2010) MAFFT version 6.864 (http://mafft.cbrc.jp/alignment/server/). Multiple sequence alignments shown in the Supplementary section were created using the Multialin Interface webpage (http://multalin.toulouse.inra.fr/multalin/) based on published methods (Corpet 1988).

NMR spectra

^1H- and ^{13}C-NMR spectra were routinely measured with 3–30 mg samples in standard NMR solvents (Sigma-Aldrich, Germany) on a Bruker AVANCE 300 B (300 MHz) spectrometer in automated mode at the Department of Chemistry, Philipps University, Marburg. ^1H-spectra were measured at 300 MHz and ^{13}C-spectra at 75.45 MHz. Chemical shifts were measured with respect to tetramethyl silane as external standard. ^2H (deuterium only) NMR spectra were measured at 400 MHz on a Bruker BioSpin DRX400 spectrometer. The time-dependent NMR experiments were performed at 50 °C. Chemical shifts were measured with respect to 3-(trimethyl)[$^2H_6$]propane-1-sulphonate standard. ^{15}N-NMR spectra were recorded at 30.42 MHz on a Bruker AMX 300 spectrometer using 5-mm-diameter broadband frequency probe head employing a Waltz-16 composite pulse sequence. In order to obtain a good signal/noise ratio, it was necessary to accumulate 3,000–5,000 scans. Chemical shifts are quoted relative to $^{15}NH_4Cl$ (100 mM) as an external standard. The small molecule fractions for ^{15}N-NMR were prepared by removing the protein fraction by means of 3 kDa cut-off Centricon membrane filters (Millipore Corporation, USA), freezing at −80 °C followed by lyophilisation. The sample in 3-mm glass tubes was dissolved in ^2H_2O or H_2O. The TopSpin 3.0.b.7 programme from Bruker was used to evaluate the spectra.

MALDI-TOF mass spectrometry

The purified and lyophilised CoA thioester samples were dissolved in 10–40 μl water. Acetyl-CoA or free CoA was used as internal standard. The samples were mixed with a matrix consisting of alpha-cyano-4-hydroxycinnamic acid (4 mg ml^{-1} 70 % (v/v) acetonitrile) and 0.1 % (v/v) trifluoroacetic acid directly on the MALDI plate. Every sample was spread out in a sequence of spots where the sample was progressively diluted with the matrix. MALDI-TOF analysis was carried out on a 4800 Proteomics Analyser using the 4800 Series Explorer software. The mass spectrometer was operated in positive-ion reflector mode. For one main spectrum, 30 sub-spectra with 80 spots per sub-spectrum were averaged. Close external calibration was performed with the calibration standard no. 206195 from BRUKER Daltonics in the mass range 931.515–2465.199 Da.

Peptide mass fingerprinting

The peptide mixtures arising from protein samples by in-gel trypsin digestion of Coomassie-stained SDS-PAGE bands were analysed by peptide mass fingerprinting (PMF). The calibration was performed internally, using the peptides generated by trypsin autolysis. Protein samples were processed (taking precautions to avoid keratin contamination) as follows. The desired SDS gel bands were cut out of the gel and destained for several hours in 30 % isopropanol, 50 mM NH_4HCO_3, 20 mM thioglycolic acid and 20 mM

aqueous ammonia, final pH 8.2. Following removal of the supernatant, 100 % isopropanol was added. After 5–60 min, the isopropanol was removed under vacuum. The denatured proteins in the samples were treated for 20 min with trypsin (5 μg ml^{-1}), 5 mM NH_4HCO_3, 10 % acetonitrile, 8 mM dithiothreitol and 1 mM $CaCl_2$. Samples for identification by PMF (peptide mass fingerprinting) were taken after overnight incubation. Acetonitrile (20 %) was added to dry gel samples. The trypsin digestion was stopped by adding 1 μl glacial acetic acid, and further processing was done without drying of the sample. The acidic supernatant (1 μl) was extracted with 0.1 % trifluoroacetic acid and 70 % acetonitrile. The gel pieces were soaked in water to swell them between successive extractions. The extracted fractions were pooled and concentrated. The concentrated sample (1 μl) was mixed with the matrix and analysed by MALDI-TOF. MS–MS data were searched against an in-house protein database using Mascot embedded into GPS Explorer software (MDS Sciex). For software and web resources, please refer to (Hufnagel and Rabus 2006).

LC–MS analysis

Each *A. fulgidus* culture (200 ml, grown for 6–10 days) to be analysed was centrifuged at 10,000×*g* at 4 °C for 20 min. The supernatant was acidified with 5 M HCl to pH 2 and extracted three times with saturated NaCl and ethyl acetate. The organic part was dried over anhydrous sodium sulphate and concentrated under vacuum. The residue was dissolved in a minimum volume of methanol and analysed by LC–MS. A reverse phase C_{18} column (size 125/2 mm) was used on a LTQ FT Ultra-LC–MS device from Thermo Scientific. Elution was performed with an acetonitrile/water gradient from 5 to 99 % acetonitrile. The UV detection was at 215 nm. The peaks appearing on the HPLC were scanned by ESI–MS in the negative mode with a mass window of 50–500 Da. Each compound was assumed to be present only if the mass in the recorded spectrum was identical to that in the simulated spectrum by at least 3 decimal places. The concentration of each compound could be estimated by integrating the peak area using a photodiode array (PDA) detector and by comparison with a series of standards.

Results

Growth with different media containing phenylalanine and intermediates of the proposed pathway

The main products of the proposed phenylalanine degradation pathway are phenylacetate, phenyllactate, cinnamate and phenylpropionate. To establish a redox balance, only the oxidised phenylacetate (−4 electrons) and the reduced phenylpropionate (+2 electrons) have to be considered, whereas phenyllactate and cinnamate have the same redox state as phenylalanine. Complete sulphate reduction to sulphide needs +8 electrons. Since nearly all the sulphate consumed is reduced to sulphide (Table 1), it can be inferred that a redox balance is established in each case. 1 L of an *A. fulgidus* culture growing with phenylalanine as the sole carbon source in the presence of 36 mM sulphate for 7 days yielded 0.40 g of cells (wet weight). The growth yield with phenylalanine and 0.7 mM sulphate was 0.42 g of cells L^{-1} of culture (wet weight). When grown with lactate and yeast extract in the presence of sulphate as electron acceptor, 0.45 g L^{-1} (wet weight) was obtained; in the literature, a value of 0.47 g L^{-1} was reported (Stetter et al. 1987).

A. fulgidus growing with 6 mM phenylalanine, vitamins and 36 mM sulphate produced 1.8 mM phenylacetate, 1.5 mM phenylpropionate and 0.5 mM sulphide. Cinnamate (1.3 mM) and 0.4 mM phenyllactate were the other products derived from the intermediate CoA thioesters. For example, here, the redox balance would be $= (1.8 \times -4) + (1.5 \times +2) + (0.5 \times +8) = 0$. Similar redox calculations for the other media can be performed: the results are seen in Table 1. The presence of lactate resulted only in small changes in the product distribution. Sulphate consumption was not measured in the phenylalanine/lactate case (Table 1) as both phenylalanine and lactate could be oxidised concomitant with sulphate reduction.

If the sulphate concentration was reduced from 36 mM to 0.7 mM, 5 mM phenylalanine was converted to 1.3 mM phenylacetate and 1.4 mM phenylpropionate, while ca. 0.3 mM sulphide was formed. Cinnamate (1.7 mM) and 0.6 mM phenyllactate were also formed. When yeast extract was used instead of phenylalanine and vitamins, 0.2 mM phenylacetate, 0.15 mM phenylpropionate, 0.18 mM cinnamate and 0.07 mM phenyllactate were formed. This is not surprising since yeast extract contains almost all proteinogenic amino acids including phenylalanine. The number of electrons from phenylalanine catabolism in case of the yeast extract medium $= (0.2 \times -4) + (0.15 \times +2) = -0.5$. In order to balance this, ca. 0.06 mM of sulphate would have to be reduced to sulphide ($0.06 \times +8$ electrons $= +0.48$). However, about 1.1 mM of sulphate was reduced (Table 1). Therefore, phenylalanine could not account for all the sulphate reduced, and the oxidation of other amino acids from yeast extract was inferred. Apparently 0.6 mM phenylalanine is sufficient to induce the production of the enzymes required for its catabolism. Growth in the control medium (lactate, sulphate, minerals and vitamins but no phenylalanine or yeast extract) did not give any aromatic products. Benzoate, benzaldehyde, phenol, glutaconate and β-glutamate were not detected in any of our cultures. A typical LC–MS spectrum for phenylalanine metabolism is shown in Fig. A2, and the masses and

Table 1 The results of growth experiments of *A. fulgidus* with different media showing the consumption of phenylalanine and sulphate, and the production of phenylacetate (oxidised end product), phenylpropionate (reduced end product) and sulphide

Medium	Phe consumed (mM)	Phenylacetate (mM)	Phenyl propionate (mM)	Initial $[SO_4^{2-}]$ (mM)	SO_4^{2-} consumed (mM)	Phe/SO_4^{2-} ratio (consumed)	Sulphide formed (mM)	Electrons $[(SO_4^{2-})-(Phe)]$
Yeast extract (0.6 mM Phe)	0.60 ± 0.05	0.20 ± 0.03	0.15 ± 0.02	36.00 ± 0.04	1.10 ± 0.10	1:2	1.00 ± 0.08	>0
6 mM Phe + vitamins (high sulphate)	5.00 ± 0.20	1.80 ± 0.20	1.50 ± 0.10	36.00 ± 0.02	0.50 ± 0.07	10:1	0.48 ± 0.04	≈0
6 mM Phe + vitamins (low sulphate)	5.00 ± 0.20	1.30 ± 0.20	1.40 ± 0.30	0.70 ± 0.02	0.32 ± 0.06	15:1	0.28 ± 0.03	≈0
6 mM Phe + lactate + vitamins	5.40 ± 0.30	2.00 ± 0.30	1.60 ± 0.20	36.00 ± 0.05	Not measured	No data	No data	No data
5 mM Trp + vitamins	3.00 ± 0.20	Not applicable	Not applicable	36.00 ± 0.08	0.35 ± 0.12	8:1 (Trp/SO_4^{2-})	0.30 ± 0.05	$[(SO_4^{2-})-(Trp)] \approx 0$

The last column shows the difference between the amount of electrons generated by sulphate reduction and the amount of electrons generated by the metabolism of Phe

retention times are listed in Table A1. These metabolites were extracted from culture supernatants, indicating their possible export out of the cell. Phenylpyruvate was not detected, because it either did not accumulate due to thermal instability or was not excreted.

Our experiments showed that tryptophan could be used instead of phenylalanine as a growth substrate and the products formed were indoleacetate, indolepropionate and indoleacrylate (Fig. A4). Indolelactate was not detected. We propose that the pathway for the catabolism of tryptophan involves the same enzymes as for phenylalanine in Fig. 1: tryptophan is converted into indolepyruvate by a tryptophan:2-oxoglutarate aminotransferase reaction, and indolepyruvate is then reduced by a dehydrogenase to indolelactate. The oxidation of indolepyruvate via the phenylpyruvate:ferredoxin oxidoreductase and ACD II yields indoleacetate and ATP. Indolelactate is activated to indolelactyl-CoA and dehydrated to indoleacryloyl-CoA. The latter is reduced to indolepropionyl-CoA, and the CoA moiety is recycled.

Other aromatic compounds

Caffeate (3,4-dihydroxycinnamate) was decarboxylated by extracts of cells grown with yeast extract–lactate–sulphate to 3,4-dihydroxystyrene (Fig. A5), but cinnamate was not.

Enzyme activities, purification of enzymes and identification of candidate genes in the genome

The activities of the phenylalanine catabolism shown below were measurable in extracts of *A. fulgidus* cells only when grown on yeast extract–lactate–sulphate, but not on vitamins–lactate–sulphate. This clearly demonstrates the induction of these activities in the presence of 0.6 mM phenylalanine from the yeast extract and confirms that they are not side reactions of enzymes involved in the lactate–sulphate metabolism. Some of the measured activities differ significantly from those of *C. sporogenes* after growth on phenylalanine (Table 2). In cell extracts of *A. fulgidus* grown on sulphate-mineral medium and lactate, complemented with either yeast extract or vitamins, no enzymatic activities associated with glutamate fermentation via 2-hydroxyglutaryl-CoA (Buckel 1980a, b; Buckel and Barker 1974; Kim et al. 2004) were detected. There was no activity measurable for β-glutamyl-CoA ammonia lyase or for phenylalanine ammonia lyase.

Phenyllactyl-CoA dehydratase

This is the key enzyme of the phenylalanine degradation pathway (Fig. 1). At 1.0 U mg^{-1}, its specific activity was relatively high (Table 2), but attempts to purify the

Table 2 Enzymes and corresponding gene candidates for the proposed pathway are shown. Activities measured (in cell extracts) of some major enzymes of the proposed phenylalanine pathway in *A. fulgidus* are compared with those from a similar pathway from the mesophilic *Clostridium sporogenes* (Dickert 2001; Dickert et al. 2000, 2002)

Enzyme	Gene candidate(s)	Specific activity (mU/mg) in *A. fulgidus* (yeast extract, lactate, sulphate)	Specific activity (mU/mg) in *A. fulgidus* (vitamins, lactate, sulphate)	Specific activity (mU/mg) in *C. sporogenes*
Phenylalanine:2-oxoglutarate aminotransferase	*aspB1-4,hisC-2*	500 ± 80	None	Not known
3-Phenyllactate dehydrogenase	AF1779	755 ± 90 (NADH + phenyllactate) 400 ± 65 (NAD^+ + phenylpyruvate)	None	5000
Phenyllactate (family III) CoA-transferase	*caiB-1*	100 ± 5	None	110
Phenyllactyl-CoA dehydratase	*hgd ABC*	1030 ± 20	None	60 (assay not optimised)
Cinnamoyl-CoA reductase/ Phenylpropionyl-CoA dehydrogenase	*acd2,5,7,8 (etfBA)*	300 ± 16 (Phenylpropionyl-CoA with ferrocenium)	None	None
Cinnamate (enoate) reductase	None	None	None	300
Phenylpyruvate ferredoxin oxidoreductase (POR) (Musfeldt and Schönheit 2002)	*iorAB*	280 ± 30	None	Not known
ADP-forming phenylacetyl-CoA synthetase (ACD II) (Musfeldt and Schönheit 2002)	AF1938	200 ± 15	None	Not known

Activities were measurable from extracts of *A. fulgidus* grown on yeast extract–sulphate–lactate which contains phenylalanine, but not when grown on vitamins-sulphate-lactate

phenyllactyl-CoA dehydratase were unsuccessful, probably due to the extremely labile nature of the activator protein which interacts with it and is required for its catalytic activity. The enzyme also acts as a hydratase, converting cinnamoyl-CoA to (*R*)-3-phenyllactyl-CoA. By performing the reaction in water enriched with $H_2^{18}O$, mass additions of 18 and 20 mass units are expected. This was indeed observed in the MALDI-TOF spectrum (Fig. 2). Under aerobic conditions or when Mg-ATP and dithionite were absent, cinnamoyl-CoA remained unchanged as detected by its peak in the MALDI-TOF spectrum (data not shown), confirming the lack of enzymatic activity. This indicates that the hydration of cinnamoyl-CoA occurs via phenyllactyl-CoA dehydratase and not via an unknown enoyl-CoA hydratase yielding 3-hydroxy-3-phenylpropionyl-CoA (3H3P-CoA). Oxidation of 3H3P-CoA would yield 3-oxo-3-phenylpropionyl-CoA, which would then be cleaved to acetyl-CoA and benzoyl-CoA. However, benzoate was not detected in any of our cultures.

BLASTP and BLASTX searches for 2-hydroxyacyl-CoA dehydratase subunits (HgdAB) from *A. fulgidus* revealed 30–50 % identities to those of well-characterised 2-hydroxyacyl-CoA dehydratases from clostridia and related bacteria. Figures A7 and A8 show that the *A. fulgidus* enzyme conserves the important features of the 2-hydroxyacyl-CoA dehydratases, namely the three [4Fe-4S] cluster forming cysteines and a catalytic glutamate on the A subunit, and the three [4Fe-4S] cluster forming cysteines on the B subunit (Knauer et al. 2011). The A subunit is predicted to contain the active site [4Fe-4S] cluster and the B subunit an electron transfer/storage [4Fe-4S] cluster of the radical dehydratase family based on the X-ray crystallographic structure of the *Clostridium difficile* 2-hydroxyisocaproyl-CoA dehydratase (Knauer et al. 2011). The putative homodimeric activator of 2-hydroxyacyl-CoA dehydratase (HgdC) from *A. fulgidus* shares 75-80 % sequence identity with the activators of the clostridial group; the 2 × 2 cysteines forming the [4Fe-4S] cluster are conserved (Knauer et al. 2012) (Fig. A9).

Phylogenetic trees (Fig. 3) show that the *A. fulgidus* dehydratase branches off from the clostridial enzymes; for the A subunit, it forms its own sub-clade with many SRB or sulphate-reducing bacteria (Fig. 3). For the B subunit, *A. fulgidus* HgdB again falls within the SRB sub-clade (Fig. 3), which is less closely related to the clostridia than in the subunit A case and has a few close relatives among the benzoyl-CoA reductases (Bcr). The entries from the thermophilic archaea are only distantly related to each other and are closely related to different bacterial entries (Fig. 3). For the activator, the SRB sub-clade does not exist, but the *A. fulgidus* HgdC still is closely related to that of the true clostridia (Fig. 4). The benzoyl-CoA reductase (Bcr) subunits BcrBC from *Thauera aromatica* (Boll and Fuchs 1995) occur in a complex responsible for the reduction of benzoyl-CoA. However, benzoate and benzaldehyde were absent in our cultures, and there is no biochemical evidence for benzoate reduction under our growth conditions in *A. fulgidus*. Also, there are no homologues encoded by

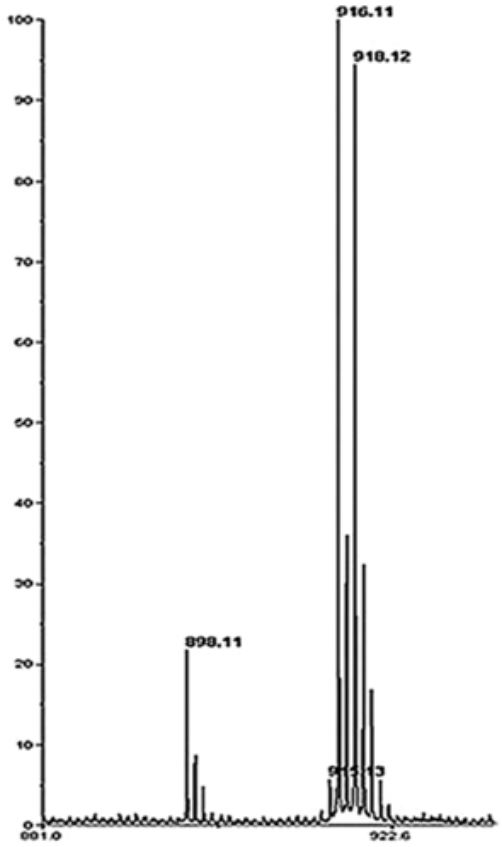

Fig. 2 The MALDI-TOF spectrum (*x*-axis m/z; *y*-axis relative intensity) of a cinnamoyl-CoA hydratase assay (with Mg-ATP and dithionite) showing the hydration of cinnamoyl-CoA (898.11 Da). The products phenyllactyl-CoA-^{16}O (916.11 Da) and phenyllactyl-CoA-^{18}O (918.12 Da) are formed, respectively, by the addition of H_2 ^{16}O and H_2 ^{18}O

any known genes for benzene ring catabolism in the whole genome except HgdABC. Thus, due to the close phylogenetic relationship of the *A. fulgidus* sequence to the well-known clostridial sequences and clear distinction from the Bcr in case of the catalytic A subunit and the activator, the function of HgdABC is suggested to be dehydration rather than aromatic ring reduction.

Phenylalanine:2-oxoglutarate aminotransferase

Since the spectrophotometric assay at 340 nm performed (Table 2) depends on the NADH-dependent reduction of phenylpyruvate to (*R*)-3-phenyllactate formed from the initial aminotransferase reaction, discriminating between the activities of the aminotransferase and the phenyllactate dehydrogenase is difficult. Therefore, we needed to confirm the aminotransferase activity by using NMR spectroscopy. Thus, L-phenyl[^{15}N]alanine was incubated for 1 h with cell extract under assay conditions previously described in the Methods section. Since the enzymatic reaction started without any [^{15}N]glutamate, the label must have been transferred from phenyl[^{15}N]alanine to 2-oxoglutarate yielding [^{15}N]glutamate by aminotransferase activity. The ^{15}N-NMR spectrum is shown in Fig. A10. The unidentified peak at 6.3 ppm could be [^{15}N]aspartate due to further transamination(s). Again, no phenylalanine ammonia lyase activity was detected.

The genome of *A. fulgidus* does not include any gene for phenylalanine ammonia lyase, an enzyme occurring in plants that catalyses the formation of cinnamate from phenylalanine in a single step. We therefore looked for an aminotransferase, which could initiate the fermentation of phenylalanine. An alanine aminotransferase is probably not present in *A. fulgidus* because this amino acid is synthesised from pyruvate mediated by an alanine dehydrogenase (Schröder et al. 2004). However, *A. fulgidus* contains two aminotransferases annotated as aspartate aminotransferase (AspB1-4) and histidinol aminotransferase (HisC-2). In other organisms, tyrosine, histidinol phosphate and aspartate aminotransferases are homologous (Mehta et al. 1989) and mutations in the active site can change the specificity from aspartate to phenylalanine (Onuffer and Kirsch 1995). Therefore, AspB1-4 or HisC-2 may correspond to phenylalanine:2-oxoglutarate aminotransferase.

Phenyllactate dehydrogenase

The activity was measured with phenylpyruvate and NADH or with phenyllactate and NAD^+ at pH 8.0 (Table 2). The enzyme is very likely *R*-specific, since this activity was only observed with the racemate or the *R*-isomer but not with the *S*-enantiomer. Apart from using the spectrophotometric measurements, we also decided to demonstrate the enzyme activity by a direct and chemically specific method. Therefore, we synthesised (*R,S*)-3-phenyl[2-^{2}H]lactate by reduction of phenylpyruvate with sodium borodeuteride. The chemical shift of the singlet ^{2}H-signal (4.4 ppm) of 3-phenyl[2-^{2}H]lactate in the ^{2}H-only spectrum in H_2O was the same as that of the multiplet (4.4 ppm) in the ^{1}H-NMR spectrum of 3-phenyllactate in ^2H_2O at an identical pH of 8.0 (Fig. A11). The NAD^+-dependent oxidation of 3-phenyl[2-^{2}H]lactate to non-deuterated phenylpyruvate catalysed by the cell extract was measured following the disappearance of the corresponding deuterium signal in a ^{2}H-only NMR spectrum (Fig. A12). The peak at 2.45 ppm corresponding to [4-^{2}H]NADH (NADD) slowly increases in intensity over time. This demonstrates the occurrence of a specific deuteride ($^2H^-$) transfer from 3-phenyllactate (substrate) to NAD^+ (cofactor).

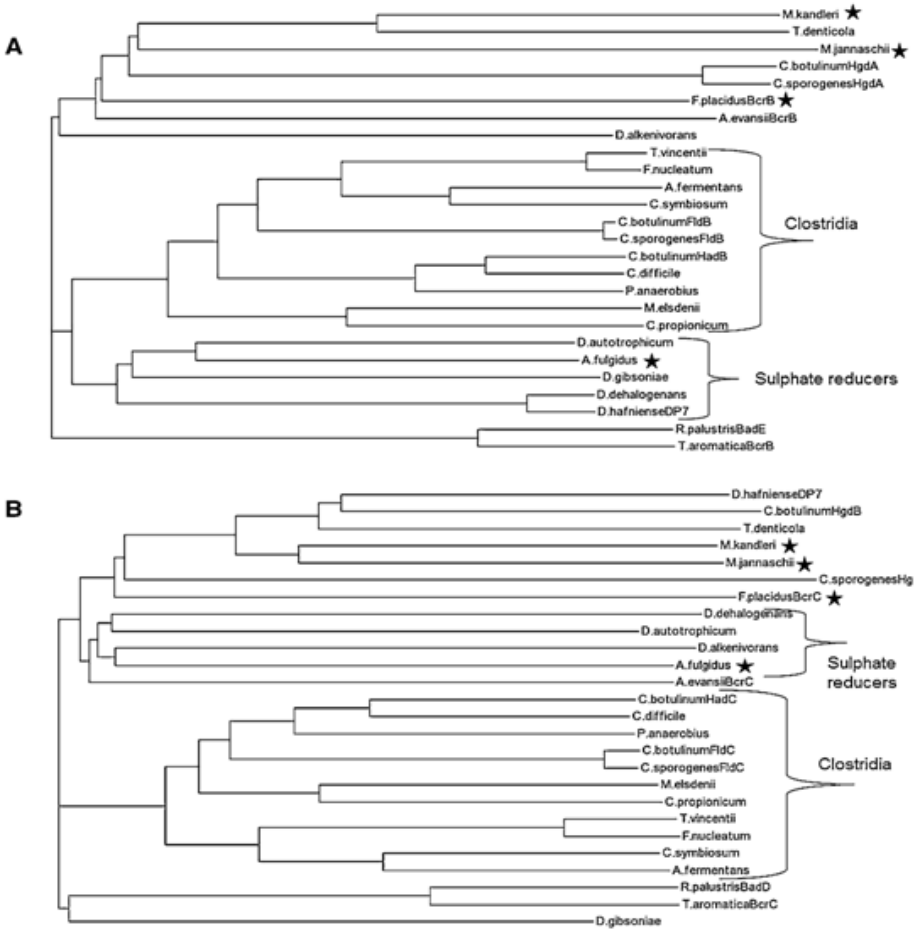

Fig. 3 **a** Phylogenetic tree of the (*R*)-2-hydroxyacyl-CoA dehydratases in the ClustalW mode: Subunit A: Clostridia and their relatives: *C. difficile, C. sporogenes* contains two forms HgdA and FldB,*C. propionicum, C. symbiosum,C. botulinum* Hall str. A contains three putative forms HadA, HgdB and FldB, *Acidaminococcus fermentans, Fusobacterium nucleatum, Treponema vincentii, Megasphaera elsdenii, Peptostreptococcus anaerobius.* Other entries are *Treponema denticola, Methanocaldococcus jannaschii, Methanopyrus kandleri* and the sulphate reducers *Desulfatibacillum alkenivorans, Desulfitobacterium hafniense* DP7, *Desulfotomaculum gibsoniae, Desulfitobacterium dehalogenans* and *Desulfobacterium autotrophicum.* The BcrB from *Thauera aromatica, Azoarcus evansii* and *Ferroglobus placidus* as well as the *Rhodopseudomonas palustris* BadE are benzoyl-CoA reductase subunits. The starred entries indicate thermophilic archaea. **b** Corresponding entries for the subunit B of the (*R*)-2-hydroxyacyl-CoA dehydratases are shown. The dehydratase subunits here are HgdB (shown for *C. sporogenes* as Hg), HadC and FldC. BcrC and BadD are the benzoyl-CoA reductase subunits. Accession numbers for some entries which also appear in the multiple sequence alignments in the Supplements section are given in that section in the legends to figures A7 and A8

The gene AF1779 is annotated as the only putative 2-hydroxyacid dehydrogenase in *A. fulgidus*. Comparison of the amino acid sequence of AF1779 with those of putative and well-characterised enzymes of the 2-hydroxyacid dehydrogenase family revealed sequence identities of 20–32 %. However, the catalytic triad of arginine, glutamate and histidine, based on the X-ray diffraction structure of the (*R*)-2-hydroxyglutarate dehydrogenase from *Acidaminococcus fermentans* (Martins et al. 2005) was not only conserved in several clostridia and lactobacilli, but also in *A. fulgidus* (Fig. A13).

Phenyllactate CoA-transferase

Apart from measuring the activity via spectrophotometry with phenylpropionyl-CoA and cinnamate (Table 2),

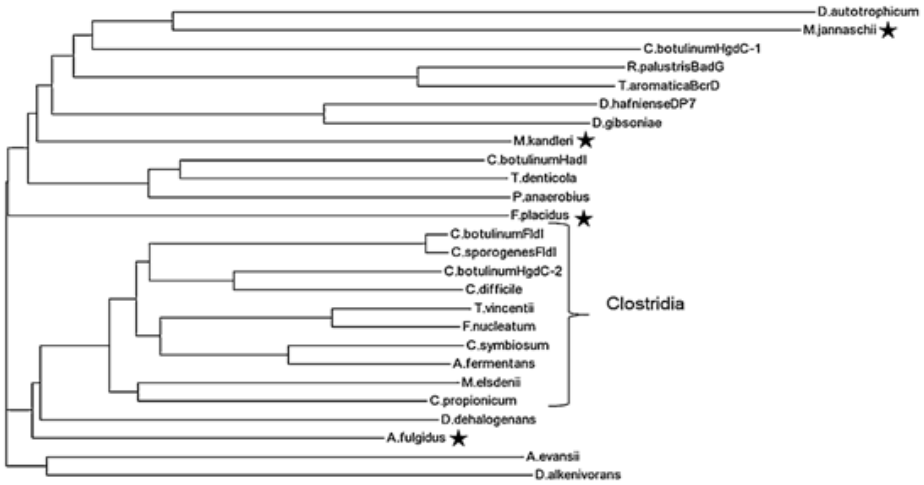

Fig. 4 Phylogenetic trees of the activators of the (*R*)-2-hydroxyacyl-CoA dehydratases in the ClustalW mode are shown: the organisms are the same as in the Fig. 3. Accession numbers are shown in the legend to fig. A9 of the Supplements

MALDI-TOF mass spectrometry was used to analyse the enzymatic reaction. Cinnamoyl-CoA at 898.13 Da and phenylpropionyl-CoA at 900.15 Da were detected after an incubation of cell extracts with the latter compound and cinnamate (data not shown, but see Fig. A14). The phenyllactate CoA-transferase from *C. sporogenes*, an organism with a very similar phenylalanine degradation pathway to *A. fulgidus,* co-purifies with the 3-phenyllactyl-CoA dehydratase (Dickert et al. 2000). Additionally, family III CoA-transferases to which phenyllactate CoA-transferase belongs differ in their catalytic mechanisms from the other types of CoA-transferases (Heider 2001). All the CoA-transferases involved in clostridial amino acid fermentations except glutaconate CoA-transferase (from glutamate fermentation) belong to family III. We speculate that the most likely candidate for the phenyllactate CoA-transferase activity in *A. fulgidus* also belongs to family III of the CoA-transferases.

There are several putative CoA-transferases in *A. fulgidus*; CaiB-1 (carnitine CoA-transferase), GctA (large subunit of glutaconate CoA-transferase) as well as Cat2-1 and Cat2-2 (both 4-hydroxybutyrate CoA-transferase subunits). The only putative family III CoA-transferase in *A. fulgidus* is CaiB-1 which has a modest 28 % amino acid sequence similarity to the *C. sporogenes* enzyme. The overall sequence similarity is less important for conserved enzymatic function than the presence of critical residues and regions. The CaiB-1 sequence was compared to some other family III CoA-transferases suggested in a review on this topic (Heider 2001). A highly conserved region near the N-terminus and a potentially catalytic aspartate are present in all the family III CoA-transferases. The X-ray structure of CaiB (carnitine:crotonobetaine CoA-transferase) from *E. coli* (Stenmark et al. 2004) suggests that the amino acids 37–41 in the alignment in Fig. A15 contain key amino acid residues important for binding the CoA moiety.

Cinnamoyl-CoA reductase/phenylpropionyl-CoA dehydrogenase

Unlike in *C. sporogenes* (Dickert et al. 2000, 2002) that contains a NAD-dependent cinnamate reductase, the redox reaction of cinnamate/phenylpropionate in *A. fulgidus* occurs at the CoA-ester level. Cinnamate or cinnamoyl-CoA could not be reduced with NADH either in the presence or absence of oxygen. Therefore, the cinnamoyl-CoA reductase activity was measured in the backward direction with phenylpropionyl-CoA as substrate and ferrocenium hexafluorophosphate as electron acceptor (Lehman and Thorpe 1990). The results of the spectrophotometrical assay were confirmed by analysing the CoA thioesters purified from an assay mixture by MALDI-TOF mass spectrometry: cinnamoyl-CoA (898.13 Da) and phenylpropionyl-CoA (900.15 Da) in Fig. A14. To identify the gene encoding phenylpropionyl-CoA dehydrogenase, we had to partially purify the enzyme (1.2 U mg^{-1}) as described in the methods section, because *A. fulgidus* contains eight acyl-CoA dehydrogenase genes. Peptide mass fingerprinting (PMF) of the SDS-PAGE helped us to identify band 4 as a mixture of the β-subunit of sulphite reductase (DsrB) and the 8th acyl-CoA dehydrogenase (Acd-8; Fig. 5, Table A2). No activity was observed with butyryl-CoA or propionyl-CoA as substrates. There are 8 putative

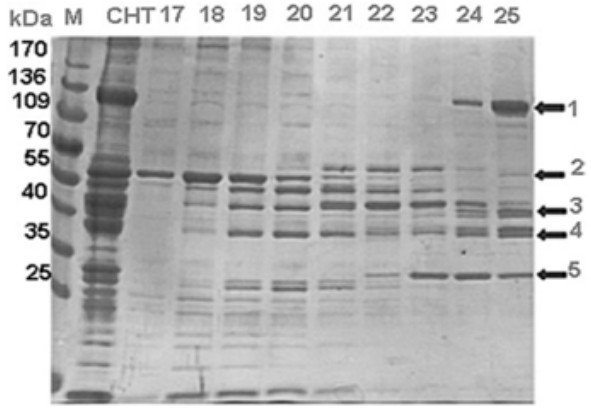

Fig. 5 SDS-PAGE showing partial purification of Acd-8: *M* = protein marker mixture, *CHT* = active fraction before loading on CHT (hydroxyapatite) column, *17–25* = active fractions eluted from the CHT column. The five gel bands of the most active fraction 25 indicated by *arrows* were analysed by PMF and Acd-8 was found in band 4 (complete data in Table A2 of Supplements)

acyl-CoA dehydrogenases in *A. fulgidus* (Acd1-8). Of these, only Acd-2, 5, 7 and 8 conserve the glutamate residue suggested in previous studies to act as base to remove the α-proton of acyl-CoA (Ghisla and Thorpe 2004). Among those, we identified Acd-8 as the cinnamoyl-CoA reductase/phenylpropionyl-CoA dehydrogenase.

Electron-transferring flavoprotein (Etf)

The INT assay (see methods) was used to identify the active fractions, whereby the pure protein showed a specific activity of 10 mU mg^{-1}. Although its specific activity is low, Etf appeared to be an abundant protein in *A. fulgidus*. PMF of the SDS gel bands in Fig. 6 was used to verify the amino acid sequence of the purified Etf. An assay showing a potential electron bifurcation (Herrmann et al. 2008: Li et al. 2008) according to Eq. (1) catalysed by the purified Etf and phenylpropionyl-CoA dehydrogenase did not show activity. Possibly, the ferredoxin from *Clostridium tetanomorphum* (Jayamani 2008) could not substitute for the ferredoxin from *A. fulgidus*.

$$2\ \mathrm{NADH} + \mathrm{cinnamoyl-CoA} + \mathrm{ferredoxin\ (oxidised)} = 2\ \mathrm{NAD^+} + \mathrm{phenylpropionyl-CoA} + \mathrm{ferredoxin^{2-}\ (reduced)} \quad (1)$$

There is only one copy each of *etfA* and *etfB* in the genome. NADH-dependent reduction of cinnamoyl-CoA may be coupled to ferredoxin reduction and electron bifurcation via EtfBA (electron-transferring flavoprotein) subunits. However, the *A. fulgidus* EtfBA have about 15–18 % identity to EtfBA from several clostridia (Herrmann et al. 2008; Li et al. 2008; Buckel and Thauer 2013) and therefore may have a function other than electron bifurcation.

Discussion

Metabolism of phenylalanine and tryptophan

We have presented evidence for the pathway of phenylalanine degradation in *A. fulgidus* proposed in Fig. 1. Phenylpyruvate oxidation via the phenylpyruvate:ferredoxin oxidoreductase can be coupled to substrate-level phosphorylation. In addition, the enzyme generates reduced ferredoxin, which is necessary to activate phenyllactyl-CoA dehydratase (Thamer et al. 2003). Therefore, in the absence of lactate and yeast extract, growth can occur by coupling phenylalanine oxidation and sulphate reduction, while also allowing phenylalanine reduction. We have shown that tryptophan is also degraded to indoleacetate and indolepropionate linked to sulphate reduction although a more detailed quantitative analysis was not performed. We propose that the pathway for the catabolism of tryptophan would involve the same enzymes as for phenylalanine in Fig. 1. Due to the promiscuity of the enzymes involved, the substrates would only differ in having an indole ring instead of the benzene ring as in Fig. 1. The absence of indolelactate as a product in the latter metabolism may be simply due to the different equilibrium constants for the enzymatic dehydrations which are dependent on the substrate structure in each case (Parthasarathy et al. 2010). Further, a shikimate dehydrogenase (Lim et al. 2004) and a trifunctional chorismate mutase/prephenate dehydratase/prephenate dehydrogenase (Lim et al. 2009) have been characterised in *A. fulgidus*. The archaeon can possibly synthesise all three proteinogenic aromatic amino acids via chorismate. Since we have also demonstrated aromatic amino acid catabolism, it follows that *A. fulgidus* must have a mechanism to sense and regulate the metabolism of these amino acids.

Adaptation and energy conservation

Archaeoglobus species are found in both marine and freshwater environments. They do not ferment, although the lactate catabolism in *A. fulgidus* strain Z changes from about 1:1 lactate/sulphate at 14 mM sulphate to 2:1 at 0.3 mM sulphate (Habicht et al. 2005). It was suggested that this shift occurs because marine environments are rich in sulphate (28 mM) but poor in organic matter, whereas in freshwater, organic matter may be more abundant and sulphate is usually low (0.3 mM). Similarly, in the phenylalanine degradation in *A. fulgidus*, the ratio of Phe/sulphate changes from 10:1 at 36 mM sulphate to about 15:1 at 0.7 mM sulphate.

Sulphate reduction via the classical pathway involving adenosine phosphosulphate (APS) occurs in *A. fulgidus* (Stetter et al. 1987; Stetter 1988) and requires an investment of ATP before sulphate can be reduced. Therefore, any mechanism that allows the organism to gain or conserve energy would confer an adaptive advantage. Energy conservation through electron bifurcation involving ferredoxin and NADH via Etf and phenylpropionyl-CoA dehydrogenase could be envisaged, but was not measurable in this study using *C. tetanomorphum* ferredoxin. There are 8 putative ferredoxin genes and one flavodoxin gene in the genome of which one may encode a protein needed for this reaction. On the other hand, *A. fulgidus* contains a menaquinone derivative (Hemmi et al. 2005). We speculate that an electron confurcating Qmo-like (quinone monooxygenase) membrane complex with ferredoxin as low potential donor and menaquinone ($E^{\circ\prime} = -71$ mV, +150 mV membrane potential) as high potential donor could use Etf together with cinnamoyl-CoA ($E^{\circ\prime}$ ca. 0 mV) as acceptor, similar to APS (adenosinephosphosulfate) (Grein et al. 2013).

Metabolism of other aromatic compounds

The decarboxylation of caffeate may be attributed to the activity of the product of the *pad-1* (phenylacrylate decarboxylase) gene. This may be an indication that *A. fulgidus* is able to degrade a wider range of aromatic compounds than previously suspected.

Ecological significance and horizontal gene transfer

In marine environments, amino acids can comprise from 1 to 50 % of the organic carbon, and 10–100 % of the organic nitrogen, decreasing with the depth of sediments (Lee 1988). A 'composite' marine organism tissue averaged for different organisms contains about 5 % phenylalanine in the total amino acid pool (Phillips 1984). Up to 4 % of the total amino acid pool in sediments is phenylalanine, but other amino acids such as glutamate, aspartate and glycine are more abundant (Dauwe and Middelburg 1998; Lee 1988). Nevertheless, hyperthermophilic archaea such as *Pyrococcus furiosus* may scavenge peptides/amino acids and have evolved ways to degrade phenylalanine. This may reflect the niche specialisation where the more abundant amino acids are degraded first in complex communities, while the aromatic amino acids are accessible only to those with unusual metabolic capabilities. Further, the ability to regulate sulphate-dependent catabolism of organic substrates could be of adaptive advantage since *A. fulgidus* is found in both marine and freshwater habitats.

The presence of a *pheS* gene coding for a subunit of phenylalanine-tRNA synthetase, a gene encoding the DNA-binding protein Alba (Zhao et al. 2003) and *hgdABC* in the same module (archaea lack well-defined operons) may suggest regulatory interaction between them. The phylogenetic trees for the HgdAB subunits suggest a possible horizontal gene transfer with mesophilic bacteria (Fig. 3 and 4). Evidence of lateral gene transfer between bacteria and archaea in the marine environment comes from the genome sequencing of the thermophilic bacterium *T. maritima* (Nelson et al. 1999), which revealed conservation of gene order between *T. maritima* and archaea in many of the clustered regions (81 archaeal-like genes in 15 regions of the genome). Amino acid degradation pathways known originally from a few mesophilic species of clostridia may in fact be widespread in thermophilic bacteria and archaea in diverse freshwater and marine environments. Some of those pathways may involve enzymes of interest to future investigators.

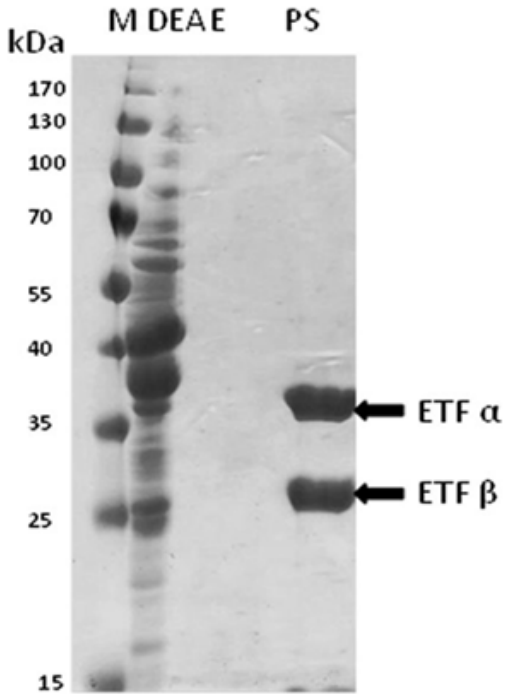

Fig. 6 SDS–PAGE analysis showing the purification of Etf subunits: *M* = Protein marker mixture (molecular masses in kDa), *DEAE* = active fraction eluted from the DEAE-Sepharose column and *PS* = active fraction eluted from the phenyl Sepharose column. PMF analysis results are shown in Table A3

Acknowledgments The authors most gratefully acknowledge the assistance of the following people: Gert Häde, Klaus Putzer and Dr. Xiulan Xie of the NMR Division, Jan Bamberger and Dr. Uwe Linne of the Mass Spectrometry Division, and all at the Philipps-Universität Marburg. They also thank Dr. Harald Huber of the Lehrstuhl für

Mikrobiologie, Universität Regensburg, for the providing cells of *A. fulgidus*. Finally, we thank the Max Planck Society and the Zentrum für synthetische Mikrobiologie (Synmikro), Marburg, Germany, for funding this work.

References

Atlas RM (1993) Handbook of microbiological media. CRC Press, Boca Raton, USA. http://nar.oxfordjournals.org/content/40/W1/W573

Boc A, Philippe H, Makarenkov V (2010) Inferring and validating horizontal gene transfer events using bipartition dissimilarity. Syst Biol 59:195–211

Boll M, Fuchs G (1995) Benzoyl-coenzyme A reductase (dearomatizing), a key enzyme of anaerobic aromatic metabolism: ATP dependence of the reaction, purification and some properties of the enzyme from *Thauera aromatica* strain K172. Eur J Biochem 234:921–933

Buckel W (1980a) Analysis of the fermentation pathways of clostridia using double labelled glutamate. Arch Microbiol 127:167–169

Buckel W (1980b) The reversible dehydration of (*R*)-2-hydroxyglutarate to (*E*)-glutaconate. Eur J Biochem 106:439–447

Buckel W (2001) Sodium ion-translocating decarboxylases. Biochim Biophys Acta 1505:15–27

Buckel W, Barker HA (1974) Two pathways of glutamate fermentation by anaerobic bacteria. J Bacteriol 117:1248–1260

Buckel W, Keese R (1995) One-electron redox reactions of CoASH esters in anaerobic bacteria—a mechanistic proposal. Ang Chem Intl Ed Eng 34:1502–1505

Buckel W, Semmler R (1983) Purification, characterisation and reconstitution of glutaconyl-CoA decarboxylase, a biotin-dependent sodium pump from anaerobic bacteria. Eur J Biochem 136:427–434

Buckel W, Thauer RK (2013) Energy conservation via electron bifurcation ferredoxin reduction and proton/Na^+ translocating ferredoxin reduction. Biochim Biophys Acta 1827:94–113

Buckel W, Zhang J, Friedrich P, Parthasarathy A, Li H, Djurdjevic I, Dobbek H, Martins BM (2011) Enzyme catalyzed radical dehydrations of hydroxy acids. Biochim Biophys Acta 1824:1278–1290

Bult CJ, White O, Olsen GJ, Zhou L, Fleischmann RD, Sutton GG, Blake JA, FitzGerald FM, Clayton RA, Gocayne JD, Kerlavage AR, Dougherty BA, Tomb J-F, Adams MD, Reich CI, Overbeek R, Kirkness EF, Weinstock KG, Merrick JM, Glodek A, Scott JL, Geoghagen NSM, Weidman JF, Fuhrmann JL, Nguyen D, Utterback TR, Kelley JM, Peterson JD, Sadow PW, Hanna MC, Cotton MD, Roberts KM, Hurst MA, Kaine BP, Borodovsky M, Klenk H-P, Fraser CM, Smith HO, Woese CR, Venter JC (1996) Complete genome sequence of the methanogenic archaeon, *Methanococcus jannaschii*. Science 273:1058–1073

Çinkaya I (2002) Substrat induzierte Radikalbildung in dem Eisen-Schwefel-Flavoenzym 4-Hydroxybutyryl-CoA-Dehydratase aus *Clostridium aminobutyricum*. Dissertation, Philipps University, Marburg

Ciulla RA, Roberts MF (1999) Effects of osmotic stress on *Methanococcus thermolithotrophicus*: ^{13}C-edited ^{1}H-NMR studies of osmolyte turnover. Biochim Biophys Acta 1427:193–204

Cline JD (1969) Spectrophotometric determination of hydrogen sulfide in natural waters. Limnol Oceanogr 14:454–458

Corpet F (1988) Multiple sequence alignment with hierarchical clustering. Nucleic Acids Res 16:10881–10890

Dauwe B, Middelburg JJ (1998) Amino acids and hexosamines as indicators of organic matter degradation state in North Sea sediments. Limnol Oceanogr 43:782–798

Dickert S (2001) Fermentation von L-phenylalanin in *Clostridium sporogenes*: Charakterisierung der Phenyllactat-Dehydratase. Dissertation, Philipps University, Marburg

Dickert S, Pierik AJ, Linder D, Buckel W (2000) The involvement of coenzyme A esters in the dehydration of (*R*)-phenyllactate to (*E*)-cinnamate by *Clostridium sporogenes*. Eur J Biochem 267:3874–3884

Dickert S, Pierik AJ, Buckel W (2002) Molecular characterization of phenyllactate dehydratase and its initiator from *Clostridium sporogenes*. Mol Microbiol 44:49–60

Djurdjevic I, Zelder O, Buckel W (2010) Method for the production of glutaconate. International patent application WO/2010/081885

Djurdjevic I, Zelder O, Buckel W (2011) Production of glutaconic acid in a recombinant *Escherichia coli* strain. Appl Env Microbiol 77:320–322

D'Ordine RL, Tonge PJ, Carey PR, Anderson VE (1994) Electronic rearrangement induced by substrate analog binding to the enoyl-CoA hydratase active site: evidence for substrate activation. Biochemistry 33:12635–12643

Gerhardt A, Çinkaya I, Linder D, Huisman G, Buckel W (2000) Fermentation of 4-aminobutyrate by *Clostridium aminobutyricum*: cloning of two genes involved in the formation and dehydration of 4-hydroxybutyryl-CoA. Arch Microbiol 174:189–199

Ghisla S, Thorpe C (2004) Acyl-CoA dehydrogenases. A mechanistic overview. Eur J Biochem 271:494–508

Gokarn RR, Selifonova OV, Jessen HJ, Gort SJ, Selmer T, Buckel W (2004) 3-Hydroxypropionic acid and other organic compounds. US Patent Application 20040076982, Cargill Incorporated, Minneapolis, MN, USA

Graupner M, Xu H, White RH (unpublished) In: Roberts MF (2005) Organic compatible solutes of halotolerant and halophilic microorganisms. Saline Syst Open Access J 1:5

Grein F, Ramos AR, Venceslau SS, Pereira IAC (2013) Unifying concepts in anaerobic respiration: Insights from dissimilatorysulfur metabolism. Biochim Biophys Acta 1827:145–160

Habicht KS, Salling L, Thamdrup B, Canfield DE (2005) Effect of low sulfate concentrations on lactate oxidation and isotope fractionation during sulfate reduction by *Archaeoglobus fulgidus* Strain Z. Appl Env Microbiol 71:3770–3777

Hans M, Sievers J, Müller U, Bill E, Vorholt JA, Linder D, Buckel W (1999) 2-Hydroxyglutaryl-CoA dehydratase from *Clostridium symbiosum*. Eur J Biochem 265:404–414

Hartzell PL, Reed DW (2006) The genus Archaeoglobus. Prokaryotes 3:82–100

Havir EA, Hanson KR (1970) L-phenylalanine ammonia-lyase (potato tubers). Methods Enzymol 17A:575–581

Heider J (2001) A new family of CoA-transferases. FEBS Lett 509:345–349

Hemmi H, Takahashi Y, Shibuya K, Nakayama T, Nishino T (2005) Menaquinone-specific prenyl reductase from the hyperthermophilic archaeon *Archaeoglobus fulgidus*. J Bacteriol 187:1937–1944

Herrmann G, Selmer T, Jessen HJ, Gokarn RR, Selifonova O, Gort SJ, Buckel W (2005) Two beta-alanyl-CoA:ammonia lyases in Clostridium propionicum. FEBS J 272:813–821

Herrmann G, Jayamani E, Mai G, Buckel W (2008) Energy conservation via electron-transferring flavoprotein in anaerobic bacteria. J Bacteriol 190:784–791

Hetzel M, Brock M, Selmer T, Pierik AJ, Golding BT, Buckel W (2003) Acryloyl-CoA reductase from *Clostridium propionicum*, an enzyme complex of propionyl-CoA dehydrogenase and electron-transferring flavoprotein. Eur J Biochem 270: 902–910

Hodgins DS (1971) Yeast phenylalanine ammonia-lyase. Purification, properties, and the identification of catalytically essential dehydroalanine. J Biol Chem 246:2977–2985

Holmes DE, Risso C, Smith JA, Lovely DE (2011) Anaerobic oxidation of benzene by the hyperthermophilic archaeon *Ferroglobus placidus*. Appl Env Microbiol 17:5926–5933

Hufnagel P, Rabus R (2006) Mass spectrometric identification of proteins in complex post-genomic projects. Soluble proteins of the metabolically versatile, denitrifying '*Aromatoleum*' sp. strain EbN1. J Mol Microbiol Biotech 11:53–81

Jayamani E (2008) A unique way of energy conservation in glutamate fermenting clostridia. Dissertation, Philipps Universität, Marburg

Kandasamy V, Vaidyanathan H, Djurdjevic I, Jayamani E, Ramachandran KB, Buckel W, Jayaraman G, Ramalingam S (2013) Engineering *Escherichia coli* with acrylate pathway genes for propionic acid synthesis and its impact on mixed-acid fermentation. Appl Microbiol Biotechnol 97:1191–1200

Katoh K, Kuma K, Toh H, Miyata T (2005) MAFFT version 5: improvement in accuracy of multiple sequence alignment. Nucleic Acids Res 33:511–518

Kawaguchi A, Yoshimura T, Okuda S (1981) A new method for the preparation of acyl-CoA thioesters. J Biochem 89:337–339

Kim J, Hetzel M, Boiangiu CD, Buckel W (2004) Dehydration of (*R*)-2-hydroxyacyl-CoA to enoyl-CoA in the fermentation of alpha-amino acids by anaerobic bacteria. FEMS Microbiol Rev 28:455–468

Kim J, Darley DJ, Buckel W, Pierik AJ (2008) An allylic ketyl radical intermediate in clostridial amino-acid fermentation. Nature 452:239–242

Klees AG, Linder D, Buckel W (1992) 2-Hydroxyglutaryl-CoA dehydratase from *Fusobacterium nucleatum (subsp. nucleatum)*: an iron-sulfur flavoprotein. Arch Microbiol 158:294–301

Klenk H-P, Clayton RA, Tomb JF, White O, Nelson KE, Ketchum KA, Dodson RJ, Gwinn M, Hickey EK, Peterson JD, Richardson DL, Kerlavage AR, Graham DE, Kyrpides NC, Fleischmann RD, Quackenbush J, Lee NH, Sutton GG, Gill S, Kirkness EF, Dougherty BA, McKenney K, Adams MD, Loftus B, Peterson S, Reich CI, McNeil LK, Badger JH, Glodek A, Zhou L, Overbeek R, Gocayne JD, Weidman JF, McDonald L, Utterback T, Cotton MD, Spriggs T, Artiach P, Kaine BP, Sykes SM, Sadow PW, D'Andrea KP, Bowman C, Fujii C, Garland SC, Mason TM, Olsen GJ, Fraser CM, Smith HO, Woese CR, Venter JC (1997) The complete genome sequence of the hyperthermophilic, sulphate-reducing archaeon *Archaeoglobus fulgidus*. Nature 390:364–370

Knauer SH, Buckel W, Dobbek H (2011) Structural basis for reductive radical formation and electron recycling in (*R*)-2-hydroxyisocaproyl-CoA dehydratase. J Am Chem Soc 133:4342–4347

Knauer SH, Buckel W, Dobbek H (2012) On the ATP-dependent activation of the radical enzyme (R)-2-hydroxyisocaproyl-CoA dehydratase. Biochemistry 51:6609–6622

Laemmli UK (1970) Cleavage of structural proteins during the assembly of the head of bacteriophage T4. Nature 227:680–685

Lee C (1988) Amino acid and amine biogeochemistry in marine particulate material and sediments. In: Blackburn TH, Sørensen J (eds) Nitrogen cycling in coastal marine environments. Wiley, New York, pp 125–141

Lehman TC, Thorpe C (1990) Alternate electron acceptors for medium-chain acyl-CoA dehydrogenase: use of ferricenium salts. Biochemistry 29:10594–10602

Li F, Hinderberger J, Seedorf H, Zhang J, Buckel W, Thauer RK (2008) Coupled ferredoxin and crotonyl Coenzyme A (CoA) Reduction with NADH catalyzed by the butyryl-CoA dehydrogenase/Etf complex from *Clostridium kluyveri*. J Bacteriol 190:843–850

Lim S, Springstead JR, Yu M, Bartkowski W, Schröder I, Monbouquette HG (2004) A thermostable shikimate 5-dehydrogenase from the archaeon *Archaeoglobus fulgidus*. FEMS Microbiol Lett 238:101–106

Lim S, Springstead JR, Yu M, Bartkowski W, Schröder I, Monbouquette HG (2009) Characterization of a key trifunctional enzyme for aromatic amino acid biosynthesis in *Archaeoglobus fulgidus*. Extremophiles 13:191–198

MacKellar WJ, Wiederanders RS, Tallman DE (1978) Indirect determination of sulfate ion by spectrophotometric titration of excess barium (II) ion with ethylenediaminetetraacetate. Anal Chem 50:160–163

Mai X, Adams MWW (1994) Indolepyruvate ferredoxin oxidoreductase from the hyperthermophilic archaeon *Pyrococcus furiosus:* a new enzyme involved in peptide fermentation. J Biol Chem 269:16726–16732

Martins BM, Macedo-Ribeiro S, Bresser J, Buckel W, Messerschmidt A (2005) Structural basis for stereo-specific catalysis in NAD^+-dependent (*R*)-2-hydroxyglutarate dehydrogenase from *Acidaminococcus fermentans*. FEBS J 272:269–281

Mayhew SG (1978) The redox potential of dithionite and SO_4^{2-} from equilibrium reactions with flavodoxins, methyl viologen and hydrogen plus hydrogenase. Eur J Biochem 85:535–547

Mehta PK, Hale TI, Christen P (1989) Evolutionary relationships among aminotransferases: tyrosine aminotransferase, histidinol-phosphate aminotransferase, and aspartate aminotransferase are homologous proteins. Eur J Biochem 186:249–253

Möllering H, Wahlefeld, AW, Michal G (1974) Visualisierung NAD(P)-abhängiger Reaktionen. In: Bergmeyer HU (ed) Methoden der enzymatischen Analyse. Verlag Chemie, Weinheim/Bergstrasse, Germany, pp 145–153

Musfeldt M, Schönheit P (2002) Novel type of ADP-forming acetyl coenzyme A synthetase in hyperthermophilic archaea: heterologous expression and characterization of isoenzymes from the sulfate reducer, *Archaeoglobus fulgidus* and the methanogen *Methanococcus jannaschii*. J Bacteriol 184:636–644

Nelson KE, Clayton RA, Gill SR, Gwinn ML, Dodson RJ, Haft DH, Hickey EK, Peterson JD, Nelson WC, Ketchum KA, McDonald L, Utterback TR, Malek JA, Linher KD, Garrett MM, Stewart AM, Cotton MD, Pratt MS, Phillips CA, Richardson D, Heidelberg J, Sutton GG, Fleischmann RD, Eisen JA, White O, Salzberg SL, Smith HO, Venter JC, Fraser CM (1999) Evidence for lateral gene transfer between archaea and bacteria from genome sequence of *Thermotoga maritima*. Nature 399: 323–329

Onuffer JJ, Kirsch JF (1995) Redesign of the substrate specificity of *Escherichia coli* aspartate aminotransferase to that of *Escherichia coli* tyrosine aminotransferase by homology modeling and site-directed mutagenesis. Protein Sci 4:1750–1757

Parthasarathy A, Buckel W, Smith DM (2010) On the thermodynamic equilibrium between (*R*)-2-hydroxyacyl-CoA and 2-enoyl-CoA. FEBS J 277:1738–1746

Parthasarathy A, Pierik AJ, Kahnt J, Zelder O, Buckel W (2011) Substrate specificity of 2-hydroxyglutaryl-CoA dehydratase from *Clostridium symbiosum*: towards a bio-based production of adipic acid. Biochemistry 50:3540–3550

Phillips NW (1984) Role of different microbes and substrates as potential food suppliers of specific essential nutrients to marine detritivores. Bull Mar Sci 35:283–298

Riddles PW, Blakeley RL, Zerner B (1979) Ellman's reagent: 5,5′-dithiobis(2-nitrobenzoic acid)-a reexamination. Anal Biochem 94:75–81

Schröder I, Vadas A, Johnson E, Lim S, Monbouquette HG (2004) A novel archaeal alanine dehydrogenase homologous to ornithine cyclodeaminase and mu-crystallin. J Bacteriol 186:7680–7689

Simon EJ, Shemin D (1953) The preparation of S-succinyl Coenzyme A. J Am Chem Soc 75:2520–2520

Steen IH, Hvoslef H, Lien T, Birkeland N-K (2001) Isocitrate dehydrogenase, malate dehydrogenase, and glutamate dehydrogenase

from *Archaeoglobus fulgidus*. Methods Enzymol 331: 13–26

Stenmark P, Gurmu D, Nordlund P (2004) Crystal structure of CaiB, a Type-III CoA transferase in carnitine metabolism. Biochemistry 43:13996–14003

Stetter KO (1988) *Archaeoglobus fulgidus* gen. nov., sp. nov.: a new taxon of extremely thermophilic Archaebacteria. Syst Appl Microbiol 10:172–173

Stetter KO, Lauerer G, Thomm M, Neuner A (1987) Isolation of extremely thermophilic sulfate reducers: evidence for a novel branch of archaebacteria. Science 236:822–824

Stetter KO, Fiala G, Huber G, Huber R, Segerer A (1990) Hyperthermophilic microorganisms. FEMS Microbiol Rev 75:117–124

Tamannaei A (2003) Untersuchungen zum Katalysemechanismus der 2-Hydroxyglutaryl-CoA-Dehydratase aus *Fusobacterium nucleatum.* Diploma thesis, Philipps-Universität, Marburg

Thamer W, Cirpus I, Hans M, Pierik AJ, Selmer T, Bill E, Linder D, Buckel W (2003) A two [4Fe-4S]-cluster-containing ferredoxin as an alternative electron donor for 2-hydroxyglutaryl-CoA dehydratase from *Acidaminococcus fermentans*. Arch Microbiol 179:197–204

Wöhlbrand L, Jacob JH, Kube M, Mussmann M, Jarling R, Beck A, Amann R, Wilkes H, Reinhardt R, Rabus R (2013) Complete genome, catabolic sub-proteomes and key metabolites of *Desulfobacula toluolica* ol2, a marine, aromatic compound degrading, sulphate-reducing bacterium. Environ Microbiol 15:1334–1355

Zhao K, Chai X, Marmorstein R (2003) Structure of a Sir2 Substrate, Alba, reveals a mechanism for deacetylation-induced enhancement of DNA binding. J Biol Chem 278:26071–26077

Ziegenhorn J, Senn M, Bücher T (1976) Molar absorptivities of beta-NADH and beta-NADPH. Clin Chem 22:151–160

Acknowledgements

I would like to take this opportunity to thank my advisor Prof. Wolfgang Buckel who accepted me as a doctoral candidate and let me continue my research in his group. Actually, I will fall short of my words to forward my earnest gratitude and to explain how I enjoyed his regular company, discussing not only science but also regular topics beyond work. It is not only science; I learnt how to become a better human being. This is what I feel is more important in my own life. I will highly value the 5-10 minutes we shared everyday over a cigarette discussing everything and anything. I really feel that I was lucky to have him as my instructor.

Secondly, I would like to thank our collaborator PD. Ulrich Ermler, one of the coolest person I have met till date. His patience and perseverance with my over-enthusiastic nature is highly appreciated.

Thirdly, I would like to thank my advisory and thesis committee members Prof. Johann Heider, Prof. Mohammed Marahiel, Prof. Ulrich Mosch, and Dr. Seigo Shima for their efforts.

I would like to thank my previous laboratory members who were involved in the electron-bifurcation project: Gloria Herrmann, Elamparithi Jayamani, Sebastian Koelzer, Zhen Li and Amr Mowafy. It's said that Rome wasn't built in one day and so is this study. I highly regard the technical assistance of Marco Hornung during my initial days of protein purification and Jorg Kahnt with MALDI.

Generally 2/3rd of my day was well spent only due to the presence of my lab-members and the entire AG Heider group, they made me feel home even though I was 4500 miles away.

A special thanks goes to Anutthaman Parthasarathy and Ankan Banerjee for every reason of my presence in Marburg.

I would also like to thank two of my bachelor co-workers, Katharina Klomann and Arno Fricke who made me learn, how to be a better instructor.

I thank Patricia Wagner for her administrative help.

Thanks to Max Planck Institute for providing me the funding for my doctoral study and Philipps-Universität, Marburg for providing me the lab space.

Finally I would like to thank my family, specially my Mother for making me what I am today.

Curriculum Vitae

Personal details

Name:	Nilanjan Pal Chowdhury
Date of birth:	03.06.1985
Place of birth:	Kolkata
Nationality:	Indian
Marital status:	Single

Education and Professional experience

2002	Secondary education examination, Vivekananda Mission School, Joka, Kolkata, India
2004	Senior secondary education examination, Vivekananda Mission School, Joka, Kolkata, India
2004 – 2007	Bachelor of Science (Biochemistry), University of Calcutta, Kolkata, India
2007 – 2009	Masters of Science (Biochemistry), University of Calcutta, Kolkata, India
09/2009 – 01/2010	Clinical Analyst, Sun Knowledge India Pvt. Ltd, Kolkata, India
02/2010 – 08/2011	Research & Development Associate, Phyto Biotech India Pvt. Ltd., Bangalore, India
09/2011 – 10/2014	Doctoral student in the group of Prof. Wolfgang Buckel and International Max Planck Research School (IMPRS-Mic), Marburg, Germany

Erklärung

Hiermit versichere ich, dass ich meine Dissertation mit dem Titel:

On the Mechanism of Electron-Bifurcation by Electron Transferring Flavoprotein and Butryl-CoA Dehydrogenase

selbständig, ohne unerlaubte Hilfe angefertigt und mich dabei keiner anderen als der von mir ausdrücklich bezeichneten Quellen und Hilfen bedient habe. Die vorliegende Dissertation wurde in der jetzigen oder einer ähnlichen Form noch bei keiner anderen deutschen Hochschule eingereicht und hat noch keinen sonstigen Prüfungszwecken gedient.

_____ _____

(Ort, Datum) (Unterschrift)

(Verfasser)

_____

(Unterschrift)

(Betreuer)